Vol. 5, 3, 243–301 (1998)

Archives of Computational Methods in Engineering
State of the art reviews

Numerical Analysis of Coupled Thermomechanical Frictional Contact Problems. Computational Model and Applications

C. Agelet de Saracibar

E.T.S. Ingenieros de Caminos, Canales y Puertos
Universitat Politècnica de Catalunya
Barcelona, Spain

Summary

In this paper a numerical model for the analysis of coupled thermomechanical multi-body frictional contact problems at finite deformations is presented. The multi-body frictional contact formulation is fully developed on the continuum setting and then a spatial (Galerkin projection) and temporal (time-stepping algorithm) discretization is applied. A contact pressure and temperature dependent thermal contact model has been used. A fractional step method arising from an operator split of the governing equations has been used to solve the coupled nonlinear system of equations, leading to a staggered solution algorithm.
The numerical model has been implemented into an enhanced version of the computational finite element program FEAP. Numerical examples and simulation of industrial metal forming processes show the performance of the numerical model in the analysis of coupled thermomechanical frictional contact problems.

1. INTRODUCTION. MOTIVATION AND GOALS

Numerical analysis of coupled thermomechanical frictional contact problems has been one of the research topics of main interest over the last years. Coupled thermomechanical frictional contact problems arises in many application fields such as metal forming processes, crashworthiness and projectile impact, among others. In spite of important progresses achieved in the computational mechanics, the large scale numerical simulation of these topics continues to be nowadays a very complex task due mainly nowadays a very complex task due mainly to the highly nonlinear nature of the problem, usually involving nonlinear kinematics, large deformations, large inelastic strains, nonlinear boundary conditions, frictional contact interaction, wear phenomena,large slips and coupled thermomechanical effects. During the last decade, a growing interest on these and related topics, has been shown by many industrial companies, such as automotive and aeronautical, motivated by the need to get high quality final products and to reduce manufacturing costs.

Mathematically, the numerical analysis of frictional contact problems amounts to finding the solution of an Initial Boundary Value Problem (IBVP) within a constrained solution space. Consideration of the weak form of momentum balance equations induces limitations on admissible variations in the tangent solution space, imposed by the physical constraints, leading to variational inequalities (VI). See, for example, Kikuchi & Oden (1988) and Duvaut & Lions (1972). A regularization of the frictional contact constraints, using for instance penalty or augmented Lagrangian methods, allows to bypass the need to find a solution within a constrained solution space and provides a very convenient displacement-driven frictional contact formulation. The penalty method has been used by Oden & Pires (1984), Cheng & Kikuchi (1985), Hallquist, Goudreau & Benson (1985), Simo, Wriggers & Taylor (1985), Curnier & Alart (1988), Wriggers, Vu Van & Stein (1990), Belytschko & Neal (1991), Laursen (1992) and Laursen & Simo (1992,1993) among others. On the other hand, the augmented Lagrangian method has been used, for example, by Laursen (1992), Simo

©1998 by CIMNE, Barcelona (Spain). ISSN: 1134–3060 Received: October 1996

& Laursen (1992), Laursen & Simo (1992,1994) and Laursen & Govindjee (1994). Furthermore, the displacement-driven formulation of frictional contact problems, allows to widely exploit the framework developed for computational plasticity. See, for example, Simo & Hughes (1994) and Simo (1994), for an excellent presentation of current topics and last developments in computational plasticity. In particular, return mapping algorithms developed for plasticity can be applied to integrate the frictional traction. Frictional return mapping algorithms have been used by Giannakopoulos (1989), Wriggers, Wan & Stein (1990) and Laursen & Simo (1993,1994), among others. Enhanced Coulomb frictional models, using a non-constant friction coefficient have been used, for example, by Wriggers (1987) and Owen *et al.* (1995). Numerical models for coupled thermomechanical frictional contact problems have been used by Wriggers & Miehe (1992,1994) and Wriggers & Zavarise (1993) among others. A fully nonlinear kinematics formulation of frictionless contact problems, including the derivation of the algorithmic contact operators, was developed by Wriggers & Simo (1985) for 2D linear surface elements and by Parish (1989) for 3D linear surface elements. An extension to frictional contact problems for 2D linear surface elements was provided by Wriggers (1987). A general fully nonlinear kinematics formulation of multi-body frictional contact problems at finite strain was first developed on a continuum setting for 3D and 2D contact surfaces, by Laursen & Simo (1993). A new frictional time integration algorithm for large slip multi-body frictional contact problems at finite deformations has been recently proposed by Agelet de Saracibar (1995a). An extension of the fully nonlinear kinematics formulation to account for wear phenomena was given by Agelet de Saracibar & Chiumenti (1995).

Coupled thermomechanical problems tipically involve different time scales associated with the mechanical and thermal fields. It is widely accepted that an effective numerical integration scheme for the full coupled thermomechanical problem should take advantage of these different time scales. These considerations motivate the so-called staggered algorithms, whereby the problem is partitioned into several smaller sub-problems which are solved sequentially. This technique is specially attractive since the large and generally non-symmetric system that results from a monolithic solution scheme is replaced by much smaller, typically symmetric, sub-systems. For thermomechanical problems the standard approach exploits a natural partitioning of the problem in a mechanical phase, with the temperature held constant, followed by a thermal phase at fixed configuration. As noted in Simo & Miehe (1991) this class of staggered algorithms falls within the class of product formula algorithms arising from an operator split of the governing evolution equations into an isothermal step followed by a heat-conduction step at fixed configuration. A recent analysis in Armero & Simo (1992a,1992b,1993) shows that this isothermal split does not preserve the contractivity property of the coupled problem of (nonlinear) thermoelasticity, leading to staggered schemes that are at best only conditionally stables. Armero & Simo (1992a,1992b,1993) proposed an alternative operator split, henceforth referred to as the isentropic split, whereby the problem is partitioned into an isentropic mechanical phase, with total entropy held constant, followed by a thermal phase at fixed configuration. It was shown by Armero & Simo (1992a,1992b,1993) that such operator split leads to an unconditionally stable staggered algorithm, which preserves the crucial properties of the coupled problem.

The remaining of the paper is as follows. Section 2, deals with the numerical analysis of thermomechanical frictional contact problems. The multi-body frictional contact formulation proposed by Laursen & Simo (1993,1994), fully developed on a continuum setting, and extended by Agelet de Saracibar & Chiumenti (1995) to accomodate wear phenomena, has been extended now to incorporate thermal effects within a fully coupled thermomechanical analysis.

In Section 3, the discretization of the initial boundary value problem including thermomechanical frictional contact constraints is presented. The focuss has been placed on the time integration of the constrained frictional evolution problem. Two time integra-

SCIPEDIA
Register for free at https://www.scipedia.com to download the version without the watermark

tion algorithms are presented. First, the lower Backward-Difference (BD) method, the Backward-Euler (BE) algorithm. Second, within the Implicit Runge-Kutta (IRK) methods, the generalized Projected Mid-Point (PMP) algorithm. This algorithm was first proposed, within a J2 plasticity context, by Simo (1994). See also Agelet de Saracibar (1995b). Both algorithms are amenable to exact linearization and the algorithmic frictional contact tangent operators are derived.

The thermomechanical frictional contact model has been implemented into an enhanced version of the computational finite element program FEAP developed by R.L. Taylor and J.C. Simo and described in Zienkiewicz & Taylor (1991). Numerical examples and metal forming simulations are provided in Section 4. Finally some concluding remarks are included.

2. FORMULATION OF THE COUPLED THERMOMECHANICAL MULTI-BODY FRICTIONAL CONTACT PROBLEM

In this section we present the *continuum* formulation of the coupled thermomechanical multi-body frictional contact problem.

2.1 Notation

Let $2 \leq n_{dim} \leq 3$ be the space dimension and $I := [0, T] \subset \mathbb{R}_+$ the time interval of interest. Let the open sets $\Omega^{(1)} \subset \mathbb{R}^{n_{dim}}$ and $\Omega^{(2)} \subset \mathbb{R}^{n_{dim}}$ with smooth boundaries $\partial\Omega^{(1)}$ and $\partial\Omega^{(2)}$ and closures $\bar{\Omega}^{(1)} := \Omega^{(1)} \cup \partial\Omega^{(1)}$ and $\bar{\Omega}^{(2)} := \Omega^{(2)} \cup \partial\Omega^{(2)}$, be the reference placement of two continuum bodies $\mathcal{B}^{(1)}$ and $\mathcal{B}^{(2)}$, with material particles labeled $\boldsymbol{X} \in \bar{\Omega}^{(1)}$ and $\boldsymbol{Y} \in \bar{\Omega}^{(2)}$ respectively.

Denote by $\varphi^{(i)} : \bar{\Omega}^{(i)} \times \mathbb{I} \to \mathbb{R}^{n_{dim}}$ the orientation preserving deformation map of the body $\mathcal{B}^{(i)}$, with material velocities $\boldsymbol{V}^{(i)} := \partial_t \varphi^{(i)}$, deformation gradients $\boldsymbol{F}^{(i)} := D\varphi^{(i)}$ and absolute temperature $\Theta^{(i)} : \bar{\Omega}^{(i)} \times \mathbb{I} \to \mathbb{R}$. For each time $t \in I$, the mapping $t \in \mathbb{I} \mapsto \varphi_t^{(i)} := \varphi^{(i)}(\cdot, t)$ represents a one-parameter family of configurations indexed by time t, with $\varphi_0^{(i)}$ the reference placement of body $\mathcal{B}^{(i)}$ onto its current placement $\mathcal{S}_t^{(i)} : \varphi_t^{(i)}(\mathcal{B}^{(i)}) \subset \mathbb{R}^{n_{dim}}$.

We will assume that no contact forces are present between the two bodies at the reference configuration. Subsequent configurations cause the two bodies to physically contact and produce interactive forces during some portion of $I = [0, T]$.

We will denote as the *contact surface* $\Gamma^{(i)} \subset \partial\Omega^{(i)}$ the part of the boundary of the body $\mathcal{B}^{(i)}$ such that all material points where contact will occur at any time $t \in \mathbb{I}$ are included. The current placement of the contact surface $\Gamma^{(i)}$ is given by $\gamma^{(i)} := \boldsymbol{\varphi}_t^{(i)}(\Gamma^{(i)})$.

Attention will be focussed to material points on these surfaces denoted as $\boldsymbol{X} \in \Gamma^{(1)}$ and $\boldsymbol{Y} \in \Gamma^{(2)}$. Current placement of these particles is given by $\boldsymbol{x} = \boldsymbol{\varphi}_t^{(1)}(\boldsymbol{X}) \in \gamma^{(1)}$ and $\boldsymbol{y} = \boldsymbol{\varphi}_t^{(2)}(\boldsymbol{Y}) \in \gamma^{(2)}$. See Figure 2.1 for an illustration of the notation to be used.

(A) *Parametrization of the contact surfaces* Let $\mathcal{A}^{(i)} \subset \mathbb{R}^{n_{dim}-1}$ be a parent domain for the contact surface of body $\mathcal{B}^{(i)}$. A parametrization of the contact surface for each body $\mathcal{B}^{(i)}$ is introduced by a family of (orientation preserving) one-parameter mappings indexed by time, $\boldsymbol{\psi}_t^{(i)} : \mathcal{A}^{(i)} \subset \mathbb{R}^{n_{dim}-1} \to \mathbb{R}^{n_{dim}}$ such that $\Gamma^{(i)} := \boldsymbol{\psi}_0^{(i)}(\mathcal{A}^{(i)})$ and $\gamma^{(i)} := \boldsymbol{\psi}_t^{(i)}(\mathcal{A}^{(i)})$. Using the mapping composition rule, it also follows that $\boldsymbol{\psi}_t^{(i)} = \boldsymbol{\varphi}_t^{(i)} \circ \boldsymbol{\psi}_0^{(i)}$.

In particular, for any material point $\boldsymbol{Y} \in \Gamma^{(2)}$ with current placement $\boldsymbol{y} \in \gamma^{(2)}$, there exist some point $\boldsymbol{\xi} \in \mathcal{A}^{(2)}$ such that $\boldsymbol{Y} := \boldsymbol{\psi}_0^{(2)}(\boldsymbol{\xi})$ and $\boldsymbol{y} := \boldsymbol{\psi}_t^{(2)}(\boldsymbol{\xi})$. It will be assumed in what follows that these parametrizations have the required smoothness conditions. Figure 2.2 shows the parametrization map of reference and current placement of a contact surface.

SCIPEDIA
Register for free at https://www.scipedia.com to download the version without the watermark

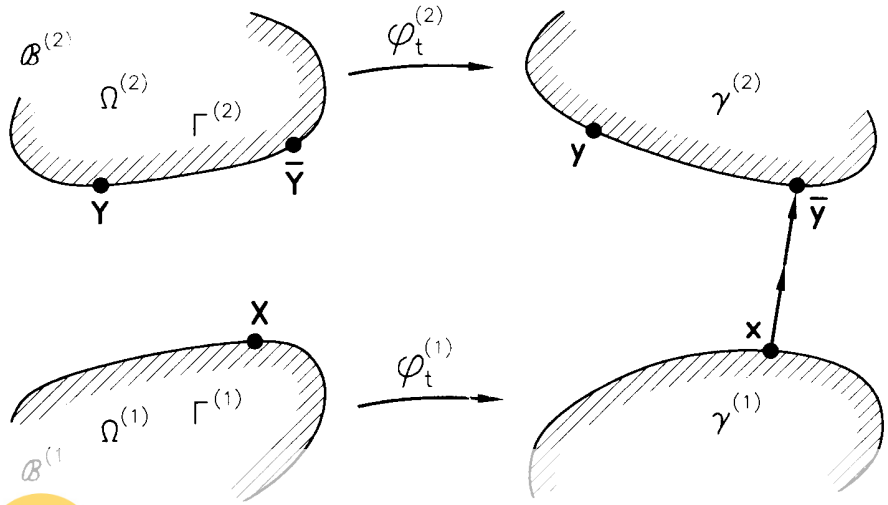

Figure 2.1. Schematic description of two interacting bodies at reference and current placements. Reference and current placement of contact surfaces

SCIPEDIA
Register for free at https//www.scipedia.com to download the version without the watermark

Figure 2.2. Contact surfaces parametrization. Parametrization map of reference and current placement of a contact surface

2.2 Frictional Contact Constraints

Using a standard notation in contact mechanics we will assign to each pair of contact surfaces involved in the problem, the roles of *slave* and *master* surface. In particular, let $\Gamma^{(1)}$ be the *slave surface* and $\Gamma^{(2)}$ be the *master surface*. Additionally, we will denote *slave particles* and *master particles* to the material points of the slave and master surfaces, respectively. With this notation in hand, we will require that any slave particle may not penetrate the master surface, at any time $t \in \mathbb{I}$.

Although in the continuum setting the slave-master notation plays no role, in the discrete setting this choice becomes important.

(A) *Closest-point projection of a slave particle onto a master surface.* Attention is focussed to any slave particle $\boldsymbol{X} \in \Gamma^{(1)}$ with current placement $\boldsymbol{x} := \boldsymbol{\varphi}_t^{(1)}(\boldsymbol{X}) \in \gamma^{(1)}$ and to the master surface $\Gamma^{(2)}$, with particles $\boldsymbol{Y} \in \Gamma^{(2)}$ and current placement $\boldsymbol{y} := \boldsymbol{\varphi}_t^{(2)}(\boldsymbol{Y}) \in \gamma^{(2)}$.

Let $\bar{\boldsymbol{y}}(\boldsymbol{X}, t) \in \gamma^{(2)}$ be the closest-point projection of the current position of the slave particle $\boldsymbol{X}$ onto the current placement of the master surface $\Gamma^{(2)}$, defined as

$$\bar{\boldsymbol{Y}}(\boldsymbol{X}, t) := \arg \min_{\boldsymbol{Y} \in \Gamma^{(2)}} \{\|\boldsymbol{\varphi}_t^{(1)}(\boldsymbol{X}) - \boldsymbol{\varphi}_t^{(2)}(\boldsymbol{Y})\|\} \tag{2.1}$$

$$\bar{\boldsymbol{y}}(\boldsymbol{X}, t) := \boldsymbol{\varphi}_t^{(2)}(\bar{\boldsymbol{Y}}) \tag{2.2}$$

The definition of the closest-point projection allows us to define the distance between any slave particle and the master surface at any time $t \in \mathbb{I}$.

Let $g_N(\boldsymbol{X}, t)$ be the gap function defined for any slave particle $\boldsymbol{X} \in \Gamma^{(1)}$ and for any time $t \in \mathbb{I}$ as (minus) the distance of the current placement of this particle to the current placement of the master surface $\gamma^{(2)} := \boldsymbol{\varphi}_t^{(2)}(\Gamma^{(2)})$. Using the definition of the closest-point projection stated above, the gap function $g_N(\boldsymbol{X}, t)$ may be defined as

$$g_N(\boldsymbol{X}, t) := -[\boldsymbol{\varphi}_t^{(1)}(\boldsymbol{X}) - \boldsymbol{\varphi}_t^{(2)}(\bar{\boldsymbol{Y}}(\boldsymbol{X}, t))] \cdot \boldsymbol{\nu} \tag{2.3}$$

where $\boldsymbol{\nu} : \gamma^{(2)} \to S^2$ is the unit outward normal field to the current placement of the master surface particularized at the closest-point projection $\bar{\boldsymbol{y}}(\boldsymbol{X}, t) \in \gamma^{(2)}$. Here S^2 denotes the unit sphere defined as

$$S^2 := \{\boldsymbol{\nu} \in \mathbb{R}^{n_{dim}} \; : \; \|\boldsymbol{\nu}\| = 1\} \tag{2.4}$$

Register for free at https//www.scipedia.com to download the version without the watermark

(B) *Contact pressure.* Let $\boldsymbol{P}^{(1)}(\boldsymbol{X}, t)$ be the first Piola-Kirchhoff stress tensor and $\boldsymbol{N}^{(1)}(\boldsymbol{X})$ the unit outward normal to the slave surface $\Gamma^{(1)}$ in the reference configuration. The nominal (Piola) frictional contact traction at $\boldsymbol{X} \in \Gamma^{(1)}$ is given as

$$\boldsymbol{t}^{(1)}(\boldsymbol{X}, t) = \boldsymbol{P}^{(1)}(\boldsymbol{X}, t) \cdot \boldsymbol{N}^{(1)}(\boldsymbol{X}) \tag{2.5}$$

Additionally one defines the contact pressure $t_N(\boldsymbol{X}, t)$ as minus the projection of the nominal frictional contact traction $\boldsymbol{t}^{(1)}$ onto the unit outward normal to the current placement of the slave surface $\boldsymbol{n}^{(1)}(\boldsymbol{X}, t)$. Then we can split the nominal frictional contact as

$$\boldsymbol{t}^{(1)}(\boldsymbol{X}, t) = -t_N(\boldsymbol{X}, t) \; \boldsymbol{n}^{(1)}(\boldsymbol{X}, t) + \mathbb{P}_{n^{(1)}} \boldsymbol{t}^{(1)}(\boldsymbol{X}, t) \tag{2.6}$$

where $\mathbb{P}_{n^{(1)}} \boldsymbol{t}^{(1)}$ is the projection of $\boldsymbol{t}^{(1)}$ onto the associated tangent plane.

With the required surface smoothness conditions, when the slave particle $\boldsymbol{X}$ comes in to contact with the master surface, the following relation holds

$$\boldsymbol{\nu} = \boldsymbol{n}^{(2)}(\bar{\boldsymbol{Y}}(\boldsymbol{X}, t), t) = -\boldsymbol{n}^{(1)}(\boldsymbol{X}, t) \tag{2.7}$$

Here $\boldsymbol{n}^{(1)}$ is the unit outward normal to the slave surface at the point $\boldsymbol{x} = \boldsymbol{\varphi}_t^{(1)}(\boldsymbol{X})$ and $\boldsymbol{\nu} := \boldsymbol{n}^{(2)}$ is the unit outward normal to the the master surface at the point $\bar{\boldsymbol{y}} = \boldsymbol{\varphi}_t^{(2)}(\bar{\boldsymbol{Y}})$.

Then an equivalent expression for the nominal frictional contact traction split is given as

$$\boxed{\boldsymbol{t}^{(1)}(\boldsymbol{X},t) = t_N(\boldsymbol{X},t)\ \boldsymbol{\nu}(\bar{\boldsymbol{Y}}(\boldsymbol{X},t),t) + \mathbb{P}_{\nu}\boldsymbol{t}^{(1)}(\boldsymbol{X},t)} \tag{2.8}$$

(C) *Contact normal constraints* With the preceding definitions for the gap function $g_N(\boldsymbol{X},t)$ and the contact pressure $t_N(\boldsymbol{X},t)$ we can introduce the normal constraints induced by the frictionless contact problem.

i. Impenetrability kinematic constraint The kinematic constraint induced by the impenetrability requirement can be expressed in terms of the gap function $g_N(\boldsymbol{X},t)$ as

$$g_N(\boldsymbol{X},t) \leq 0 \tag{2.9}$$

ii. Non-adhesion constraint. The non-adhesion constraint implies that the contact pressure must be non-negative. Mathematically this condition can be expressed as

$$\begin{aligned} t_N(\boldsymbol{X},t) &\geq 0 \qquad \text{if} \quad g_N(\boldsymbol{X},t) = 0 \\ t_N(\boldsymbol{X},t) &= 0 \qquad \text{if} \quad g_N(\boldsymbol{X},t) < 0 \end{aligned} \tag{2.10}$$

iii. Contact persistency condition. This condition implies the requirement that the rate of separation at the contact points must be zero for positive contact pressure. Mathematically, this persistency condition takes the form

$$t_N(\boldsymbol{X},t)\ \dot{g}_N(\boldsymbol{X},t) = 0 \tag{2.11}$$

The above expressions for impenetrability, non-adhesion and contact persistency can be expressed as Kuhn-Tucker complementarity conditions as

$$\boxed{\begin{aligned} g_N(\boldsymbol{X},t) &\leq 0 \\ t_N(\boldsymbol{X},t) &\geq 0 \\ t_N(\boldsymbol{X},t)\ g_N(\boldsymbol{X},t) &= 0 \\ t_N(\boldsymbol{X},t)\ \dot{g}_N(\boldsymbol{X},t) &= 0 \end{aligned}} \tag{2.12}$$

(D) *Convected basis on the master surface* Exploiting the geometric structure induced by the impenetrability constraint through the definition of the gap function $g_N(\boldsymbol{X},t)$, we introduce an associated convected basis, suitable for definition of the frictional constraints. The definitions of the convected frames emanate from the differentiation of the contact surfaces with respect to the convected coordinates. Along with the convected basis, dual or reciprocal convected basis are defined following a standard procedure. Attention in what follows will be restricted to $n_{dim} = 3$. Particularization for $n_{dim} = 2$ is trivial once the three-dimensional case has been considered.

Using the parametrization of the contact surfaces introduced above we consider a point $\boldsymbol{\xi} := (\xi^1, \xi^2) \in \mathcal{A}^{(2)}$ of the parent domain, such that

$$\boldsymbol{Y} := \boldsymbol{\psi}_0^{(2)}(\boldsymbol{\xi})\ , \qquad \boldsymbol{y} := \boldsymbol{\psi}_t^{(2)}(\boldsymbol{\xi}) \tag{2.13}$$

SCIPEDIA
Register for free at https://www.scipedia.com to download the version without the watermark

Attached to each master particle $\boldsymbol{Y} \in \Gamma^{(2)}$ we introduce the convected surface basis $\boldsymbol{E}_\alpha(\boldsymbol{\xi})$ and $\boldsymbol{e}_\alpha(\boldsymbol{\xi})$, $\alpha = 1, 2$ on the reference and current configurations, respectively as

$$\boldsymbol{E}_\alpha(\boldsymbol{\xi}) := \boldsymbol{\psi}^{(2)}_{0,\alpha}(\boldsymbol{\xi}) \ , \qquad \boldsymbol{e}_\alpha(\boldsymbol{\xi}) := \boldsymbol{\psi}^{(2)}_{t,\alpha}(\boldsymbol{\xi}) \tag{2.14}$$

where $(\cdot)_{,\alpha}$ denotes partial derivative with respect to ξ^α. Using the composition map $\boldsymbol{\psi}^{(2)}_t = \boldsymbol{\varphi}^{(2)}_t \circ \boldsymbol{\psi}^{(2)}_0$ the following relation holds

$$\boldsymbol{e}_\alpha(\boldsymbol{\xi}) = \boldsymbol{F}^{(2)}_t(\boldsymbol{\psi}^{(2)}_0(\boldsymbol{\xi})) \cdot \boldsymbol{E}_\alpha(\boldsymbol{\xi}) \tag{2.15}$$

where $\boldsymbol{F}^{(2)}_t := D\boldsymbol{\varphi}^{(2)}_t$ is the deformation gradien t.

Let consider now for any slave particle $\boldsymbol{X} \in \Gamma^{(1)}$ the master particle $\bar{\boldsymbol{Y}}(\boldsymbol{X}, t) \in \Gamma^{(2)}$ such that satisfies the closest-point projection minimization condition given by (2.1). Then for some poin t$\bar{\boldsymbol{\xi}} := (\bar{\xi}^1, \bar{\xi}^2) \in \mathcal{A}^{(2)}$ of the parent domain we have

$$\bar{\boldsymbol{Y}}(\boldsymbol{X}, t) := \boldsymbol{\psi}^{(2)}_0(\bar{\boldsymbol{\xi}}(\boldsymbol{X}, t)) \ , \qquad \bar{\boldsymbol{y}}(\boldsymbol{X}, t) := \boldsymbol{\psi}^{(2)}_t(\bar{\boldsymbol{\xi}}(\boldsymbol{X}, t)) \tag{2.16}$$

Attached to the master particle$\bar{\boldsymbol{Y}}(\boldsymbol{X}, t) \in \Gamma^{(2)}$ we define the convected surface basis on the reference and current configurations, respectively, as

$$\boldsymbol{\tau}^{ref}_\alpha(\boldsymbol{X}, t) := \boldsymbol{E}_\alpha(\bar{\boldsymbol{\xi}}(\boldsymbol{X}, t)) \ , \qquad \boldsymbol{\tau}_\alpha(\boldsymbol{X}, t) := \boldsymbol{e}_\alpha(\bar{\boldsymbol{\xi}}(\boldsymbol{X}, t)) \tag{2.17}$$

Using the composition map $\boldsymbol{\psi}^{(2)}_t = \boldsymbol{\varphi}^{(2)}_t \circ \boldsymbol{\psi}^{(2)}_0$ the following relation holds

$$\boldsymbol{\tau}_\alpha = \boldsymbol{F}^{(2)}_t(\boldsymbol{\psi}^{(2)}_0(\bar{\boldsymbol{\xi}})) \cdot \boldsymbol{\tau}^{ref}_\alpha \tag{2.18}$$

showing that the surface basis v ectors$\boldsymbol{\tau}^{ref}_\alpha$ and $\boldsymbol{\tau}_\alpha$ are convected through the deformation gradient map $\boldsymbol{F}^{(2)}_t$ at the master particle $\bar{\boldsymbol{Y}}(\boldsymbol{X}, t)$.

Additionaly, the unit outward normals$\boldsymbol{\nu}^{ref} \in S^2$ and $\boldsymbol{\nu} \in S^2$ at the master particle $\bar{\boldsymbol{Y}}(\boldsymbol{X}, t)$ on the reference and current configurations, respectively, can be defined as

$$\boldsymbol{\nu}^{ref} := \frac{\boldsymbol{\tau}^{ref}_1 \times \boldsymbol{\tau}^{ref}_2}{\|\boldsymbol{\tau}^{ref}_1 \times \boldsymbol{\tau}^{ref}_2\|} \ , \qquad \boldsymbol{\nu} := \frac{\boldsymbol{\tau}_1 \times \boldsymbol{\tau}_2}{\|\boldsymbol{\tau}_1 \times \boldsymbol{\tau}_2\|} \tag{2.19}$$

The vectors $\boldsymbol{\tau}^{ref}_\alpha \in T_{\nu^{ref}} S^2$ and $\boldsymbol{\tau}_\alpha \in T_\nu S^2$, $\alpha = 1, 2$ span the tangent spaces $T_{\nu^{ref}} S^2$ and $T_\nu S^2$ to the S^2 unit sphere at $\boldsymbol{\nu}^{ref}$ and $\boldsymbol{\nu}$, respectively. Here the tangen t space to theS^2 unit sphere at $\boldsymbol{\nu} \in S^2$ is defined as

$$T_\nu S^2 := \{\delta\boldsymbol{\nu} \in \mathbb{R}^{n_{dim}} \ : \ \delta\boldsymbol{\nu} \cdot \boldsymbol{\nu} = 0\} \tag{2.20}$$

The convected surface basis vectors $\boldsymbol{\tau}^{ref}_\alpha$ and $\boldsymbol{\tau}_\alpha$, $\alpha = 1, 2$, augmen ted with the unit out ward normals $\boldsymbol{\nu}^{ref}$ and $\boldsymbol{\nu}$, provides local spatial frames at the master particle $\bar{\boldsymbol{Y}}(\boldsymbol{X}, t)$ on the reference and current configurations, respectively.

SCIPEDIA
Register for free at https//www.scipedia.com to download the version without the watermark

(E) *Surface metric and curvature on the reference and current configurations.* The convected surface basis vectors $\boldsymbol{\tau}_\alpha^{ref}$ and $\boldsymbol{\tau}_\alpha$, $\alpha = 1, 2$, induces a surface metric or first fundamental form on the reference and current configurations, defined respectively as

$$\boxed{M_{\alpha\beta} := \boldsymbol{\tau}_\alpha^{ref} \cdot \boldsymbol{\tau}_\beta^{ref} \ , \qquad m_{\alpha\beta} := \boldsymbol{\tau}_\alpha \cdot \boldsymbol{\tau}_\beta} \tag{2.21}$$

Inverse surface metrics $M^{\alpha\beta}$ and $m^{\alpha\beta}$ are defined in the usual manner. Additionally, dual surface basis on the reference and current configurations are straightforward defined respectively as

$$\boldsymbol{\tau}_{ref}^\alpha := M^{\alpha\beta} \boldsymbol{\tau}_\beta^{ref} \ , \qquad \boldsymbol{\tau}^\alpha := m^{\alpha\beta} \boldsymbol{\tau}_\beta \tag{2.22}$$

The variation of the convected surface basis along the convected coordinates, together with the unit normal, induces the second fundamental form or surface curvature defined, on the reference and current configurations, as

$$\boxed{\kappa_{\alpha\beta}^{ref} := \boldsymbol{E}_{\alpha,\beta}(\bar{\boldsymbol{\xi}}) \cdot \boldsymbol{\nu}^{ref} \ , \qquad \kappa_{\alpha\beta} := \boldsymbol{e}_{\alpha,\beta}(\bar{\boldsymbol{\xi}}) \cdot \boldsymbol{\nu}} \tag{2.23}$$

(F) *Relative slip velocity on the convected description.* We introduce the relative slip velocity on the convected (reference) configuration defined as

$$\boldsymbol{v}_T^{ref}(\boldsymbol{X}, t) := \dot{\bar{\boldsymbol{Y}}}(\boldsymbol{X}, t) \tag{2.24}$$

The relative velocity on the convected description can be expressed in terms of the rate of the parent coordinates, using the map $(2.16)_1$, the convected surface basis on the reference configuration given by $(2.17)_1$ and applying the chain rule derivation, as

$$\boldsymbol{v}_T^{ref}(\boldsymbol{X}, t) = \dot{\bar{\xi}}^\alpha \boldsymbol{\tau}_\alpha^{ref} \tag{2.25}$$

As expected, the convected relative slip velocity defined by (2.24) or (2.25) lies in the tangent plane to the master surface at the master point $\bar{\boldsymbol{Y}}(\boldsymbol{X}, t)$.

The relative velocity on the current configuration can be defined as the push-forward of the relative velocity in the convected description with the deformation gradient $\boldsymbol{F}_t^{(2)}$, as

$$\boldsymbol{v}_T(\boldsymbol{X}, t) := \boldsymbol{F}_t^{(2)}(\bar{\boldsymbol{\xi}}(\boldsymbol{X}, t)) \cdot \boldsymbol{v}_T^{ref}(\boldsymbol{X}, t) \tag{2.26}$$

The one-form associated to the relative velocity in the convected description is defined as

$$\boldsymbol{v}_T^{\flat\, ref}(\boldsymbol{X}, t) := \dot{\bar{\xi}}^\alpha M_{\alpha\beta} \boldsymbol{\tau}_{ref}^\beta \tag{2.27}$$

while the one-form associated to the relative velocity in the current configuration is defined as the push-forward of the corresponding one-form in the convected description, as

$$\boxed{\boldsymbol{v}_T^\flat(\boldsymbol{X}, t) := \dot{\bar{\xi}}^\alpha M_{\alpha\beta} \boldsymbol{\tau}^\beta} \tag{2.28}$$

REMARK 2.1. The definition of $\boldsymbol{v}_T^\flat(\boldsymbol{X}, t)$ is *frame indifferent* despite the fact that the material and spatial velocity fields are not. This crucial property arises because the definition of $\boldsymbol{v}_T^\flat(\boldsymbol{X}, t)$ uses the convected basis. □

SCIPEDIA
Register for free at https://www.scipedia.com to download the version without the watermark

REMARK 2.2. We note that the definition of the one-form associated to the relative velocity involves the metric $M_{\alpha\beta}$ at the point $\bar{\boldsymbol{Y}}(\boldsymbol{X},t)$ in the reference configuration, and *not* the metric $m_{\alpha\beta}$ in the current configuration. This is because we define $\boldsymbol{v}_T^\flat$ as the push-forward of the corresponding one-form in the convected description and not as the one-form associated to the spatial vector $\boldsymbol{v}_T$ in the current configuration. This last definition leads to an increase in the computational cost, due to the complexities involved in the linearization of the frictional integration algorithm. □

(G) *Frictional traction.* We define the nominal frictional tangent traction $\boldsymbol{t}_T(\boldsymbol{X},t)$ as (minus) the projection of the nominal frictional contact traction $\boldsymbol{t}^{(1)}(\boldsymbol{X},t)$ onto the unit normal $\boldsymbol{\nu}$, as

$$t_T(\boldsymbol{X},t) := -\mathbb{P}_\nu \boldsymbol{t}^{(1)}(\boldsymbol{X},t) = t_T^\alpha(\boldsymbol{X},t)\ \boldsymbol{\tau}_\alpha \tag{2.29}$$

Additionally the one-form associated to this object is defined as

$$\boxed{t_T^\flat(\boldsymbol{X},t) := -\mathbb{P}_\nu \boldsymbol{t}^{\flat(1)}(\boldsymbol{X},t) = t_{T_\alpha}(\boldsymbol{X},t)\ \boldsymbol{\tau}^\alpha} \tag{2.30}$$

(H) *Frictional constraints.* With the preceding definitions for the relative slip velocity and frictional traction, the frictional constraints are introduced as follows:

i. Slip function. Admissible traction space. We define a *slip function* $\Phi : T_\nu S^2 \times \mathbb{R}_+ \times \mathbb{R}_+ \to \mathbb{R}$ such that the states $(t_T^\flat, t_N) \in T_\nu S^2 \times \mathbb{R}_+$ in the traction space and the internal variable $\alpha \in \mathbb{R}_+$ are constrained to lie in the closed set of admissible states defined as

$$\mathbb{E}_t := \{(t_T^\flat, t_N, \alpha) \in T_\nu S^2 \times \mathbb{R}_+ \times \mathbb{R}_+ \ :\ \Phi(t_T^\flat, t_N, \alpha) \le 0\} \tag{2.31}$$

Register for free at https//www.scipedia.com to download the version without the watermark

In particular, the classical friction Coulomb law can be extended to accomodate wear effects using a friction coefficient defined as a function of an internal variable α, such as the frictional dissipation or the slip amount. Then the admissible states space is defined by the slip function:

$$\Phi(\boldsymbol{t}_T^\flat, t_N, \alpha) := \|\boldsymbol{t}_T^\flat\| - \mu(\alpha) t_N \tag{2.32}$$

where $\|\cdot\|$ denotes the norm of its argument and $\mu(\alpha)$ is the Coulomb friction coefficient.

ii. Slip rule and internal evolution equation. The slip rule is defined as follows

$$\begin{aligned} \boldsymbol{v}_T^\flat(\boldsymbol{X},t) &:= 0 \qquad \text{if} \quad \Phi(\boldsymbol{t}_T^\flat, t_N, \alpha) < 0 \\ \boldsymbol{v}_T^\flat(\boldsymbol{X},t) &:= \gamma\ \boldsymbol{p}_T^\flat \qquad \text{if} \quad \Phi(\boldsymbol{t}_T^\flat, t_N, \alpha) = 0 \end{aligned} \tag{2.33}$$

where $\boldsymbol{p}_T^\flat := \partial_{t_T^\flat} \Phi(\boldsymbol{t}_T^\flat, t_N, \alpha)$ and $\gamma \in \mathbb{R}_+$ is the non-negative slip consistency factor. For the frictional Coulomb law $\boldsymbol{p}_T^\flat$ is the normalized one-form frictional traction defined as $\boldsymbol{p}_T^\flat := \boldsymbol{t}_T^\flat / \|\boldsymbol{t}_T^\flat\|$.

Additionally one needs to define an evolution equation for the internal variable α. As stated above, one may define α as the slip amount leading to the following evolution equation:

$$\begin{aligned} \dot{\alpha}(\boldsymbol{X},t) &:= 0 \qquad \text{if} \quad \Phi(\boldsymbol{t}_T^\flat, t_N, \alpha) < 0 \\ \dot{\alpha}(\boldsymbol{X},t) &:= \gamma \qquad \text{if} \quad \Phi(\boldsymbol{t}_T^\flat, t_N, \alpha) = 0 \end{aligned} \tag{2.34}$$

or, alternatively, one may define α as the frictional dissipation, leading to the following evolution equation:

$$\begin{aligned} \dot{\alpha}(\boldsymbol{X},t) &:= 0 && \text{if} \quad \Phi(\boldsymbol{t}_T^\flat, t_N, \alpha) < 0 \\ \dot{\alpha}(\boldsymbol{X},t) &:= \boldsymbol{t}_T^\flat \cdot \boldsymbol{v}_T^\flat = \gamma \, \|\boldsymbol{t}_T^\flat\| && \text{if} \quad \Phi(\boldsymbol{t}_T^\flat, t_N, \alpha) = 0 \end{aligned} \tag{2.35}$$

where the last expression in $(2.35)_2$ comes out using the slip rule (2.33).

These two alternative definitions can be easily accomodated in to a single expression in the form:

$$\begin{aligned} \dot{\alpha}(\boldsymbol{X},t) &:= 0 && \text{if} \quad \Phi(\boldsymbol{t}_T^\flat, t_N, \alpha) < 0 \\ \dot{\alpha}(\boldsymbol{X},t) &:= \gamma \, [(1-w) + w\|\boldsymbol{t}_T^\flat\|] && \text{if} \quad \Phi(\boldsymbol{t}_T^\flat, t_N, \alpha) = 0 \end{aligned} \tag{2.36}$$

where $w \in [0,1]$ is a constant such that, for $w = 0$ one recovers (2.34) and α is defined as the slip amount, for $w = 1$ one recovers (2.35) and α is defined as the frictional dissipation, and additionally for $w \in (0,1)$ α is defined as a linear combination of slip amount and frictional dissipation. In what follows, we will use this single expression for the evolution equation of α, allowing to easily recover both alternative definitions as a particular case.

iii. Slip consistency condition. The slip consistency condition states that the rate of change of the slip function must be zero for positive values of the slip consistency factor. Mathematically this condition is expressed as

$$\gamma \, \dot{\Phi}(\boldsymbol{t}_T^\flat, t_N, \alpha) = 0 \tag{2.37}$$

The above expressions lead to a constrained evolution problem defined by the evolution equations

$$\boxed{\begin{aligned} \boldsymbol{v}_T^\flat(\boldsymbol{X},t) &= \gamma \, \boldsymbol{p}_T^\flat \\ \dot{\alpha}(\boldsymbol{X},t) &= \gamma \, [(1-w) + w\|\boldsymbol{t}_T^\flat\|] \end{aligned}} \tag{2.38}$$

subjected to the constraints, expressed as Kuhn-Tucker complementarity conditions as,

$$\boxed{\begin{aligned} \Phi(\boldsymbol{t}_T^\flat, t_N, \alpha) &\leq 0 \\ \gamma &\geq 0 \\ \gamma \, \Phi(\boldsymbol{t}_T^\flat, t_N, \alpha) &= 0 \\ \gamma \, \dot{\Phi}(\boldsymbol{t}_T^\flat, t_N, \alpha) &= 0 \end{aligned}} \tag{2.39}$$

(I) *Regularization of frictional contact constraints* As discussed in Kikuchi & Oden (1988], for instance, solution of initial boundary value problems (IBVP) subject to constraints such as (2.12) and (2.39) amounts to finding a solution within a constrained solution space. Consideration of corresponding weak forms induces limitations on admissible variations in the tangent solution space, imposed by the physical constraints, leading to variational inequalities. See, for example, Kikuchi & Oden (1988) or Duvaut & Lions (1972).

Different methods have been used to bypass the need to find a solution within a constrained configuration solution space. Here we will use the *penalty* method to remove the restrictions associated to the constrained solution space and enforce the constraints through the introduction of constituve equations for the frictional contact traction.

SCIPEDIA
Register for free at https//www.scipedia.com to download the version without the watermark

The normal constraints induced by the contact problem are regularized in troducing a *normal p enalty* parameter ϵ_N and substituting the Kuhn-Tucker complementarity conditions defined in (2.12) with the follo wing constitutiv e-like equation for the contact pressure

$$\boxed{t_N(\boldsymbol{X},t) := \epsilon_N \langle g_N(\boldsymbol{X},t)\rangle} \tag{2.40}$$

where $\langle\cdot\rangle$ is the Macauley brac ket, representing the positive part of its operand. Expression (2.40) can be viewed as a Yosida regularization of the Kuhn-T ucker complementarity conditions given by (2.12), providing a constitutive-like equation for the contact pressure and leading to a convenient displacemen t-driven form ulation.

Comparison of (2.40) with (2.12) reveals that now a (hopefully small) violation of the constraints (2.12) is allowed, and that the constraints will be exactly satisfied as $\epsilon_N \to \infty$.

The regularization of the constrained frictional evolution problem defined by (2.38) and (2.39) is performed in troducing a *tangential penalty* parameter ϵ_T playing the role of constitutive parameter in the relativ e slip velocity evolution equation. Then the regularized constrained frictional evolution problem tak es the form:

$$\boxed{\begin{aligned} \boldsymbol{v}_T^\flat(\boldsymbol{X},t) &= \gamma\ \boldsymbol{p}_T^\flat + \frac{1}{\epsilon_T}\mathcal{L}_{v_T}\boldsymbol{t}_T^\flat \\ \dot{\alpha}(\boldsymbol{X},t) &= \gamma\ [(1-w) + w\|\boldsymbol{t}_T^\flat\|] \end{aligned}} \tag{2.41}$$

subjected to the following constrain ts

$$\boxed{\begin{aligned} \Phi(\boldsymbol{t}_T^\flat, t_N, \alpha) &\le 0 \\ \gamma &\ge 0 \\ \gamma\ \Phi(\boldsymbol{t}_T^\flat, t_N, \alpha) &= 0 \\ \gamma\ \dot{\Phi}(\boldsymbol{t}_T^\flat, t_N, \alpha) &= 0 \end{aligned}} \tag{2.42}$$

where $\mathcal{L}_{v_T}\boldsymbol{t}_T^\flat$ is the Lie derivative of the frictional tangent traction along the flow induced by the relative slip velocity $\boldsymbol{v}_T$, defined as

$$\mathcal{L}_{v_T}\boldsymbol{t}_T^\flat := \dot{t}_{T\alpha}\boldsymbol{\tau}^\alpha \tag{2.43}$$

Comparison of (2.41) and (2.42) with (2.38) and (2.39), reveals that the frictional constraints are exactly satisfied as $\epsilon_T \to \infty$, in which case the (plastic) slip rate γ is equal to the norm of the relative slip velocity $\boldsymbol{v}_T^\flat$. Otherwise, it is assumed that the relative slip velocity can be decomposed in to an elastic or recoverable part and a plastic or irreversible part. Introduction of the Lie derivative in the regularized relative slip velocity, main tains frame indifference of the frictional evolution equations.

Using the definition of the one-form relative slip velocity given by (2.28) and the Lie derivative of the frictional tangent traction along the flow induced by the relative slip velocity given by (2.43), the componen t form of the frictional tangen t traction evolution equation $(2.41)_1$, along with the in ternal variable evolution equation, takes the form

$$\begin{aligned} \dot{t}_{T\alpha} &= \epsilon_T\ (M_{\alpha\beta}\dot{\xi}^\beta - \gamma\ p_{T\alpha}) \\ \dot{\alpha} &= \gamma\ [(1-w) + w\|\boldsymbol{t}_T^\flat\|] \end{aligned} \tag{2.44}$$

As we have seen above, the regularization of the frictional constraint problem leads to the following frictional constrained evolution problem

$$\begin{aligned} \mathcal{L}_{v_T} \boldsymbol{t}_T^\flat &= \epsilon_T \ [\boldsymbol{v}_T^\flat - \gamma \ \partial_{t_T^\flat} \Phi(\boldsymbol{t}_T^\flat, t_N, \alpha)] \\ \dot{\alpha} &= \gamma \ [(1-w) + w \|\boldsymbol{t}_T^\flat\|] \\ \Phi(\boldsymbol{t}_T^\flat, t_N, \alpha) \leq 0, \quad \gamma \geq 0, \quad \gamma \ \Phi(\boldsymbol{t}_T^\flat, t_N, \alpha) &= 0 \\ \gamma \ \dot{\Phi}(\boldsymbol{t}_T^\flat, t_N, \alpha) &= 0 \end{aligned} \tag{2.45}$$

Within the context of the product formula algorithms, a *frictional operator split* of the constrained evolution problem can be introduced by means of a *trial state*, defined by freezing the irreversible (plastic) slip response, i.e. setting $\gamma = 0$, as follows

Trial state *Return mapping*

$$\left\{ \begin{array}{l} \mathcal{L}_{v_T} \boldsymbol{t}_T^\flat := \epsilon_T \ \boldsymbol{v}_T^\flat \\ \dot{\alpha} := 0 \\ \text{unconstrained} \end{array} \right\} \qquad \left\{ \begin{array}{l} \mathcal{L}_{v_T} \boldsymbol{t}_T^\flat := -\epsilon_T \ \gamma \ \partial_{t_T^\flat} \Phi(\boldsymbol{t}_T^\flat, t_N, \alpha) \\ \dot{\alpha} := \gamma \ [(1-w) + w \|\boldsymbol{t}_T^\flat\|] \\ \Phi(\boldsymbol{t}_T^\flat, t_N, \alpha) \leq 0, \ \gamma \geq 0, \ \gamma \ \Phi(\boldsymbol{t}_T^\flat, t_N, \alpha) = 0 \end{array} \right\} \tag{2.46}$$

REMARK 2.3. We point out that here only the regularization of the slip rule has been performed and (2.41) and (2.42) can be viewed as the governing equations of a *rate-independent* constrained frictional evolution problem. On the other hand, a Yosida regularization of the complementary Kuhn-Tucker frictional conditions (2.39), analogously to the regularization of the complementary Kuhn-Tucker contact normal conditions (2.12), would lead to a *rate-dependent* frictional evolution equations. □

2.3 Thermal Contact Model at the Contact Interface

A thermal contact model at the contact interface is considered, taking into account the phenomena of heat conduction flux through the contact surface and the heat source term due to frictional dissipation at the interface.

(A) *Heat conduction at the contact surface* The heat conduction flux through the contact surface $\Gamma^{(1)}$ can be expressed as

$$\boxed{Q_{hc} := Q_{hc}^{(1)}(\boldsymbol{X}, t) = \hat{h}(t_N, \theta_G) \ g_\theta(\boldsymbol{X}, t)} \tag{2.47}$$

where the heat transfer coefficient at the contact surface $\hat{h}(t_N, \theta_G)$ is assumed to be a function of the contact pressure t_N and the current mean gas temperature $\theta_G := \hat{\theta}_G(\Theta^{(1)}, \Theta^{(2)})$, and $g_\theta := \hat{g}_\theta(\Theta^{(1)}, \Theta^{(2)})$ is the thermal gap at the contact surface. The thermal gap and the current mean gas temperature at the contact interface are defined as

$$\boxed{\begin{aligned} g_\theta(\boldsymbol{X}, t) &:= \Theta^{(1)}(\boldsymbol{X}, t) - \Theta^{(2)}(\bar{\boldsymbol{Y}}(\boldsymbol{X}, t), t) \\ \theta_G(\boldsymbol{X}, t) &:= h_\epsilon \ \Theta^{(1)}(\boldsymbol{X}, t) + (1 - h_\epsilon) \ \Theta^{(2)}(\bar{\boldsymbol{Y}}(\boldsymbol{X}, t), t) \end{aligned}} \tag{2.48}$$

where h_ϵ is the relative effusivity (constant) coefficient of the surface $\Gamma^{(1)}$, i.e. the effusivity of the surface $\Gamma^{(1)}$ divided by the sum of the effusivities of the surfaces $\Gamma^{(1)}$ and $\Gamma^{(2)}$.

i. General contact pressure-temperature dependent heat conduction model. The resistance against heat transfer is mainly due to the low percentage of surface area which is really in contact. The presence of a reduced set of spots surrounded by microcavities characterizes the contact area. Hence heat transfer takes place by heat conduction through the spots and heat conduction through the gas contained in the microcavities. Other effects such radiation between microcavities surfaces can in general be omitted since both bodies are very close to each other. Making the usual assumption that both heat conduction mechanisms, through the spots and through the the gas contained in the microcavities, act in parallel, the heat transfer coefficient $\hat{h}(\theta_G, t_N)$ can be expressed as

$$\hat{h}(t_N, \theta_G) := \hat{h}_S(t_N) + \hat{h}_G(t_N, \theta_G) \tag{2.49}$$

where $\hat{h}_S(t_N)$ is the heat transfer coefficient through the spots, assumed to be a function of the contact pressure t_N, and $\hat{h}_G(t_N, \theta_G)$ is the heat transfer coefficient through the gas contained in the microcavities, assumed to be a function of the contact pressure and the current mean gas temperature.

Based on a statistical model and taking into account the dependence upon surface roughness parameters and Vickers microhardness coefficients, hardness variation with the mean planes approach, the following heat transfer through the spots was proposed by Song & Yovanovich (1987):

$$\hat{h}_S(t_N) := \frac{1.25\ \hat{k}\ \bar{m}}{\sigma}\Big[\frac{t_N}{c_1}(1.62\frac{10^6\ \sigma}{\bar{m}})^{-c_2}\Big]^{\frac{0.95}{1+0.71c_2}} \tag{2.50}$$

where $\hat{k}$ is the mean thermal conductivity, depending on the conductivities of the two bodies being in contact, σ is the surface roughness, $\bar{m}$ is the mean absolute asperity slope and c_1, c_2 describe the hardness variation.

The heat transfer through the gas or liquid contained in the microcavities is mainly governed by conduction. This fact rsults from the small height of the microcavities which do not allow convective flow. Based on this assumption and taking into account the change of microcavity height by the contact pressure t_N, Yovanovich (1981) derived the following expression for the heat conduction coefficient through the gas within the microcavities:

$$\hat{h}_G(t_N, \theta_G) := \frac{k_g}{1.36\ \sigma\sqrt{-\log(5.59\frac{t_N}{H_e})} + C_{PC}\theta_G} \tag{2.51}$$

where k_g is the gas conductivity, C_{PC} is a constitutive constant for the gas, H_e is the Vickers hardness and σ the surface roughness.

ii. Simplified contact pressure dependent heat conduction model. For high pressures, a simplified contact pressure dependent model can be derived from the above equations, in terms of the Vickers hardness H_e and introducing a contact resistance coefficient h_{co} and an exponent ϵ, leading to a heat transfer coefficient $\hat{h}(t_N)$ given by

$$\hat{h}(t_N) := h_{co}\Big[\frac{t_N}{H_e}\Big]^{\epsilon} \tag{2.52}$$

(B) *Heat source at the contact surface* The heat source term $R^{(1)}_{fric}$ for the contact surface $\Gamma^{(1)}$, due to frictional dissipation at the contact interface, is assumed to be given by

$$\boxed{R^{(1)}_{fric} := h_\epsilon \; \mathcal{D}_{fric}} \tag{2.53}$$

where h_ϵ is the relative effusivity of the surface $\Gamma^{(1)}$ and $\mathcal{D}_{fric} := \|\boldsymbol{t}^\flat_T\|\gamma$ is the frictional dissipation at the contact interface.

2.4 The Coupled Thermomechanical IBVP with Frictional Contact Constraints

We describe below the system of quasi-linear partial differential equations governing the evolution of the coupled thermomechanical initial boundary value problem, including frictional contact constraints. We will adopt general constitutive equations which incorporate current models of finite strain plasticity and, in particular, micromechanically motivated models based on a multiplicative decomposition of the deformation gradient, the tangent deformation map, and an additive split of the local entropy. Frictional contact constraints will be introduced using a penalized regularization technique, leading to a constitutive-like set of evolution equations within the framework of a displacement-driven formulation, and we will adopt a pressure-temperature dependent thermal contact model.

(A) *Local governing equations.* The local system of partial differential equations governing the coupled thermomechanical initial boundary value problem is defined by the momentum balance equation and the energy balance equation, restricted by the second law of the thermodynamics. This system must be supplemented by suitable constitutive equations. Additionaly, one must supply suitable prescribed boundary and initial conditions, and to consider the equilibrium equations at the contact interface.

i. Local form of momentum and energy balance (reduced dissipation) equations. The material form of the local governing equations for the initial boundary value problem, the local momentum and energy (reduced dissipation) balance equations for the body $\mathcal{B}^{(i)}$ can be written as

$$\left.\begin{aligned} \dot{\boldsymbol{\varphi}}^{(i)} &= \boldsymbol{V}^{(i)} \\ \rho^{(i)}_0 \dot{\boldsymbol{V}}^{(i)} &= \mathrm{DIV}[\boldsymbol{P}^{(i)}] + \boldsymbol{B}^{(i)} \\ \Theta^{(i)} \dot{H}^{(i)} &= -\mathrm{DIV}[\boldsymbol{Q}^{(i)}] + R^{(i)} + \mathcal{D}^{(i)}_{int} \end{aligned}\right\} \quad \text{in} \quad \bar{\Omega}^{(i)} \times \mathbb{I} \tag{2.54}$$

where $\boldsymbol{\varphi}^{(i)} : \bar{\Omega}^{(i)} \times \mathbb{I} \to \mathbb{R}^{n_{dim}}$ is the deformation map in the time interval of interest $\mathbb{I} := [0, T]$, $\boldsymbol{V}^{(i)} : \bar{\Omega}^{(i)} \times \mathbb{I} \to \mathbb{R}^{n_{dim}}$ is the velocity field, $\rho^{(i)}_0 : \bar{\Omega}^{(i)} \to \mathbb{R}_+$ is the reference density, $\boldsymbol{B}^{(i)} : \bar{\Omega}^{(i)} \times \mathbb{I} \to \mathbb{R}^{n_{dim}}$ the (prescribed) reference body forces, DIV[$\cdot$] the reference divergence operator and $\boldsymbol{P}^{(i)}$ the non-symmetric nominal or first Piola-Kirchhoff stress tensor, $\Theta^{(i)}$ the absolute temperature, $H^{(i)}$ the entropy, $\boldsymbol{Q}^{(i)}$ the nominal heat flux, $R^{(i)}$ the (prescribed) reference heat source and $\mathcal{D}^{(i)}_{int}$ the internal dissipation per unit reference volume. In addition, the entropy $H^{(i)}$ and the nominal stress tensor $\boldsymbol{P}^{(i)}$ are defined via constitutive relations, typically formulated in terms of the internal energy $E^{(i)}$, and subjected to the following restriction on the internal dissipation $\mathcal{D}^{(i)}_{int}$:

$$\mathcal{D}^{(i)}_{int} = \boldsymbol{P}^{(i)} : \dot{\boldsymbol{F}}^{(i)} + \Theta^{(i)} \dot{H}^{(i)} - \dot{E}^{(i)} \geq 0 \qquad \text{in} \quad \bar{\Omega}^{(i)} \times \mathbb{I} \tag{2.55}$$

where $\boldsymbol{F}^{(i)} := D\boldsymbol{\varphi}^{(i)}$ is the deformation gradient or tangent deformation map.

The nominal heat flux $\boldsymbol{Q}^{(i)}$ is defined via constitutive equations, say Fourier's law, subjected to the restriction on the dissipation by conduction $\mathcal{D}^{(i)}_{con}$:

$$\mathcal{D}^{(i)}_{con} = -\frac{1}{\Theta^{(i)}}\mathrm{GRAD}[\Theta^{(i)}]\cdot\boldsymbol{Q}^{(i)} \geq 0 \qquad \text{in} \quad \Omega^{(i)}\times\mathbb{I} \tag{2.56}$$

ii. Boundary conditions. We will assume that the deformation $\boldsymbol{\varphi}^{(i)}$ is prescribed on $\Gamma^{(i)}_{\varphi}\subset\partial\Omega^{(i)}$, the nominal traction $\boldsymbol{t}^{(i)}$ is prescribed on the part of the boundary $\Gamma^{(i)}_{\sigma}\subset\partial\Omega^{(i)}$, with unit outward normal field $\boldsymbol{N}^{(i)}:\Gamma^{(i)}_{\sigma}\to S^2$, the temperature $\Theta^{(i)}$ is prescribed on $\Gamma^{(i)}_{\Theta}\subset\partial\Omega^{(i)}$ and the outward normal heat flux is prescribed on the part of the boundary $\Gamma^{(i)}_{Q}\subset\partial\Omega^{(i)}$, with unit outward normal field $\boldsymbol{N}^{(i)}:\Gamma^{(i)}_{\sigma}\to S^2$, as

$$\left.\begin{aligned}
\boldsymbol{\varphi}^{(i)} &= \bar{\boldsymbol{\varphi}}^{(i)} && \text{on} && \Gamma^{(i)}_{\varphi}\times\mathbb{I}\\
\boldsymbol{t}^{(i)} &= \boldsymbol{P}^{(i)}\cdot\boldsymbol{N}^{(i)} = \bar{\boldsymbol{t}}^{(i)} && \text{on} && \Gamma^{(i)}_{\sigma}\times\mathbb{I}\\
\Theta^{(i)} &= \bar{\Theta}^{(i)} && \text{on} && \Gamma^{(i)}_{\Theta}\times\mathbb{I}\\
Q^{(i)} &= \boldsymbol{Q}^{(i)}\cdot\boldsymbol{N}^{(i)} = \bar{Q}^{(i)} && \text{on} && \Gamma^{(i)}_{Q}\times\mathbb{I}
\end{aligned}\right\} \tag{2.57}$$

where $\bar{\boldsymbol{\varphi}}^{(i)}:\Gamma^{(i)}_{\varphi}\times\mathbb{I}\to\mathbb{R}^{n_{dim}}$, $\bar{\boldsymbol{t}}^{(i)}:\Gamma^{(i)}_{\sigma}\times\mathbb{I}\to\mathbb{R}^{n_{dim}}$, $\bar{\Theta}^{(i)}:\Gamma^{(i)}_{\Theta}\times\mathbb{I}\to\mathbb{R}$ and $\bar{Q}^{(i)}:\Gamma^{(i)}_{Q}\times\mathbb{I}\to\mathbb{R}$ are prescribed deformation, nominal traction, temperature and (outward) normal heat flux maps. As usual it is assumed that the following conditions hold

$$\left.\begin{aligned}
\Gamma^{(i)}_{\varphi}\cup\Gamma^{(i)}_{\sigma}\cup\Gamma^{(i)} &= \partial\Omega^{(i)}\\
\Gamma^{(i)}_{\varphi}\cap\Gamma^{(i)}_{\sigma} = \Gamma^{(i)}_{\varphi}\cap\Gamma^{(i)} &= \Gamma^{(i)}_{\sigma}\cap\Gamma^{(i)} = \emptyset\\
\Gamma^{(i)}_{\Theta}\cup\Gamma^{(i)}_{Q}\cup\Gamma^{(i)} &= \partial\Omega^{(i)}\\
\Gamma^{(i)}_{\Theta}\cap\Gamma^{(i)}_{Q} = \Gamma^{(i)}_{\Theta}\cap\Gamma^{(i)} &= \Gamma^{(i)}_{Q}\cap\Gamma^{(i)} = \emptyset
\end{aligned}\right\} \tag{2.58}$$

iii. Initial conditions. Additionally, we will assume the following initial conditions

$$\left.\begin{aligned}
\boldsymbol{\varphi}^{(i)}(\cdot,t)|_{t=0} &= \bar{\boldsymbol{\varphi}}^{(i)}_0(\cdot)\\
\boldsymbol{V}^{(i)}(\cdot,t)|_{t=0} &= \bar{\boldsymbol{V}}^{(i)}_0(\cdot)\\
\Theta^{(i)}(\cdot,t)|_{t=0} &= \bar{\Theta}^{(i)}_0(\cdot)
\end{aligned}\right\} \qquad \text{in} \quad \bar{\Omega}^{(i)} \tag{2.59}$$

iv. Equilibrium conditions on the contact interface. For each material point $\boldsymbol{X}\in\Gamma^{(1)}$ at any time $t\in\mathbb{I}$, we require that the (differential) frictional contact force and normal heat conduction flux induced on body $\mathcal{B}^{(2)}$ at the material point $\bar{\boldsymbol{Y}}(\boldsymbol{X},t)$ be *equal* and *opposite* to that produced on body $\mathcal{B}^{(1)}$ at $\boldsymbol{X}$. Mathematically, these equilibrium conditions take the form

$$\begin{aligned}
\boldsymbol{t}^{(1)}(\boldsymbol{X},t)\ d\Gamma^{(1)} + \boldsymbol{t}^{(2)}(\bar{\boldsymbol{Y}}(\boldsymbol{X},t),t)\ d\Gamma^{(2)} &= 0\\
Q^{(1)}_{hc}(\boldsymbol{X},t)\ d\Gamma^{(1)} + Q^{(2)}_{hc}(\bar{\boldsymbol{Y}}(\boldsymbol{X},t),t)\ d\Gamma^{(2)} &= 0
\end{aligned} \tag{2.60}$$

where $Q^{(i)}_{hc} := Q^{(i)} + R^{(i)}_{fric}$ is the (outward) normal heat conduction flux at the contact interface $\Gamma^{(i)}$ and $R^{(i)}_{fric}$ is a heat source due to frictional dissipation at the contact interface

$\Gamma^{(i)}$. The heat sources due to frictional dissipation at the contact surfaces $\Gamma^{(1)}$ and $\Gamma^{(2)}$ are related to the frictional dissipation $\mathcal{D}_{fric} := \|\boldsymbol{t}_T^b\| \, \gamma$ through the relationship

$$\mathcal{D}_{fric}(\boldsymbol{X}, t) \; d\Gamma^{(1)} = R^{(1)}_{fric}(\boldsymbol{X}, t) \; d\Gamma^{(1)} + R^{(2)}_{fric}(\bar{\boldsymbol{Y}}(\boldsymbol{X}, t), t) \; d\Gamma^{(2)} \tag{2.61}$$

(B) *General thermoplastic constitutive equations.* We will consider a general thermoplastic constitutive framework defined in terms of the tangent deformation map $\boldsymbol{F}^{(i)} := D\boldsymbol{\varphi}^{(i)}$, a set of internal variables collectively denoted as $\boldsymbol{G}^{(i)}$, which characterizes the microstructural properties, and the local entropy $H^{(i)}$.

A generic expression for the internal energy $E^{(i)}$ will take the functional form

$$E^{(i)} := \hat{E}^{(i)}(\boldsymbol{F}^{(i)}, \boldsymbol{G}^{(i)}, H^{(i)}) \tag{2.62}$$

Following a standard argument, i.e., Coleman's method, the restriction placed by the second law of thermodynamics, the Clausius-Plank inequality $\mathcal{D}^{(i)}_{int} \geq 0$, yields the following constitutive equations for the nominal or first Piola-Kirchhoff stress tensor $\boldsymbol{P}^{(i)}$ and the absolute temperature $\Theta^{(i)}$, together with the reduced dissipation inequality:

$$\begin{aligned}
\boldsymbol{P}^{(i)} &:= \partial_{F^{(i)}} \hat{E}^{(i)}(\boldsymbol{F}^{(i)}, \boldsymbol{G}^{(i)}, H^{(i)}), \\
\Theta^{(i)} &:= \partial_{H^{(i)}} \hat{E}^{(i)}(\boldsymbol{F}^{(i)}, \boldsymbol{G}^{(i)}, H^{(i)}), \\
\boldsymbol{A}^{(i)} &:= -\partial_{G^{(i)}} \hat{E}^{(i)}(\boldsymbol{F}^{(i)}, \boldsymbol{G}^{(i)}, H^{(i)}), \\
\mathcal{D}^{(i)}_{int} &:= \boldsymbol{A}^{(i)} \cdot \dot{\boldsymbol{G}}^{(i)} \geq 0,
\end{aligned} \tag{2.63}$$

where we have introduced the variable $\boldsymbol{A}^{(i)}$ as the set of variables which are thermodinamically conjugate to the set of the internal variables $\boldsymbol{G}^{(i)}$.

The evolution equation for the set of internal variables $\boldsymbol{G}^{(i)}$ take the functional form

$$\dot{\boldsymbol{G}}^{(i)} = \hat{G}^{(i)}_{F^{(i)}}(\boldsymbol{P}^{(i)}, \boldsymbol{A}^{(i)}, \Theta^{(i)}) \tag{2.64}$$

where $\hat{G}^{(i)}_{F^{(i)}}$ is a prescribed function, possibly non-smooth, which depends implicitly on $\boldsymbol{F}^{(i)}$ in order to ensure frame invariance. Note that (2.64) is restricted by the reduced internal dissipation inequality given by $(2.63)_4$.

Additionally, we consider a generic constitutive equation for the heat flux $\boldsymbol{Q}^{(i)}$ taking the functional form

$$\boldsymbol{Q}^{(i)} = \hat{\boldsymbol{Q}}^{(i)}(\boldsymbol{F}^{(i)}, \boldsymbol{G}^{(i)}, H^{(i)}) \tag{2.65}$$

which is restricted by the conduction dissipation inequality $\mathcal{D}^{(i)}_{con} \geq 0$.

(B.1) *Thermoplastic constitutive equations for finite deformation multiplicative plasticity.* Micromechanically based phenomenological models of finite strain plasticity adopt a local multiplicative factorization of the deformation gradient into elastic and plastic parts. This local factorization was introduced within a phenomenological context by Lee & Liu (1967) and Lee (1969), which regard the plastic part as a microstructural internal variable. Hardening mechanisms in the material taking place at a microstructural level are characterized by an additional set of phenomenological internal variables collectively denoted here by ξ_α.

In the coupled thermomechanical theory, an additive split of the local entropy into elastic and plastic parts is adopted, where the plastic entropy is viewed as an additional internal variable arising as a result of dislocation and lattice defect motion. This additive split of the local entropy was adopted by Simo & Miehe (1992). Then the above considerations, motivates the following set of microstructural internal variables (for the sake of simplicity in the notation we will drop out the superindices $[]^{(i)}$, denoting a particular body $\mathcal{B}^{(i)}$, in all the variables, while they are not absolutely needed):

$$\boldsymbol{G} := \{\boldsymbol{F}^p, \xi_\alpha, H^p\} \tag{2.66}$$

with

$$\boldsymbol{F} := \boldsymbol{F}^e \boldsymbol{F}^p, \qquad \text{and} \qquad H := H^e + H^p \tag{2.67}$$

In the single crystal model, the internal energy function $\hat{E}$ depends on lattice distorsion, which is characterized by the elastic part $\boldsymbol{F}^e$ of the deformation gradient, on the configurational entropy H^e and on the hardening internal variables. Assuming here for simplicity that the thermoelastic and hardening contributions are uncoupled, we consider for the internal energy E the functional form

$$E := \hat{E}(\bar{\boldsymbol{C}}^e, H^e) + \hat{\mathcal{H}}(\xi_\alpha) \tag{2.68}$$

where $\bar{\boldsymbol{C}}^e := \boldsymbol{F}^{e\,T} \boldsymbol{F}^e$ is the elastic right Cauchy-Green deformation tensor, to be viewed as a second order covariant tensor at the (locally defined) intermediate configuration.

PROPOSITION 2.1. The material time derivative of the elastic right Cauchy-Green deformation tensor $\bar{\boldsymbol{C}}^e$ can be written as:

$$\frac{1}{2}\dot{\bar{\boldsymbol{C}}}^e := \bar{\boldsymbol{D}} - \bar{\boldsymbol{D}}^p \tag{2.69}$$

where

$$\begin{aligned} \bar{\boldsymbol{D}}^p &:= \mathrm{sym}[\bar{\boldsymbol{C}}^e \bar{\boldsymbol{L}}^p], \qquad \text{where} \qquad \bar{\boldsymbol{L}}^p := \dot{\boldsymbol{F}}^p \boldsymbol{F}^{p-1} \\ \bar{\boldsymbol{D}} &:= \mathrm{sym}[\bar{\boldsymbol{C}}^e \bar{\boldsymbol{L}}\,], \qquad \text{where} \qquad \bar{\boldsymbol{L}} := \boldsymbol{F}^{e-1} \boldsymbol{l} \boldsymbol{F}^e \quad \text{and} \quad \boldsymbol{l} := \dot{\boldsymbol{F}} \boldsymbol{F}^{-1} \end{aligned} \tag{2.70}$$

Here $\bar{\boldsymbol{D}}^p$ and $\bar{\boldsymbol{D}}$ are, respectively, the plastic and total deformation rate tensors. We regard these tensors as covariant tensors defined in the local intermediate configuration, as the symmetric part of the two-points (contravariant-covariant) plastic and total velocity gradient tensors at the intermediate configuration $\bar{\boldsymbol{L}}^p$ and $\bar{\boldsymbol{L}}$, respectively, where the elastic right Cauchy-Green tensor $\bar{\boldsymbol{C}}^e$ act as the metric tensor in the intermediate configuration. Consistently with these definitions, the (two-point) total velocity gradient tensor $\bar{\boldsymbol{L}}$ can be viewed as the pull-back to the local intermediate configuration of the (two-point) spatial velocity gradient tensor $\boldsymbol{l}$, with the elastic part of the deformation gradient tensor $\boldsymbol{F}^e$. □

PROPOSITION 2.2. Using the expressions derived above, the following relationship hold

$$\begin{aligned} \partial_{\bar{C}^e}\hat{E} : \dot{\bar{\boldsymbol{C}}}^e &:= 2\partial_{\bar{C}^e}\hat{E} : \bar{\boldsymbol{D}} - 2\partial_{\bar{C}^e}\hat{E} : \bar{\boldsymbol{D}}^p \\ &:= (\boldsymbol{F}^e\ 2\partial_{\bar{C}^e}\hat{E}\ \boldsymbol{F}^{p-T}) : \dot{\boldsymbol{F}} - (\boldsymbol{F}^{e\,T}\ \boldsymbol{F}^e\ 2\partial_{\bar{C}^e}\hat{E}\ \boldsymbol{F}^{p-T}) : \dot{\boldsymbol{F}}^p \end{aligned} \tag{2.71}$$

□

Using the expressions deriv ed above, the restriction placed by the second law through the Clausius-Plank inequalit y, yield the following constitutiv e equations and reduced in ternal dissipation

$$\begin{aligned} \bar{\boldsymbol{S}} &:= 2\partial_{\bar{C}^e}\hat{E}(\bar{\boldsymbol{C}}^e, H^e), \\ \Theta &:= \partial_{H^e}\hat{E}(\bar{\boldsymbol{C}}^e, H^e), \\ \beta^\alpha &:= -\partial_{\xi_\alpha}\hat{\mathcal{H}}(\xi_\alpha), \\ \mathcal{D}_{int} &:= \bar{\boldsymbol{S}} : \bar{\boldsymbol{D}}^p + \Theta\ \dot{H}^p + \beta^\alpha\ \dot{\xi}_\alpha \geq 0, \end{aligned} \tag{2.72}$$

where $\bar{\boldsymbol{S}}$ is the (contravariant) second Piola-Kirc hhoff stress tensor relative to the intermediate configuration.

Alternatively, we can get the following constitutiv e equations and reduced in ternal dissipation

$$\begin{aligned} \boldsymbol{P} &:= \boldsymbol{F}^e\ 2\partial_{\bar{C}^e}\hat{E}(\bar{\boldsymbol{C}}^e, H^e)\ \boldsymbol{F}^{p-T}, \\ \Theta &:= \partial_{H^e}\hat{E}(\bar{\boldsymbol{C}}^e, H^e), \\ \beta^\alpha &:= -\partial_{\xi_\alpha}\hat{\mathcal{H}}(\xi_\alpha), \\ \mathcal{D}_{int} &:= (\boldsymbol{F}^{eT}\boldsymbol{P}) : \dot{\boldsymbol{F}}^p + \Theta\ \dot{H}^p + \beta^\alpha\ \dot{\xi}_\alpha \geq 0, \end{aligned} \tag{2.73}$$

where the (t wo-points) nominal or first Piola-Kirchhoff stress tensor $\boldsymbol{P}$ can be expressed in terms of the (contravariant) second Piola-Kirc hhoff stress tensor at the in termediate configuration, through classical pull-bac k/push-forw ard operations, leading to the relationship $\boldsymbol{P} = \boldsymbol{F}^e\ \bar{\boldsymbol{S}}\ \boldsymbol{F}^{p-T}$. Furthermore the t wo-points stress tensor, betw een the intermediate and the reference configuration, defined as $\bar{\boldsymbol{P}} := \boldsymbol{F}^{eT}\boldsymbol{P}$ can be view ed as the conjugate tensor of the rate of the plastic deformation gradien t $\dot{\boldsymbol{F}}^p$. Note also that balance of angular momentum leading to the symmetry restriction on the second Piola-Kirchhoff stress tensor at the in termediate configuration $\bar{\boldsymbol{S}} = \bar{\boldsymbol{S}}^T$, implies the equiv alent restriction $\boldsymbol{F}^{e-1}\ \boldsymbol{P}\ \boldsymbol{F}^{pT} = \boldsymbol{F}^p\ \boldsymbol{P}^T\ \boldsymbol{F}^{e-1}$ on the nominal Piola-Kirchhoff stress tensor $\boldsymbol{P}$.

An equiv alent expression for the reduced in ternal dissipation tak es the form

$$\mathcal{D}_{int} := \bar{\boldsymbol{\Sigma}} : \bar{\boldsymbol{L}}^p + \Theta\ \dot{H}^p + \beta^\alpha\ \dot{\xi}_\alpha, \tag{2.74}$$

where $\bar{\boldsymbol{\Sigma}} := \bar{\boldsymbol{C}}^e\ \bar{\boldsymbol{S}}$ has been introduced as conjugate tensor of the plastic v elocity gradient at the intermediate configuration. Note, also that balance of angular momentum leads to the restriction $\bar{\boldsymbol{C}}^{e-1}\ \bar{\boldsymbol{\Sigma}} = \bar{\boldsymbol{\Sigma}}^T\ \bar{\boldsymbol{C}}^{e-T}$.

Here, $\boldsymbol{P}$ is the (two-point) nominal first Piola-Kirchhoff stress tensor, $\bar{\boldsymbol{S}}$ is the (contravariant) second Piola-Kirc hhoff stress tensor at the in termediate configuration and note again, that the elastic right Cauchy-Green tensor pla y the role of metric tensor at the in termediate configuration in the definition of the (t wo-point) stress tensor $\bar{\boldsymbol{\Sigma}}$ as stress conjugate of the (two-point) plastic velocity gradient tensor at the intermediate configuration $\bar{\boldsymbol{L}}^p$.

Within a coupled thermomechanical framew ork the reduced in ternal dissipation can be splitted into a mechanical and a thermal dissipation, according to

$$\mathcal{D}_{int} := \mathcal{D}_{mech} + \mathcal{D}_{ther} \tag{2.75}$$

where

$$\mathcal{D}_{mech} := \bar{\boldsymbol{S}} : \bar{\boldsymbol{D}}^p + \beta^\alpha\ \dot{\xi}_\alpha = \bar{\boldsymbol{\Sigma}} : \bar{\boldsymbol{L}}^p + \beta^\alpha\ \dot{\xi}_\alpha, \qquad \mathcal{D}_{ther} := \Theta\ \dot{H}^p. \tag{2.76}$$

Assuming a yield criterion of the form $\Phi = \hat{\Phi}(\bar{\boldsymbol{S}}, \Theta, \beta^\alpha)$, the evolution law of the internal variables take the form

$$\begin{aligned} \bar{\boldsymbol{D}}^p &:= \gamma\ \partial_{\bar{S}}\hat{\Phi}(\bar{\boldsymbol{S}}, \Theta, \beta^\alpha), \\ \dot{H}^p &:= \gamma\ \partial_{\Theta}\hat{\Phi}(\bar{\boldsymbol{S}}, \Theta, \beta^\alpha), \\ \dot{\xi}_\alpha &:= \gamma\ \partial_{\beta^\alpha}\hat{\Phi}(\bar{\boldsymbol{S}}, \Theta, \beta^\alpha). \end{aligned} \tag{2.77}$$

Alternatively, assuming a yield critrerion of the form $\Phi = \tilde{\Phi}(\bar{\boldsymbol{\Sigma}}, \Theta, \beta^\alpha)$, the evolution law of the internal variables take the form

$$\begin{aligned} \bar{\boldsymbol{L}}^p &:= \gamma\ \partial_{\bar{\Sigma}}\tilde{\Phi}(\bar{\boldsymbol{\Sigma}}, \Theta, \beta^\alpha), \\ \dot{H}^p &:= \gamma\ \partial_{\Theta}\tilde{\Phi}(\bar{\boldsymbol{\Sigma}}, \Theta, \beta^\alpha), \\ \dot{\xi}_\alpha &:= \gamma\ \partial_{\beta^\alpha}\tilde{\Phi}(\bar{\boldsymbol{\Sigma}}, \Theta, \beta^\alpha). \end{aligned} \tag{2.78}$$

REMARK 2.4. The representative thermoplastic model showed above has been defined by the internal energy $E = \hat{E}(\bar{\boldsymbol{C}}^e, H^e) + \mathcal{H}(\xi_\alpha)$ as a function of the elastic right Cauchy-Green tensor (at the intermediate configuration) and the elastic part of the entropy plus a hardening potential as a function of the internal hardening variables. Alternatively we can adopt the absolute temperature in place of the elastic entropy as an independent variable by introducing the free energy function $\Psi = \hat{\Psi}(\bar{\boldsymbol{C}}^e, \Theta) + \hat{\mathcal{H}}(\xi_\alpha)$ via the standard Legendre transformation $\hat{\Psi} = \hat{E} - \Theta H^e$.

In terms of the free energy , the internal dissipation takes the form

$$\mathcal{D}_{int} := \boldsymbol{P} : \dot{\boldsymbol{F}} + H^e\ \dot{\Theta} - \dot{\Psi} + \Theta\ \dot{H}^p \geq 0 \tag{2.79}$$

with $\mathcal{D}_{int} := \mathcal{D}_{mech} + \mathcal{D}_{ther}$, where

$$\mathcal{D}_{mech} := \boldsymbol{P} : \dot{\boldsymbol{F}} + H^e\ \dot{\Theta} - \dot{\Psi} \geq 0, \qquad \text{and} \qquad \mathcal{D}_{ther} := \Theta\ \dot{H}^p \tag{2.80}$$

Taking the time derivative of the free energy function and applying the chain rule, a straightforward argument yields the following constitutive equations and reduced dissipation inequality

$$\begin{aligned} \bar{\boldsymbol{S}} &:= 2\partial_{\bar{C}^e}\hat{\Psi}(\bar{\boldsymbol{C}}^e, \Theta), \\ H^e &:= -\partial_{\Theta}\hat{\Psi}(\bar{\boldsymbol{C}}^e, \Theta), \\ \beta^\alpha &:= -\partial_{\xi_\alpha}\hat{\mathcal{H}}(\xi_\alpha), \\ \mathcal{D}_{int} &:= \bar{\boldsymbol{S}} : \bar{\boldsymbol{D}}^p + \Theta\dot{H}^p + \beta^\alpha\ \dot{\xi}_\alpha \geq 0, \end{aligned} \tag{2.81}$$

Using the additive split of the total entropy into the elastic and plastic parts, the additive split of the internal dissipation into mechanical and thermal, and the constitutive equation obtained for the elastic part of the entropy, the reduced energy equation can be expressed in the alternative temperature-form as:

$$c_0\dot{\Theta} = -\mathrm{DIV}[\boldsymbol{Q}] + R - \mathcal{H}^{ep} + \mathcal{D}_{mech} \tag{2.82}$$

where $c_0 := -\Theta\partial^2_{\Theta\Theta}\hat{\Psi}(\bar{\boldsymbol{C}}^e, \Theta)$ is the reference heat capacity, $\mathcal{H}^{ep} := -\Theta\partial^2_{\Theta\bar{C}^e}\hat{\Psi}(\bar{\boldsymbol{C}}^e, \Theta) : \dot{\bar{\boldsymbol{C}}}^e$ is the elastoplastic structural heating and $\mathcal{D}_{mech} := \bar{\boldsymbol{S}} : \bar{\boldsymbol{D}}^p + \beta^\alpha\ \dot{\xi}_\alpha$ is the reduced (plastic) mechanical dissipation. □

2.5 Variational Formulation. Weak Form of the IBVP Including Frictional Contact Constraints

(A) *Configuration and admissible temperature spaces.* Let the configuration space and the admissible temperature space for the body $\mathcal{B}^{(i)}$ be defined by the inifinite dimensional configuration manifolds, denoted here respectiv ely as

$$\begin{aligned} \mathcal{C}^{(i)}_{mech} &:= \{\boldsymbol{\varphi}^{(i)} \in W^{1,p}(\Omega^{(i)})^{n_{dim}} : \ \det[D\boldsymbol{\varphi}^{(i)}] > 0 \text{ in } \Omega^{(i)} \quad \text{and} \quad \boldsymbol{\varphi}^{(i)}|_{\Gamma^{(i)}_{\varphi}} = \bar{\boldsymbol{\varphi}}^{(i)}\} \\ \mathcal{C}^{(i)}_{ther} &:= \{\Theta^{(i)} \in W^{1,q}(\Omega^{(i)})^{n_{dim}} : \ \Theta^{(i)} > 0 \text{ in } \Omega^{(i)} \quad \text{and} \quad \Theta^{(i)}|_{\Gamma^{(i)}_{\Theta}} = \bar{\Theta}^{(i)}\} \end{aligned} \tag{2.83}$$

where $W^{1,p}(\Omega^{(i)})$ is the Sobolev space of order $(1,p)$ for some p such that $2 \leq p < \infty$.

(B) *Admissible variations spaces.* Associated with the configuration and admissible temperature manifolds, we have the tangent (linear) spaces of (time independen t) material displacemen ts and temperature test functions, respectively, defined as

$$\begin{aligned} \mathcal{V}^{(i)}_0 &:= \{\boldsymbol{\eta}^{(i)}_0 : \bar{\Omega}^{(i)} \to \mathbb{R}^{n_{dim}} \mid \boldsymbol{\eta}^{(i)}_0|_{\Gamma^{(i)}_{\varphi}} = 0\} \\ \mathcal{T}^{(i)}_0 &:= \{\zeta^{(i)}_0 : \bar{\Omega}^{(i)} \to \mathbb{R}^{n_{dim}} \mid \zeta^{(i)}_0|_{\Gamma^{(i)}_{\Theta}} = 0\} \end{aligned} \tag{2.84}$$

(C) *W eak form of the IBVP.* Using standard procedures, the weak form of the momentum balance and reduced energy equations can be formally justified by taking the L_2–inner product of $(2.47)_{1,2}$ and $(2.47)_3$ with an y $\boldsymbol{\eta}^{(i)}_0 \in \mathcal{V}^{(i)}_0$ and any $\zeta^{(i)}_0 \in \mathcal{T}^{(i)}_0$, respectively, and making a straigh tforward use of the divergence theorem, leading to the follo wing expressions:

$$\begin{aligned} \langle \dot{\boldsymbol{\varphi}}^{(i)}, \boldsymbol{\eta}^{(i)}_0 \rangle &= \langle \boldsymbol{V}^{(i)}, \boldsymbol{\eta}^{(i)}_0 \rangle \\ \langle \rho^{(i)}_0 \dot{\boldsymbol{V}}^{(i)}, \boldsymbol{\eta}^{(i)}_0 \rangle + \langle \boldsymbol{P}^{(i)}, \text{GRAD}[\boldsymbol{\eta}^{(i)}_0] \rangle &= \langle \boldsymbol{B}^{(i)}, \boldsymbol{\eta}^{(i)}_0 \rangle + \langle \bar{\boldsymbol{t}}^{(i)}, \boldsymbol{\eta}^{(i)}_0 \rangle_{\Gamma^{(i)}_{\sigma}} + \langle \boldsymbol{t}^{(i)}, \boldsymbol{\eta}^{(i)}_0 \rangle_{\Gamma^{(i)}} \\ \langle \Theta^{(i)} \dot{H}^{(i)}, \zeta^{(i)}_0 \rangle - \langle \boldsymbol{Q}^{(i)}, \text{GRAD}[\zeta^{(i)}_0] \rangle &= \langle R^{(i)} + \mathcal{D}^{(i)}_{int}, \zeta^{(i)}_0 \rangle - \langle \bar{Q}^{(i)}, \zeta^{(i)}_0 \rangle_{\Gamma^{(i)}_Q} - \langle Q^{(i)}, \zeta^{(i)}_0 \rangle_{\Gamma^{(i)}} \end{aligned} \tag{2.85}$$

which m ust hold for an y (material) test function $\boldsymbol{\eta}^{(i)}_0 \in \mathcal{V}^{(i)}_0$ and $\zeta^{(i)}_0 \in \mathcal{T}^{(i)}_0$. Here $\langle \cdot, \cdot \rangle$ denotes the $L_2(\Omega^{(i)})$–inner product and with a sligh t abuse in notation $\langle \cdot, \cdot \rangle_{\Gamma^{(i)}_{\sigma}}$, $\langle \cdot, \cdot \rangle_{\Gamma^{(i)}_Q}$ and $\langle \cdot, \cdot \rangle_{\Gamma^{(i)}}$ denote the $L_2(\Gamma^{(i)}_{\sigma})$, $L_2(\Gamma^{(i)}_Q)$ and $L_2(\Gamma^{(i)})$–inner products on the boundaries $\Gamma^{(i)}_{\sigma}$, $\Gamma^{(i)}_Q$ and $\Gamma^{(i)}$, respectively.

Denoting b y $G^{(i)}_{dyn,mech}(\boldsymbol{V}^{(i)}, \boldsymbol{P}^{(i)}; \boldsymbol{\eta}^{(i)}_0)$ and $G^{(i)}_{stat,mech}(\boldsymbol{P}^{(i)}; \boldsymbol{\eta}^{(i)}_0)$ the dynamic and quasi-static w eak forms of the momentum balance equations, respectively, excluding frictional contact contributions, and by $G^{(i)}_{c,mech}(\boldsymbol{P}^{(i)}; \boldsymbol{\eta}^{(i)}_0)$ the frictional contact contribution to the w eak form of the momentum balance equations, respectiv ely defined as

$$\begin{aligned} G^{(i)}_{dyn,mech}(\boldsymbol{V}^{(i)}, \boldsymbol{P}^{(i)}; \boldsymbol{\eta}^{(i)}_0) &:= \langle \rho^{(i)}_0 \dot{\boldsymbol{V}}^{(i)}, \boldsymbol{\eta}^{(i)}_0 \rangle + G^{(i)}_{stat,mech}(\boldsymbol{P}^{(i)}; \boldsymbol{\eta}^{(i)}_0) \\ G^{(i)}_{stat,mech}(\boldsymbol{P}^{(i)}; \boldsymbol{\eta}^{(i)}_0) &:= \langle \boldsymbol{P}^{(i)}, \text{GRAD}[\boldsymbol{\eta}^{(i)}_0] \rangle - \langle \boldsymbol{B}^{(i)}, \boldsymbol{\eta}^{(i)}_0 \rangle - \langle \bar{\boldsymbol{t}}^{(i)}, \boldsymbol{\eta}^{(i)}_0 \rangle_{\Gamma^{(i)}_{\sigma}} \\ G^{(i)}_{c,mech}(\boldsymbol{P}^{(i)}; \boldsymbol{\eta}^{(i)}_0) &:= -\langle \boldsymbol{t}^{(i)}, \boldsymbol{\eta}^{(i)}_0 \rangle_{\Gamma^{(i)}} = -\langle \boldsymbol{P}^{(i)} \cdot \boldsymbol{N}^{(i)}, \boldsymbol{\eta}^{(i)}_0 \rangle_{\Gamma^{(i)}} \end{aligned} \tag{2.86a}$$

and denoting by $G^{(i)}_{dyn,ther}(\Theta^{(i)}, \boldsymbol{Q}^{(i)}; \zeta^{(i)}_0)$ and $G^{(i)}_{stat,ther}(\boldsymbol{Q}^{(i)}; \zeta^{(i)}_0)$ the dynamic (transien t) and quasi-static w eak forms of the energy balance equations, respectiv ely, excluding ther-

mal frictional con tact contributions, and by $G^{(i)}_{c,ther}(\boldsymbol{Q}^{(i)};\zeta_0^{(i)})$ the thermal frictional con tact contribution to the w eak form of the momentum balance equations, respectiv ely defined as

$$\begin{aligned} G^{(i)}_{dyn,ther}(\Theta^{(i)},H^{(i)},\boldsymbol{Q}^{(i)};\zeta_0^{(i)}) &:= \langle \Theta^{(i)}\dot{H}^{(i)},\zeta_0^{(i)}\rangle + G^{(i)}_{stat,ther}(\boldsymbol{Q}^{(i)};\zeta_0^{(i)}) \\ G^{(i)}_{stat,ther}(\boldsymbol{Q}^{(i)};\zeta_0^{(i)}) &:= -\langle \boldsymbol{Q}^{(i)},\mathrm{GRAD}[\zeta_0^{(i)}]\rangle - \langle R^{(i)}+\mathcal{D}^{(i)}_{int},\zeta_0^{(i)}\rangle + \langle \bar{Q}^{(i)},\zeta_0^{(i)}\rangle_{\Gamma^{(i)}_Q} \\ G^{(i)}_{c,ther}(\boldsymbol{Q}^{(i)};\zeta_0^{(i)}) &:= \langle Q^{(i)},\zeta_0^{(i)}\rangle_{\Gamma^{(i)}} = \langle \boldsymbol{Q}^{(i)}\cdot\boldsymbol{N}^{(i)},\zeta_0^{(i)}\rangle_{\Gamma^{(i)}} \end{aligned} \tag{2.86b}$$

the weak form of the momentum balance and energy equations for body $\mathcal{B}^{(i)}$ can be expressed in short hand notation as

$$\left.\begin{aligned} \langle \dot{\boldsymbol{\varphi}}^{(i)} - \boldsymbol{V}^{(i)},\boldsymbol{\eta}_0^{(i)}\rangle &= 0 \\ G^{(i)}_{dyn,mech}(\boldsymbol{V}^{(i)},\boldsymbol{P}^{(i)};\boldsymbol{\eta}_0^{(i)}) + G^{(i)}_{c,mech}(\boldsymbol{P}^{(i)};\boldsymbol{\eta}_0^{(i)}) &= 0 \\ G^{(i)}_{dyn,ther}(\Theta^{(i)},H^{(i)},\boldsymbol{Q}^{(i)};\zeta_0^{(i)}) + G^{(i)}_{c,ther}(\boldsymbol{Q}^{(i)};\zeta_0^{(i)}) &= 0 \end{aligned}\right\} \quad \forall\ \boldsymbol{\eta}_0^{(i)}\in\mathcal{V}_0^{(i)},\ \zeta_0^{(i)}\in\mathcal{T}_0^{(i)} \tag{2.87}$$

For the m ulti-body dynamics system, the momentum balance and energy equations tak e the form

$$\left.\begin{aligned} \sum_{i=1}^{n}\langle \dot{\boldsymbol{\varphi}}^{(i)} - \boldsymbol{V}^{(i)},\boldsymbol{\eta}_0^{(i)}\rangle &= 0 \\ \sum_{i=1}^{n} G^{(i)}_{dyn,mech}(\boldsymbol{V}^{(i)},\boldsymbol{P}^{(i)};\boldsymbol{\eta}_0^{(i)}) + \sum_{i=1}^{n} G^{(i)}_{c,mech}(\boldsymbol{P}^{(i)};\boldsymbol{\eta}_0^{(i)}) &= 0 \\ \sum_{i=1}^{n} G^{(i)}_{dyn,ther}(\Theta^{(i)},H^{(i)},\boldsymbol{Q}^{(i)};\zeta_0^{(i)}) + \sum_{i=1}^{n} G^{(i)}_{c,ther}(\boldsymbol{Q}^{(i)};\zeta_0^{(i)}) &= 0 \end{aligned}\right\} \quad \forall\ \boldsymbol{\eta}_0^{(i)}\in\mathcal{V}_0^{(i)},\ \zeta_0^{(i)}\in\mathcal{T}_0^{(i)} \tag{2.88}$$

In particular, for two intertacting bodies $\mathcal{B}^{(1)}$ and $\mathcal{B}^{(2)}$, the frictional contact mec hanical and thermal con tributions to the w eak form of the momentum and energy balance equations, at the material con tact points $\boldsymbol{X}\in\Gamma^{(1)}$ and $\bar{\boldsymbol{Y}}(\boldsymbol{X},t)\in\Gamma^{(2)}$, at any time $t\in\mathbb{I}$, take the form

$$\begin{aligned} \hat{G}^{(1,2)}_{c,mech}(\boldsymbol{P}^{(1)},\boldsymbol{P}^{(2)};\boldsymbol{\eta}_0^{(1)},\boldsymbol{\eta}_0^{(2)}) &:= G^{(1)}_{c,mech}(\boldsymbol{P}^{(1)};\boldsymbol{\eta}_0^{(1)}) + G^{(2)}_{c,mech}(\boldsymbol{P}^{(2)};\boldsymbol{\eta}_0^{(2)}) \\ \hat{G}^{(1,2)}_{c,ther}(\boldsymbol{Q}^{(1)},\boldsymbol{Q}^{(2)};\zeta_0^{(1)},\zeta_0^{(2)}) &:= G^{(1)}_{c,ther}(\boldsymbol{Q}^{(1)};\zeta_0^{(1)}) + G^{(2)}_{c,ther}(\boldsymbol{Q}^{(2)};\zeta_0^{(2)}) \end{aligned} \tag{2.89}$$

The weak form of the equilibrium conditions at the contact interface given by (2.60), can be expressed as

$$\begin{aligned} \langle \boldsymbol{t}^{(1)}(\boldsymbol{X},t),\boldsymbol{\eta}_0^{(2)}\rangle_{\Gamma^{(1)}} + \langle \boldsymbol{t}^{(2)}(\bar{\boldsymbol{Y}}(\boldsymbol{X},t),t),\boldsymbol{\eta}_0^{(2)}\rangle_{\Gamma^{(2)}} &= 0 \\ \langle Q^{(1)}_{hc}(\boldsymbol{X},t),\zeta_0^{(2)}\rangle_{\Gamma^{(1)}} + \langle Q^{(2)}_{hc}(\bar{\boldsymbol{Y}}(\boldsymbol{X},t),t),\zeta_0^{(2)}\rangle_{\Gamma^{(2)}} &= 0 \end{aligned} \tag{2.90}$$

and the w eak form of (2.61) tak es the form

$$\langle \mathcal{D}_{fric}(\boldsymbol{X},t),\zeta_0^{(2)}\rangle_{\Gamma^{(1)}} = \langle R^{(1)}_{fric}(\boldsymbol{X},t),\zeta_0^{(2)}\rangle_{\Gamma^{(1)}} + \langle R^{(2)}_{fric}(\bar{\boldsymbol{Y}}(\boldsymbol{X},t),t),\zeta_0^{(2)}\rangle_{\Gamma^{(2)}} \tag{2.91}$$

Using (2.86) and (2.89)-(2.91) the mechanical and thermal frictional con tact contributions to the w eak form of the momentum and energy balance equations, at the material contact

points $\boldsymbol{X} \in \Gamma^{(1)}$ and $\bar{\boldsymbol{Y}}(\boldsymbol{X},t) \in \Gamma^{(2)}$, at any time $t \in \mathbb{I}$, take the simple form

$$\boxed{\begin{array}{l} G^{(1,2)}_{c,mech}(\boldsymbol{P}^{(1)};\boldsymbol{\eta}^{(1)}_0,\boldsymbol{\eta}^{(2)}_0) := -\langle \boldsymbol{t}^{(1)}, \boldsymbol{\eta}^{(1)}_0 - \boldsymbol{\eta}^{(2)}_0 \rangle_{\Gamma^{(1)}} \\ G^{(1,2)}_{c,ther}(\boldsymbol{Q}^{(1)};\zeta^{(1)}_0,\zeta^{(2)}_0) := \langle Q^{(1)}_{hc} - R^{(1)}_{fric}, \zeta^{(1)}_0 - \zeta^{(2)}_0 \rangle_{\Gamma^{(1)}} - \langle \mathcal{D}_{fric}, \zeta^{(2)}_0 \rangle_{\Gamma^{(1)}} \end{array}} \tag{2.92}$$

where the relation $\boldsymbol{t}^{(1)} := \boldsymbol{P}^{(1)} \cdot \boldsymbol{N}^{(1)}$, and the arguments in $\boldsymbol{t}^{(1)}(\boldsymbol{X},t)$, $\boldsymbol{\eta}^{(1)}_0(\boldsymbol{X})$ and $\boldsymbol{\eta}^{(2)}_0(\bar{\boldsymbol{Y}}(\boldsymbol{X},t))$ have been implicitly considered.

2.6 Linearization of the Frictional Contact and Thermal Kinematics

(A) *Directional derivative.* Given the configurations $\boldsymbol{\varphi}^{(i)}$ and the admissible variations $\boldsymbol{\eta}^{(i)}_0$, for the bodies $\mathcal{B}^{(i)}$, $i = 1,2$, we define the perturbed configurations $\boldsymbol{\varphi}^{(i)}_\epsilon$ as

$$\boldsymbol{\varphi}^{(i)}_\epsilon := \boldsymbol{\varphi}^{(i)} + \epsilon\ \boldsymbol{\eta}^{(i)}_0 \tag{2.93}$$

where the ϵ is a scalar perturbation parameter (not to be confused with the penalty parameters ϵ_N and ϵ_T).

Then, for an arbitrary field $A(\boldsymbol{X},\boldsymbol{\varphi}^{(1)},\boldsymbol{\varphi}^{(2)})$ given for any $\boldsymbol{X} \in \Gamma^{(1)}$, the linearized variation $\delta A(\boldsymbol{X},\boldsymbol{\varphi}^{(1)},\boldsymbol{\varphi}^{(2)})$ is defined through the use of the directional derivative, as

$$\delta A(\boldsymbol{X},\boldsymbol{\varphi}^{(1)},\boldsymbol{\varphi}^{(2)}) := \left.\frac{d}{d\epsilon}\right|_{\epsilon=0} A(\boldsymbol{X},\boldsymbol{\varphi}^{(1)}_\epsilon,\boldsymbol{\varphi}^{(2)}_\epsilon) \tag{2.94}$$

(B) *Linearized variation of the gap function g_N.* Using the definition of the gap function $g_N(\boldsymbol{X},t)$ given by (2.3) and exploiting the definition of directional derivative (2.94), the linearized variation of the gap function $g_N(\boldsymbol{X},t)$ takes the form

$$\begin{aligned} \delta g_N = &- [\boldsymbol{\eta}^{(1)}_0(\boldsymbol{X}) - \boldsymbol{\eta}^{(2)}_0(\bar{\boldsymbol{Y}}(\boldsymbol{X},t)) - \boldsymbol{\tau}_\alpha(\bar{\boldsymbol{Y}}(\boldsymbol{X},t),t)\ \delta\bar{\xi}^\alpha(\boldsymbol{X},t)] \cdot \boldsymbol{\nu} \\ &- [\boldsymbol{\varphi}^{(1)}(\boldsymbol{X},t) - \boldsymbol{\varphi}^{(2)}(\bar{\boldsymbol{Y}}(\boldsymbol{X},t),t)] \cdot \delta\boldsymbol{\nu} \end{aligned} \tag{2.95}$$

Using the relation $\boldsymbol{\tau}_\alpha \in T_\nu S^2$ along with (2.3) and the constrain $\delta\boldsymbol{\nu} \in T_\nu S^2$ the directional derivative (2.95) can be written as

$$\boxed{\delta g_N = -[\boldsymbol{\eta}^{(1)}_0(\boldsymbol{X}) - \boldsymbol{\eta}^{(2)}_0(\bar{\boldsymbol{Y}}(\boldsymbol{X},t))] \cdot \boldsymbol{\nu}} \tag{2.96}$$

(C) *Linearized variation of the contact parent coordinate $\bar{\boldsymbol{\xi}}(\boldsymbol{X},t)$.* The linearized variation of the contact parent coordinate $\bar{\boldsymbol{\xi}}(\boldsymbol{X},t)$ can be obtained in the following way. Using the definition of closest-point projection, the following normality condition holds for $\alpha = 1,2$,

$$[\boldsymbol{\varphi}^{(1)}(\boldsymbol{X},t) - \boldsymbol{\varphi}^{(2)}(\bar{\boldsymbol{Y}}(\boldsymbol{X},t),t)] \cdot \boldsymbol{\tau}_\alpha = 0 \tag{2.97}$$

The directional derivative of (2.97) leads to the following key expression

$$A_{\alpha\beta}\delta\bar{\xi}^\beta = [\boldsymbol{\eta}^{(1)}_0(\boldsymbol{X}) - \boldsymbol{\eta}^{(2)}_0(\bar{\boldsymbol{Y}}(\boldsymbol{X},t))] \cdot \boldsymbol{\tau}_\alpha - g_N(\boldsymbol{X},t)\ \boldsymbol{\nu} \cdot \boldsymbol{\eta}^{(2)}_{0,\alpha}(\bar{\boldsymbol{Y}}(\boldsymbol{X},t)) \tag{2.98}$$

where

$$A_{\alpha\beta} = m_{\alpha\beta} + g_N \ \kappa_{\alpha\beta} \tag{2.99}$$

Determination of $\delta\bar{\xi}^{\alpha}$ thus, will requires in version of a two by two symmetric matrix $\boldsymbol{A} = [A_{\alpha\beta}]$, with components $A_{\alpha\beta}$ defined by (2.99). Denoting by $A^{\alpha\beta}$ the componen ts of the inverse matrix $\boldsymbol{A}^{-1} = [A^{\alpha\beta}]$ the linearized variation $\delta\bar{\xi}^{\alpha}$ takes the form

$$\boxed{\delta\bar{\xi}^{\alpha} = A^{\alpha\beta}\{[\boldsymbol{\eta}_0^{(1)}(\boldsymbol{X}) - \boldsymbol{\eta}_0^{(2)}(\bar{\boldsymbol{Y}}(\boldsymbol{X},t))]\cdot\boldsymbol{\tau}_{\beta} - g_N(\boldsymbol{X},t)\ \boldsymbol{\nu}\cdot\boldsymbol{\eta}_{0,\beta}^{(2)}(\bar{\boldsymbol{Y}}(\boldsymbol{X},t))\}} \tag{2.100}$$

When $g_N = 0$ then $A_{\alpha\beta} = m_{\alpha\beta}$, $A^{\alpha\beta} = m^{\alpha\beta}$ and (2.100) simplifies to

$$\boxed{\delta\bar{\xi}^{\alpha}|_{g_N=0} = [\boldsymbol{\eta}_0^{(1)}(\boldsymbol{X}) - \boldsymbol{\eta}_0^{(2)}(\bar{\boldsymbol{Y}}(\boldsymbol{X},t))]\cdot\boldsymbol{\tau}^{\alpha}} \tag{2.101}$$

(D) *Linearized variation of* δg_N. Following a standard use of the directional deriv ative and after a reasonable amoun t of algebra, the linearization of δg_N given by (2.96), leads to

$$\boxed{\begin{aligned}\Delta(\delta g_N) = {} & g_N\ (\boldsymbol{\nu}\cdot\boldsymbol{\eta}_{0,\alpha}^{(2)} + \kappa_{\alpha\gamma}\ \delta\bar{\xi}^{\gamma})\ m^{\alpha\beta}(\boldsymbol{\nu}\cdot\Delta\boldsymbol{\varphi}_{,\beta}^{(2)} + \kappa_{\beta\delta}\Delta\bar{\xi}^{\delta}) \\ & + \boldsymbol{\nu}\cdot(\delta\bar{\xi}^{\alpha}\Delta\boldsymbol{\varphi}_{,\alpha}^{(2)} + \Delta\bar{\xi}^{\alpha}\boldsymbol{\eta}_{0,\alpha}^{(2)}) + \kappa_{\alpha\beta}\ \delta\bar{\xi}^{\alpha}\Delta\bar{\xi}^{\beta}\end{aligned}} \tag{2.102}$$

(E) *Linearized variation of* $\delta\bar{\xi}^{\alpha}$. The linearized variation of $\delta\bar{\xi}^{\alpha}$ m ust be computed implicitly, by computing the directional deriv ative of (2.100). Since the calculation is quite lengthy we merely state the result, which is:

$$\boxed{\begin{aligned}A_{\alpha\beta}\Delta(\delta\bar{\xi}^{\beta}) = {} & -(\boldsymbol{\tau}_{\alpha}\cdot\boldsymbol{\eta}_{0,\beta}^{(2)} + g_N\ \boldsymbol{\nu}\cdot\boldsymbol{\eta}_{0,\alpha\beta}^{(2)})\ \Delta\bar{\xi}^{\beta} \\ & - (\boldsymbol{\tau}_{\alpha}\cdot\Delta\boldsymbol{\varphi}_{,\beta}^{(2)} + g_N\ \boldsymbol{\nu}\cdot\Delta\boldsymbol{\varphi}_{,\alpha\beta}^{(2)})\ \delta\bar{\xi}^{\beta} \\ & + (\boldsymbol{\eta}_0^{(1)} - \boldsymbol{\eta}_0^{(2)} - \delta\bar{\xi}^{\gamma}\boldsymbol{\tau}_{\gamma})\cdot(\Delta\boldsymbol{\varphi}_{,\alpha}^{(2)} + \boldsymbol{e}_{\alpha,\beta}(\bar{\boldsymbol{\xi}})\ \Delta\bar{\xi}^{\beta}) \\ & + (\Delta\boldsymbol{\varphi}^{(1)} - \Delta\boldsymbol{\varphi}^{(2)} - \Delta\bar{\xi}^{\gamma}\boldsymbol{\tau}_{\gamma})\cdot(\boldsymbol{\eta}_{0,\alpha}^{(2)} + \boldsymbol{e}_{\alpha,\beta}(\bar{\boldsymbol{\xi}})\ \delta\bar{\xi}^{\beta}) \\ & - [\boldsymbol{\tau}_{\alpha}\cdot\boldsymbol{e}_{\beta,\gamma}(\bar{\boldsymbol{\xi}}) + g_N\boldsymbol{\nu}\cdot\boldsymbol{e}_{\alpha,\beta\gamma}(\bar{\boldsymbol{\xi}})]\delta\bar{\xi}^{\beta}\Delta\bar{\xi}^{\gamma}\end{aligned}} \tag{2.103}$$

P articularizing (2.103) for $g_N = 0$, after some algebraic manipulation and using (2.23) and (2.96), the linearized variation of $\delta\bar{\xi}^{\alpha}$ at $g_N = 0$, takes the form:

$$\boxed{\begin{aligned}m_{\alpha\beta}\Delta(\delta\bar{\xi}^{\beta}) = {} & -(\boldsymbol{\tau}_{\alpha}\cdot\boldsymbol{\eta}_{0,\beta}^{(2)}\ \Delta\bar{\xi}^{\beta}|_{g_N=0} + \boldsymbol{\tau}_{\alpha}\cdot\Delta\boldsymbol{\varphi}_{,\beta}^{(2)}\ \delta\bar{\xi}^{\beta}|_{g_N=0} \\ & - \delta g_N(\Delta\boldsymbol{\varphi}_{,\alpha}^{(2)}\cdot\boldsymbol{\nu} + \kappa_{\alpha\beta}\Delta\bar{\xi}^{\beta}|_{g_N=0}) \\ & - \Delta g_N(\boldsymbol{\eta}_{0,\alpha}^{(2)}\cdot\boldsymbol{\nu} + \kappa_{\alpha\beta}\delta\bar{\xi}^{\beta}|_{g_N=0}) \\ & - \boldsymbol{\tau}_{\alpha}\cdot\boldsymbol{e}_{\beta,\gamma}(\bar{\boldsymbol{\xi}})\ \delta\bar{\xi}^{\beta}|_{g_N=0}\Delta\bar{\xi}^{\gamma}|_{g_N=0}\end{aligned}} \tag{2.104}$$

(F) *Linearized variation of the thermal gap* g_{θ}. Using the definition of the thermal gap g_{θ} given by $(2.48)_1$, its linearized variation at *a fixed configuration* is trivial and takes the simple form:

$$\boxed{\delta g_{\theta} = \zeta_0^{(1)}(\boldsymbol{X}) - \zeta_0^{(2)}(\bar{\boldsymbol{Y}}(\boldsymbol{X},t))} \tag{2.105}$$

(G) *Linearized variation of the mean gas temperature* θ_G. Using the definition of the mean gas temperature at the microcavities θ_G given by $(2.48)_2$, its linearized variation *at a fixed configuration* is defined as:

$$\boxed{\delta\theta_G = h_\epsilon\ \zeta_0^{(1)}(\boldsymbol{X}) + (1-h_\epsilon)\ \zeta_0^{(2)}(\bar{\boldsymbol{Y}}(\boldsymbol{X},t))} \tag{2.106}$$

2.7 Frictional Contact Mechanical and Thermal Contributions to the Weak Form

Starting with the expression for the frictional contact mechanical and thermal contributions given by (2.89), using the split of the frictional contact traction (2.8) and (2.30), the linearized variations (2.96) and (2.100), and the thermal expressions (2.105) and (2.106), the frictional contact mechanical and thermal contributions to the weak form can be conveniently expressed as

$$\boxed{\begin{aligned} G_c^{mech}(\boldsymbol{\varphi},\boldsymbol{\eta}_0) &:= \langle t_N, \delta g_N\rangle_{\Gamma^{(1)}} + \langle t_{T\alpha}, \delta\bar{\xi}^\alpha\rangle_{\Gamma^{(1)}} \\ G_c^{ther}(\Theta,\zeta_0) &:= \langle Q_{hc}, \delta g_\theta\rangle_{\Gamma^{(1)}} - \langle \mathcal{D}_{fric}, \delta\theta_G\rangle_{\Gamma^{(1)}} \end{aligned}} \tag{2.107}$$

where a short hand notation has been introduced, denoting as $\boldsymbol{\varphi} \in \mathcal{C}_{mech}$ and $\boldsymbol{\eta}_0 \in \mathcal{V}_0$ the collection of mappings $\boldsymbol{\varphi}^{(i)} \in \mathcal{C}_{mech}^{(i)}$ and $\boldsymbol{\eta}_0^{(i)} \in \mathcal{V}_0^{(i)}$, $i=1,2$, and $\Theta \in \mathcal{C}_{ther}$ and $\zeta_0 \in \mathcal{T}_0$ the collection of mappings $\Theta^{(i)} \in \mathcal{C}_{ther}^{(i)}$ and $\zeta_0^{(i)} \in \mathcal{T}_0^{(i)}$, $i=1,2$, such that the restriction of each of the maps $\boldsymbol{\varphi}$, $\boldsymbol{\eta}_0$, Θ and ζ_0 to the domain $\bar{\Omega}^{(i)}$ gives identically $\boldsymbol{\varphi}^{(i)}$, $\boldsymbol{\eta}_0^{(i)}$, $\Theta^{(i)}$ and $\zeta_0^{(i)}$ respectively.

3. THE DISCRETE INITIAL BOUNDARY VALUE PROBLEM INCLUDING FRICTIONAL CONTACT CONSTRAINTS

The numerical solution of the IBVP including frictional contact constraints at finite strains involves the transformation of an infinite dimensional dynamical system, governed by a system of quasi-linear partial differential equations into a sequence of discrete nonlinear algebraic problems by means of the following two steps:

Step **1.** The infinite dimensional space $Z = \mathcal{C}_{mech} \times \mathcal{V}_0 \times \mathcal{C}_{ther} \times \mathcal{T}_0$ is approximated by a finite dimensional space $Z^h \subset Z$ via a Galerkin finite element projection. The projection in space of the dynamic weak form of the momentum equations and the reduced energy equations leads to a nonlinear coupled system of ordinary differential equations (ODE's) which describe the time evolution of nodal degrees of freedom in the time interval of interest I.

Step **2.** The coupled system of nonlinear ordinary differential equations describes the time evolution in the time interval $\mathbb{I}$ of interest, of the nodal degrees of freedom and the internal variables associated with the finite element Galerkin projection. A time discretization of this problem involves a partition $\mathbb{I} = \cup_{n=0}^{N}[t_n, t_{n+1}]$ of the time interval $\mathbb{I}$. Within a typical time subinterval $[t_n, t_{n+1}]$, a time marching scheme for the advancement of the configuration, velocity and temperature fields in Z^h together with a return mapping algorithm for the advancement of the internal variables results in a nonlinear algebraic problem which is solved iteratively. The use of an *operator split*, applied to the coupled system of nonlinear ordinary differential equations, and a *product formula algorithm*, leads to a *staggered algorithm* in which each one of the subproblems defined by the partition is solved sequentially, within the framework of a *fractional step method*

3.1 Time Integration of the Coupled Problem: Fractional Step Methods

(A) *Abstract evolution problem.* Given a partition $\mathbb{I} = \cup_{n=0}^{N} [t_n, t_{n+1}]$ of the time interval of interest $\mathbb{I}$, algorithms for the time integration of the coupled initial boundary problem of dynamic thermoplasticity are typically designed by rewriting this system as an abstract first order evolution problem for the primary variables.

Let us consider the following abstract first order evolution problem:

$$\begin{aligned} \frac{d}{dt} z(\cdot, t) &= \boldsymbol{A}[z(\cdot, t)] + \boldsymbol{f}(\cdot) \qquad \text{in } \Omega \times \mathbb{I}, \\ z(\cdot, t_0) &= z_0(\cdot) \qquad \text{in } \Omega, \end{aligned} \tag{3.1}$$

where $z(\cdot, t) \in \mathcal{Z}$ lies in a suitable function space $\mathcal{Z}$, typically a Banach space of the Sobolev class, $\boldsymbol{A}[\cdot]$ is a nonlinear elliptic operator, $\boldsymbol{f}$ is a prescribed forcing term and $z_0 \in \mathcal{Z}$ is some specified initial data. Under suitable technical assumptions the homogeneous version of the abstract evolution problem defines a local semi-flow, denoted by

$$\mathcal{F}_t : \mathcal{Z} \times [t_n, t_{n+1}] \to \mathcal{Z}, \tag{3.2}$$

which advances the initial data $z(\cdot, t_0) \in \mathcal{Z}$ to the solution of the abstract evolution problem at time t according to $z(\cdot, t) = \mathcal{F}_t[z(\cdot, t_0)]$ and satisfies $\mathcal{F}_{t+s} = \mathcal{F}_t \circ \mathcal{F}_s$ for $t \geq s$. In what follows, we shall assume that the technical conditions which ensure the existence (at least locally in time) of the flow hold.

Let $\mathcal{K}_{\Delta t} : \mathcal{Z} \times \mathbb{R} \to \mathcal{Z}$ be a one-parameter family of maps, referred to as the *algorithm* in what follows, which depends continuously on the parameter $\Delta t \geq 0$ herein referred to as the *time-step*. We shall assume that the algorithm is *consistent* with the semi-flow, and hence the following two conditions hold

$$\lim_{\Delta t \to 0} \mathcal{K}_{\Delta t}[z] = z \qquad \text{and} \qquad \lim_{\Delta t \to 0} \frac{1}{\Delta t} [\mathcal{K}_{\Delta t}[z] - z] = \boldsymbol{A}[z]. \tag{3.3}$$

Now the key idea is to introduce an additive *operator split* $\boldsymbol{A}[\cdot] = \boldsymbol{A}^1[\cdot] + \boldsymbol{A}^2[\cdot]$, where $\boldsymbol{A}^1[\cdot]$ and $\boldsymbol{A}^2[\cdot]$ are two operators defining the following two (hopefully simpler) sub-problems

$$\begin{aligned} &\textit{Problem 1} && \textit{Problem 2} \\ &\frac{d}{dt} z(\cdot, t) = \boldsymbol{A}^1[z(\cdot, t)] + \boldsymbol{f}^1(\cdot) && \frac{d}{dt} z(\cdot, t) = \boldsymbol{A}^2[z(\cdot, t)] + \boldsymbol{f}^2(\cdot) \end{aligned} \tag{3.4}$$

where, additionally, a split of the prescribed forcing terms $\boldsymbol{f} = \boldsymbol{f}^1 + \boldsymbol{f}^2$ has been considered.

Now consider algorithms $\mathcal{K}^1_{\Delta t}[\cdot]$ and $\mathcal{K}^2_{\Delta t}[\cdot]$, consistent with the flows $\mathcal{F}^1$ and $\mathcal{F}^2$, respectively. Then the algorithm $\mathcal{K}_{\Delta t}[\cdot]$ is defined by the *product formula*

$$\mathcal{K}_{\Delta t}[\cdot] = \left(\mathcal{K}^2_{\Delta t} \circ \mathcal{K}^1_{\Delta t} \right)[\cdot], \qquad \text{in} \qquad \mathcal{Z} \times [t_n, t_{n+1}]. \tag{3.5}$$

Furthermore, in order that the product formula algorithm defined by (3.5), preserves crucial properties of the flow, i.e. dissipative stability, each one of the algorithms arising from the operator split must be designed to preserve those properties. Particularly in the context of coupled thermoplastic problems, it was first show by Armero & Simo (1992a,1992b,1993) than the classical isothermal operator split does not preserve the a-priori dissipative stability estimate of the continuum problem, while their new proposed isentropic operator split preserves this crucial property, leading to an unconditionally stable product formula staggered algorithm.

(B) *Product formula algorithms for coupled thermomechanical problems. Isentropic split.* The governing equations of the coupled thermomechanical evolution problem can be expressed as an abstract first order system of ordinary differential equations given by (3.1), in which the primary variables, operator and prescribed forcing terms are given by

$$z = \left\{ \begin{array}{c} \varphi \\ \boldsymbol{V} \\ H \end{array} \right\}, \qquad \boldsymbol{A}[z] = \left\{ \begin{array}{c} \boldsymbol{V} \\ \frac{1}{\rho_0} \, \mathrm{DIV}[\boldsymbol{P}] \\ -\frac{1}{\Theta} \, \mathrm{DIV}[\boldsymbol{Q}] + \frac{1}{\Theta} \, \mathcal{D}_{int} \end{array} \right\}, \qquad \boldsymbol{f} = \left\{ \begin{array}{c} 0 \\ \frac{1}{\rho_0} \boldsymbol{B} \\ \frac{1}{\Theta} R \end{array} \right\}. \tag{3.6}$$

Let consider now the following *isentropic operator split* $\boldsymbol{A}[\cdot] = \boldsymbol{A}^1_{ise}[\cdot] + \boldsymbol{A}^2_{ise}[\cdot]$, where

$$\boldsymbol{A}^1_{ise}[z] = \left\{ \begin{array}{c} \boldsymbol{V} \\ \frac{1}{\rho_0} \, \mathrm{DIV}[\boldsymbol{P}] \\ 0 \end{array} \right\}, \qquad \boldsymbol{A}^2_{ise}[z] = \left\{ \begin{array}{c} 0 \\ 0 \\ -\frac{1}{\Theta} \, \mathrm{DIV}[\boldsymbol{Q}] + \frac{1}{\Theta} \, \mathcal{D}_{int} \end{array} \right\}, \tag{3.7}$$

together with the associate prescribed forcing terms split given by

$$\boldsymbol{f}^1_{ise} = \left\{ \begin{array}{c} 0 \\ \frac{1}{\rho_0} \boldsymbol{B} \\ 0 \end{array} \right\}, \qquad \boldsymbol{f}^2_{ise} = \left\{ \begin{array}{c} 0 \\ 0 \\ \frac{1}{\Theta} R \end{array} \right\}. \tag{3.8}$$

Use of a product formula algorithm linked to the isentropic operator split leads to a staggered solution time integration algorithm in which one must solve first a mechanical problem (with heat conduction) at constant entropy, followed by a thermal heat conduction problem at constant (fixed) configuration. It was shown by Armero & Simo (1992a,1992b,1993), than in sharp contrast with classical staggered solution algorithms based on an isothermal operator split, the isentropic operator split preserves the a-priori dissipative stability estimate of the continuum, leading to an unconditionally stable product formula staggered algorithm. See Armero & Simo (1992a,1992b,1993) for details on an efficient implementation of the isentropic operator split.

(C) *Product formula algorithms for coupled thermomechanical problems. Isothermal split.* The governing equations of the coupled thermomechanical evolution problem can be expressed as an abstract first order system of ordinary differential equations given by (3.1), in which the primary variables, operator and prescribed forcing terms are given by

$$z = \left\{ \begin{array}{c} \varphi \\ \boldsymbol{V} \\ \Theta \end{array} \right\}, \qquad \boldsymbol{A}[z] = \left\{ \begin{array}{c} \boldsymbol{V} \\ \frac{1}{\rho_0} \, \mathrm{DIV}[\boldsymbol{P}] \\ -\frac{1}{c_0} \, \mathrm{DIV}[\boldsymbol{Q}] - \frac{1}{c_0} \, \mathcal{H}^{ep} + \frac{1}{c_0} \, \mathcal{D}_{mech} \end{array} \right\}, \qquad \boldsymbol{f} = \left\{ \begin{array}{c} 0 \\ \frac{1}{\rho_0} \boldsymbol{B} \\ \frac{1}{c_0} R \end{array} \right\}. \tag{3.9}$$

Let consider now the following *isothermal operator split* $\boldsymbol{A}[\cdot] = \boldsymbol{A}^1_{iso}[\cdot] + \boldsymbol{A}^2_{iso}[\cdot]$, where

$$\boldsymbol{A}^1_{iso}[z] = \left\{ \begin{array}{c} \boldsymbol{V} \\ \frac{1}{\rho_0} \, \mathrm{DIV}[\boldsymbol{P}] \\ 0 \end{array} \right\}, \qquad \boldsymbol{A}^2_{iso}[z] = \left\{ \begin{array}{c} 0 \\ 0 \\ -\frac{1}{c_0} \, \mathrm{DIV}[\boldsymbol{Q}] - \frac{1}{c_0} \, \mathcal{H}^{ep} + \frac{1}{c_0} \, \mathcal{D}_{mech} \end{array} \right\}, \tag{3.10}$$

together with the associate prescribed forcing terms split given by

$$\boldsymbol{f}^1_{iso} = \left\{ \begin{array}{c} 0 \\ \frac{1}{\rho_0} \boldsymbol{B} \\ 0 \end{array} \right\}, \qquad \boldsymbol{f}^2_{iso} = \left\{ \begin{array}{c} 0 \\ 0 \\ \frac{1}{c_0} R \end{array} \right\}. \tag{3.11}$$

Use of a product formula algorithm linked to the isothermal operator split leads to a staggered solution time integration algorithm in which one must solve first a mechanical

problem (without heat conduction) at constant temperature, followed by a thermal heat conduction problem at constant (fixed) configuration.

3.2 Spatial Discretization: The Galerkin Projection

Consider a spatial discretization $\Omega^{(i)} = \cup_{e=1}^{n_{elem}} \Omega_e^{(i)}$ of the reference configuration $\Omega^{(i)} \subset \mathbb{R}^{n_{dim}}$, generically refered as the triangularization and denoted by $\mathcal{T}^{(i)h}$ in what follows, into a disjoint collection of non-overlapping subsets $\Omega_e^{(i)}$, $i = 1, 2$. We will refer to a typical subset $\Omega_e^{(i)}$ as a finite element and denote by $h > 0$ the characteristic size of an element in a given triangularization.

Associated with the triangularization $\mathcal{T}^{(i)h}$ one introduces finite dimensional approximations $\mathcal{C}_{mech}^{(i)h} \subset \mathcal{C}_{mech}^{(i)}$ and $\mathcal{C}_{ther}^{(i)h} \subset \mathcal{C}_{ther}^{(i)}$ to the configuration and admissible temperature manifolds $\mathcal{C}_{mech}^{(i)}$ and $\mathcal{C}_{ther}^{(i)}$, respectively, defined as

$$\begin{aligned} \mathcal{C}_{mech}^{(i)h} &:= \{\boldsymbol{\varphi}^{(i)h} \in \mathcal{C}_{mech}^{(i)} \ : \ \boldsymbol{\varphi}^{(i)h} \in [C^0(\Omega^{(i)})]^{n_{dim}} \quad \text{and} \quad \boldsymbol{\varphi}^{(i)h}|_{\Omega_e^{(i)}} \in [P^k(\Omega_e^{(i)})]^{n_{dim}}\} \\ \mathcal{C}_{ther}^{(i)h} &:= \{\Theta^{(i)h} \in \mathcal{C}_{ther}^{(i)} \ : \ \Theta^{(i)h} \in [C^0(\Omega^{(i)})] \quad \text{and} \quad \Theta^{(i)h}|_{\Omega_e^{(i)}} \in [P^k(\Omega_e^{(i)})]\}, \end{aligned} \tag{3.12}$$

where $P^k(\Omega_e^{(i)})$ denotes the space of complete polynomials of degree $k \geq 1$.

The finite dimensional subspaces $\mathcal{V}_0^{(i)h} \subset \mathcal{V}_0^{(i)}$ and $\mathcal{T}_0^{(i)h} \subset \mathcal{T}_0^{(i)}$ of material test functions associated with $\mathcal{C}_{mech}^{(i)h}$ and $\mathcal{C}_{ther}^{(i)h}$ are defined as

$$\begin{aligned} \mathcal{V}_0^{(i)h} &:= \{\boldsymbol{\eta}_0^{(i)h} \in \mathcal{V}_0^{(i)} \ : \ \boldsymbol{\eta}_0^{(i)h} \in [C^0(\Omega^{(i)})]^{n_{dim}} \quad \text{and} \quad \boldsymbol{\eta}_0^{(i)h}|_{\Omega_e^{(i)}} \in [P^k(\Omega_e^{(i)})]^{n_{dim}}\} \\ \mathcal{T}_0^{(i)h} &:= \{\zeta_0^{(i)h} \in \mathcal{T}_0^{(i)} \ : \ \zeta_0^{(i)h} \in [C^0(\Omega^{(i)})] \quad \text{and} \quad \zeta_0^{(i)h}|_{\Omega_e^{(i)}} \in [P^k(\Omega_e^{(i)})]\}. \end{aligned} \tag{3.13}$$

(A) *Galerkin projection of the mechanical and thermal frictional contact contributions to the weak form.* The Galerkin projection of the mechanical and thermal frictional contact contributions to the weak form, given for the continuum case by (2.107), can be written as

$$\boxed{\begin{aligned} G_c^{mech}(\boldsymbol{\varphi}^h, \boldsymbol{\eta}_0^h) &:= \langle t_N^h, \delta g_N^h \rangle_{\Gamma^{(1)h}} + \langle t_{T\alpha}^h, \delta \bar{\xi}^{\alpha h} \rangle_{\Gamma^{(1)h}} \\ G_c^{ther}(\Theta^h, \zeta_0^h) &:= \langle Q_{hc}^h, \delta g_\theta^h \rangle_{\Gamma^{(1)h}} - \langle \mathcal{D}_{fric}^h, \delta \theta_G^h \rangle_{\Gamma^{(1)h}} \end{aligned}} \tag{3.14}$$

where $(\cdot)^h$ denotes the Galerkin projection of $(\cdot)$. In particular, using the short hand notation introduced in (3.68), $\boldsymbol{\varphi}^h$ and $\boldsymbol{\eta}_0^h$ refers to the discrete collection of mappings $\boldsymbol{\varphi}^{(i)h}$ and $\boldsymbol{\eta}_0^{(i)h}$, $i = 1, 2$, such that the restriction of each of the maps $\boldsymbol{\varphi}^h$ and $\boldsymbol{\eta}_0^h$ to the domain $\bar{\Omega}^{(i)h}$ gives identically $\boldsymbol{\varphi}^{(i)h}$ and $\boldsymbol{\eta}_0^{(i)h}$, respectively. Analogously, Θ^h and ζ_0^h refers to the discrete collection of mappings $\Theta^{(i)h}$ and $\zeta_0^{(i)h}$, $i = 1, 2$, such that the restriction of each of the maps Θ^h and ζ_0^h to the domain $\bar{\Omega}^{(i)h}$ gives identically $\Theta^{(i)h}$ and $\zeta_0^{(i)h}$, respectively.

The projections δg_N^h and $\delta \bar{\xi}^{\alpha h}$ are given by (2.96) and (2.100), and the projections δg_θ^h and $\delta \theta_G^h$ are given by (2.105) and (2.106), with discrete quantities replacing their continuous counterparts.

(B) Linearization. The linearization of the mechanical and thermal frictional contact contributions to the weak form given by (3.14), yield the following bilinear forms

$$\boxed{\begin{aligned} B_{\varphi_t^h}^{mech}(\boldsymbol{\eta}_0^h, \Delta\boldsymbol{\varphi}^h) &:= B_{\varphi_t^h}^{mech,geo}(\boldsymbol{\eta}_0^h, \Delta\boldsymbol{\varphi}^h) + B_{\varphi_t^h}^{mech,mat}(\boldsymbol{\eta}_0^h, \Delta\boldsymbol{\varphi}^h) \\ B_{\Theta_t^h}^{ther}(\zeta_0^h, \Delta\Theta^h) &:= B_{\Theta_t^h}^{ther,geo}(\zeta_0^h, \Delta\Theta^h) + B_{\Theta_t^h}^{ther,mat}(\zeta_0^h, \Delta\Theta^h) \end{aligned}} \tag{3.15}$$

Here $B^{mech,geo}_{\varphi^h_t}(\cdot,\cdot)$ is the mechanical *geometric term* defined for fixed (nominal) contact pressure t^h_N and (nominal) frictional tangent traction $t^h_{T\alpha}$ at given configuration $\varphi^h_t \in \mathcal{C}^h_{mech}$, by the bilinear form:

$$\boxed{B^{mech,geo}_{\varphi^h_t}(\eta^h_0, \Delta\varphi^h) := \langle t^h_N, \Delta(\delta g^h_N)\rangle_{\Gamma^{(1)h}} + \langle t^h_{T\alpha}, \Delta(\delta\bar{\xi}^{\alpha h})\rangle_{\Gamma^{(1)h}},} \tag{3.16}$$

$B^{mech,mat}_{\varphi^h_t}(\cdot,\cdot)$ is the mechanical *material term* defined for fixed configuration $\varphi^h_t \in \mathcal{C}^h_{mech}$, by the bilinear form:

$$\boxed{B^{mech,mat}_{\varphi^h_t}(\eta^h_0, \Delta\varphi^h) := \langle \Delta t^h_N, \delta g^h_N\rangle_{\Gamma^{(1)h}} + \langle \Delta t^h_{T\alpha}, \delta\bar{\xi}^{\alpha h}\rangle_{\Gamma^{(1)h}},} \tag{3.17}$$

$B^{ther,geo}_{\Theta^h_t}(\cdot,\cdot)$ is the thermal *geometric term* defined for fixed (nominal) heat conduction flux Q^h_{hc} at *fixed* given configuration $\varphi^h_t \in \mathcal{C}^h_{mech}$, by the bilinear form:

$$\boxed{B^{ther,geo}_{\Theta^h_t}(\zeta^h_0, \Delta\Theta^h) := \langle Q^h_{hc}, \Delta(\delta g^h_\theta)\rangle_{\Gamma^{(1)h}} - \langle \mathcal{D}^h_{fric}, \Delta(\delta\theta^h_G)\rangle_{\Gamma^{(1)h}},} \tag{3.18}$$

and $B^{ther,mat}_{\Theta^h_t}(\cdot,\cdot)$ is the thermal *material term* defined for the current fixed admissible thermal configuration $\Theta^h_t \in \mathcal{C}^h_{ther}$, by the bilinear form:

$$\boxed{B^{ther,geo}_{\Theta^h_t}(\zeta^h_0, \Delta\Theta^h) := \langle \Delta Q^h_{hc}, \delta g^h_\theta\rangle_{\Gamma^{(1)h}} - \langle \Delta\mathcal{D}^h_{fric}, \delta\theta^h_G\rangle_{\Gamma^{(1)h}}.} \tag{3.19}$$

3.3 Temporal Discretization. Frictional Return Mapping

Consider the time interval of interest $\mathbb{I} = [0, T]$ discretized into a series of non-overlapping subintervals $\mathbb{I} := \cup_{n=0}^{N}[t_n, t_{n+1}]$. The incremental solution to the IBVP is obtained applying a time stepping algorithm to integrate the evolution equations within a typical time step $[t_n, t_{n+1}]$, with given nodal and internal variables at time t_n, as initial conditions at the nodal and quadrature points of a typical element $\Omega^{(i)}_e$, respectively.

Within the framework of the *fractional step methods* arising from an *operator split* of the coupled system of nonlinear ordinary differential equations describing the time evolution of nodal degrees of freedom and internal variables, a time stepping algorithm to integrate the evolution equations is applied to each one of the partitions, using a *product formula algorithm*.

Following a standard convention, we shall denote by either $(\cdot)_n$ or $(\cdot)_{n+1}$ the algorithmic approximations at times t_n and t_{n+1} to the continuum (time dependent) variable $(\cdot)_t$.

(A) *Frictional time-stepping algorithms.* Most of the usual time-stepping algorithms will require the evaluation of the weak form and internal variables at some time $t_{n+\vartheta}$, where $\vartheta \in (0, 1]$. A class of time-stepping algorithms for dynamic plasticity, including Linear Multistep (LMS) methods, and amongst them the so-called Backward Difference (BD) methods, and Implicit Runge-Kutta (IRK) methods, are shown in Simo (1992,1994). Here, we will focussed on two algorithms for the time integration of the constrained frictional evolution problem defined by (2.41) and (2.42): the lowest order BD method, called Backward-Euler (BE) method, and amongst the Implicit Runge-Kutta (IRK) methods, the generalized Projected Mid-Point (PMP) method.

(A1) *Backward-Euler (BE) method.* Consider the approximation of (2.41) and (2.42) by the lowest order BD method, the BE scheme, to obtain the algebraic equation

$$\begin{aligned} t_{T\,n+1\,\alpha} &= t_{T\,n\,\alpha} + \epsilon_T [M_{\alpha\beta}(\bar{\xi}^{\beta}_{n+1} - \bar{\xi}^{\beta}_{n}) - \gamma_{n+1}\ p_{T\,n+1\,\alpha}] \\ \alpha_{n+1} &= \alpha_n + \gamma_{n+1}[(1-w) + w\|\boldsymbol{t}^{\flat}_{T\,n+1}\|] \end{aligned} \tag{3.20}$$

subjected to the discrete complementary Kuhn-Tucker conditions

$$\left.\begin{aligned} \Phi_{n+1} := \|\boldsymbol{t}^{\flat}_{T\,n+1}\| - \mu(\alpha_{n+1})\ t_{N\,n+1} &\le 0 \\ \gamma_{n+1} &\ge 0 \\ \gamma_{n+1}\ \Phi_{n+1} &= 0 \end{aligned}\right\} \tag{3.21}$$

The solution to the constrained incremental algebraic problem defined by (3.20) and (3.21) is obtained through the introduction of a *trial state*, obtained by freezing the irreversible-slip response, and subsequent *return mapping* algorithm to enforce the constraints.

Step **1.** *Trial state.* The frictional trial state is obtained by freezing the irreversible-slip response, i.e. assuming $\gamma_{n+1} = 0$ and that no constraints are present. Then the trial state is defined as

$$\begin{aligned} t^{trial}_{T_{n+1}\,\alpha} &:= t_{T\,n\,\alpha} + \epsilon_T M_{\alpha\beta}(\bar{\xi}^{\beta}_{n+1} - \bar{\xi}^{\beta}_{n}) \\ \alpha^{trial}_{n+1} &:= \alpha_n \\ \Phi^{trial}_{n+1} &:= \|\boldsymbol{t}^{\flat\,trial}_{T_{n+1}}\| - \mu(\alpha^{trial}_{n+1})\ t_{N_{n+1}} \end{aligned} \tag{3.22}$$

where $t_{N\,n+1} = \epsilon_N \langle g_{N\,n+1} \rangle$ is the normal contact pressure at t_{n+1}.

Step **2.** *Return mapping.* The return mapping defines the final state as the solution of the discrete constrained incremental algebraic problem:

$$\begin{aligned} t_{T_{n+1}\,\alpha} &= t^{trial}_{T_{n+1}\,\alpha} - \epsilon_T\ \gamma_{n+1}\ p_{T_{n+1}\,\alpha} \\ \alpha_{n+1} &= \alpha^{trial}_{n+1} + \gamma_{n+1}\ [(1-w) + w\|\boldsymbol{t}^{\flat}_{T\,n+1}\|] \end{aligned} \tag{3.23}$$

$$\left.\begin{aligned} \Phi_{n+1} = \|\boldsymbol{t}^{\flat}_{T_{n+1}}\| - \mu(\alpha_{n+1})\ t_{N\,n+1} &\le 0 \\ \gamma_{n+1} &\ge 0 \\ \gamma_{n+1}\ \Phi_{n+1} &= 0 \end{aligned}\right\} \tag{3.24}$$

Assuming that $\Phi^{trial}_{n+1} > 0$, otherwise $\gamma_{n+1} = 0$ and the trial state actually is the final state, the discrete consistency parameter γ_{n+1} can be computed by enforcing the discrete counterpart of the consistency condition $\Phi_{n+1} = 0$.

Introducing $\boldsymbol{p}^{\flat}_{T_{n+1}} := \boldsymbol{t}^{\flat}_{T_{n+1}} / \|\boldsymbol{t}^{\flat}_{T_{n+1}}\|$ into the intrinsic expression of the frictional traction

$$\boldsymbol{t}^{\flat}_{T_{n+1}} = \boldsymbol{t}^{\flat\,trial}_{T_{n+1}} - \epsilon_T\ \gamma_{n+1}\ \boldsymbol{p}^{\flat}_{T_{n+1}} \tag{3.25}$$

collecting terms, setting $\boldsymbol{p}^{\flat\,trial}_{T_{n+1}} := \boldsymbol{t}^{\flat\,trial}_{T_{n+1}} / \|\boldsymbol{t}^{\flat\,trial}_{T_{n+1}}\|$ and taking norms leads to,

$$\begin{aligned} \boldsymbol{p}^{\flat}_{T_{n+1}} &= \boldsymbol{p}^{\flat\,trial}_{T_{n+1}} \\ \|\boldsymbol{t}^{\flat}_{T_{n+1}}\| &= \|\boldsymbol{t}^{\flat\,trial}_{T_{n+1}}\| - \epsilon_T\ \gamma_{n+1} \end{aligned} \tag{3.26}$$

Introducing (3.26) into (3.23)-(3.25), the frictional return mapping tak es the form:

$$\begin{aligned}
\boldsymbol{t}^{\flat}_{T_{n+1}} &= (1 - \epsilon_T \ \frac{\gamma_{n+1}}{\|\boldsymbol{t}^{\flat trial}_{T_{n+1}}\|}) \ \boldsymbol{t}^{\flat trial}_{T_{n+1}} \\
\alpha_{n+1} &= \alpha^{trial}_{n+1} + \gamma_{n+1} \ [(1 - w) + w \|\boldsymbol{t}^{\flat trial}_{T_{n+1}}\| - w \ \epsilon_T \ \gamma_{n+1}] \\
\Phi_{n+1} &:= \|\boldsymbol{t}^{\flat trial}_{T_{n+1}}\| - \epsilon_T \ \gamma_{n+1} - \mu(\alpha_{n+1}) \ t_{N\,n+1} = 0
\end{aligned} \tag{3.27}$$

or alternatively, using the consistency condition,

$$\begin{aligned}
\boldsymbol{t}^{\flat}_{T_{n+1}} &= \mu(\alpha_{n+1}) \ t_{N\,n+1} \ \boldsymbol{p}^{\flat trial}_{T_{n+1}} \\
\alpha_{n+1} &= \alpha^{trial}_{n+1} + \gamma_{n+1} \ [(1 - w) + w \ \mu(\alpha_{n+1}) \ t_{N\,n+1}] \\
\Phi_{n+1} &:= \|\boldsymbol{t}^{\flat trial}_{T_{n+1}}\| - \epsilon_T \ \gamma_{n+1} - \mu(\alpha_{n+1}) \ t_{N\,n+1} = 0
\end{aligned} \tag{3.28}$$

Computation of the consistency parameter γ_{n+1} will require, in general, to solve the nonlinear equation $\Phi_{n+1} = \hat{\Phi}(\gamma_{n+1}) = 0$, were it is implicitly understood that we are looking at α_{n+1} as a function $\alpha_{n+1} = \alpha_{n+1}(\gamma_{n+1})$, using $(3.27)_2$ instead of $(3.28)_2$. Using a Newton-Raphson method the linearization of the slip function yields

$$\Phi^{(k)}_{n+1} + D\Phi^{(k)}_{n+1} \cdot \Delta\gamma^{(k)}_{n+1} = 0 \tag{3.29}$$

with

$$\begin{aligned}
\Phi^{(k)}_{n+1} &= \Phi^{trial}_{n+1} - \epsilon_T \ \gamma^{(k)}_{n+1} - [\mu(\alpha^{(k)}_{n+1}) - \mu(\alpha^{trial}_{n+1})] \ t_{N\,n+1} \\
D\Phi^{(k)}_{n+1} &= -\epsilon_T - \partial_\alpha \mu(\alpha^{(k)}_{n+1}) \ D\alpha^{(k)}_{n+1} \ t_{N\,n+1} \\
\alpha^{(k)}_{n+1} &= \alpha^{trial}_{n+1} + \gamma^{(k)}_{n+1} \ [(1 - w) + w \|\boldsymbol{t}^{\flat trial}_{T_{n+1}}\| - w \ \epsilon_T \ \gamma^{(k)}_{n+1}] \\
D\alpha^{(k)}_{n+1} &= (1 - w) + w \|\boldsymbol{t}^{\flat trial}_{T_{n+1}}\| - 2 \ w \ \epsilon_T \ \gamma^{(k)}_{n+1} \\
\Delta\gamma^{(k)}_{n+1} &= \gamma^{(k+1)}_{n+1} - \gamma^{(k)}_{n+1}
\end{aligned} \tag{3.30}$$

and with the initial condition $\gamma^{(0)}_{n+1} = 0$.

As it is well known, the BE algorithm is consistent and first order accurate. On the other hand, as it was shown b y Simo (1994) within the context of J2 perfect plasticity, in spite of its restriction to first order accuracy, the BE algorithm inherits the dissipative and contractive properties of the continuum problem and becomes optimal for a long-term behavior.

REMARK 3.1. The intrinsic form of the frictional time integration described above can be written as

$$\begin{aligned}
\boldsymbol{t}^{\flat}_{T_{n+1}} &:= \boldsymbol{t}^{\flat trial}_{T_{n+1}} - \epsilon_T \ \gamma_{n+1} \ \boldsymbol{p}^{\flat trial}_{T_{n+1}} \\
\boldsymbol{t}^{\flat trial}_{T_{n+1}} &:= \boldsymbol{F}^{-T}_{n+1} \cdot \boldsymbol{t}^{\flat ref \ trial}_{T_{n+1}} \\
\boldsymbol{t}^{\flat ref \ trial}_{T_{n+1}} &:= \boldsymbol{\Lambda}^{n}_{n+1} \cdot \boldsymbol{t}^{\flat ref}_{T_n} + \epsilon_T M_{\alpha\beta} (\bar{\xi}^{\beta}_{n+1} - \bar{\xi}^{\beta}_{n}) \ \boldsymbol{\tau}^{\alpha^{ref}}_{n+1}
\end{aligned} \tag{3.31}$$

where the surface deformation gradient $\boldsymbol{F}_{n+1}$ and the surface transport operator $\boldsymbol{\Lambda}^{n}_{n+1}$ are defined as

$$\begin{aligned}
\boldsymbol{F}^{-T}_{n+1} &:= \boldsymbol{\tau}^{\alpha}_{n+1} \otimes \boldsymbol{\tau}^{ref}_{\alpha_{n+1}} \\
\boldsymbol{\Lambda}^{n}_{n+1} &:= \boldsymbol{\tau}^{\alpha^{ref}}_{n+1} \otimes \boldsymbol{\tau}^{ref}_{\alpha_n}
\end{aligned} \tag{3.32}$$

Here the trial state defined b y $\boldsymbol{t}^{\flat trial}_{T_{n+1}} := t^{trial}_{T_{n+1}\,\alpha} \boldsymbol{\tau}^{\alpha}_{n+1}$ may be interpreted as the result of a tw o-step algorithm:

i. Time in tegration of the trial frictional traction on the reference configuration to get $\boldsymbol{t}^{\flat\,ref\;trial}_{T_{n+1}}$. This time integration consist of two steps. First, the frictional traction in the reference configuration at the last converged time step is *transported* with the operator $\boldsymbol{\Lambda}^{n}_{n+1}$ to the current closest-point projection on the reference configuration, followed by the (trial) slip contribution given by the distance, with respect to the metric $M_{\alpha\beta}$, between the current and last converged closest-point projections on the reference configuration.

ii. Push-forward to the current configuration to get $\boldsymbol{t}^{\flat\,trial}_{T_{n+1}}$.

Once the trial state has been defined the return mapping is performed on the current configuration, following standard procedures. □

(A2) *Generalized Projected Mid-Point (PMP) Implicit Runge-Kutta (IRK) method.* The Generalized Projected Mid-Point IRK method is constructed via a two-stage product formula algorithm as follows:

Stage I. A BE algorithm is applied to integrate the constrained evolution problem within a time sub-interval $[t_n, t_{n+\vartheta}] \subset [t_n, t_{n+1}]$ where $t_{n+\vartheta} := (1-\vartheta)t_n + \vartheta t_{n+1}$ and $\vartheta \in (0,1]$. Thus, the first stage of the algorithm is identical to the scheme already described above. Explicitly, the following steps are performed for prescibed initial data $\{t_{T^{ref}_{n_\alpha}}\}$ and given relative (parametrized) slip increment $\bar{g}^{\alpha}_{T_{n+\vartheta}} := \bar{\xi}^{\alpha}_{n+\vartheta} - \bar{\xi}^{\alpha}_{n}$:

Step **1.** Define the generalized mid-point trial state according to

$$\begin{aligned} t^{trial}_{T_{n+\vartheta}\alpha} &:= t_{T_n\alpha} + \epsilon_T M_{\alpha\beta}(\bar{\xi}^{\beta}_{n+\vartheta} - \bar{\xi}^{\beta}_{n}) \\ \alpha^{trial}_{n+\vartheta} &:= \alpha_n \\ \Phi^{trial}_{n+\vartheta} &:= \|\boldsymbol{t}^{\flat\,trial}_{T_{n+\vartheta}}\| - \mu(\alpha^{trial}_{n+\vartheta})\; t_{N_{n+\vartheta}} \end{aligned} \tag{3.33}$$

Step **2.** The return mapping defines the final state at the generalized mid-point configuration $\mathcal{C}_{n+\vartheta}$ as the solution of the discrete constrained incremental algebraic problem:

$$\begin{aligned} t_{T_{n+\vartheta}\alpha} &= t^{trial}_{T_{n+\vartheta}\alpha} - \epsilon_T\; \gamma_{n+\vartheta}\; p_{T_{n+\vartheta}\alpha} \\ \alpha_{n+\vartheta} &= \alpha^{trial}_{n+\vartheta} + \gamma_{n+\vartheta}\; [(1-w) + w\|\boldsymbol{t}^{\flat}_{T_{n+\vartheta}}\|] \end{aligned} \tag{3.34}$$

$$\left.\begin{aligned} \Phi_{n+\vartheta} = \|\boldsymbol{t}^{\flat}_{T\,n+\vartheta}\| - \mu(\alpha_{n+\vartheta})\; t_{N\,n+\vartheta} &\le 0 \\ \gamma_{n+\vartheta} &\ge 0 \\ \gamma_{n+\vartheta}\; \Phi_{n+\vartheta} &= 0 \end{aligned}\right\} \tag{3.35}$$

Stage IIA. Since the trial values $t^{trial}_{T_{n+\vartheta}\,\alpha}$ and the converged values $t_{T_{n+\vartheta}\,\alpha}$ are available from Stage I and within the context of a product formula algorithm, the initial data $t^{*}_{T_{n+\vartheta}\,\alpha}$ and $\alpha^{*}_{n+\vartheta}$ for the second stage are defined using the linear extrapolation:

$$\begin{aligned} t^{*}_{T_{n+\vartheta}\alpha} &:= \frac{1}{\vartheta} t_{T_{n+\vartheta}\alpha} - \frac{1-\vartheta}{\vartheta} t^{trial}_{T_{n+\vartheta}\alpha} \\ \alpha^{*}_{n+\vartheta} &:= \frac{1}{\vartheta}\alpha_{n+\vartheta} - \frac{1-\vartheta}{\vartheta}\alpha^{trial}_{n+\vartheta} \end{aligned} \tag{3.36}$$

Within a finite deformation framework, all the objects involved in the linear extrapolation given by (3.36) should be viewed as objects lying in the *same* generalized mid-point configuration $\mathcal{C}_{n+\vartheta}$. Thus, for the friction Coulomb model this extrapolation is performed on the plane $t_N = t_{N\,n+\vartheta}$ of the tractions space.

Stage IIB. The second part of Stage II is identical to Stage I, where now the initial prescribed data becomes $t^*_{T_{n+\vartheta}\,\alpha}$ and the given (parametrized) relative slip increment is $\bar{g}^\alpha_{T_{n+1}} := \bar{\xi}^\alpha_{n+1} - \bar{\xi}^\alpha_{n+\vartheta}$. The steps involved in the update are the following:

Step **1.** Define the trial state according to

$$\begin{aligned} t^{trial}_{T_{n+1}\,\alpha} &:= t^*_{T_{n+\vartheta}\,\alpha} + \epsilon_T M_{\alpha\beta}(\bar{\xi}^\beta_{n+1} - \bar{\xi}^\beta_{n+\vartheta}) \\ \alpha^{trial}_{n+1} &:= \alpha^*_{n+\vartheta} \\ \Phi^{trial}_{n+1} &:= \|\boldsymbol{t}^{\flat\,trial}_{T_{n+1}}\| - \mu(\alpha^{trial}_{n+1})\; t_{N_{n+1}} \end{aligned} \tag{3.37}$$

Step **2.** Perform the return mapping to get the final state at the configuration $\mathcal{C}_{n+1}$ as the solution of the discrete constrained incremental algebraic problem:

$$\begin{aligned} t_{T_{n+1}\,\alpha} &= t^{trial}_{T_{n+1}\,\alpha} - \epsilon_T\; \gamma_{n+1}\; p_{T_{n+1}\,\alpha} \\ \alpha_{n+1} &= \alpha^{trial}_{n+1} + \gamma_{n+1}\; [(1-w) + w\|\boldsymbol{t}^\flat_{T_{n+1}}\|] \end{aligned} \tag{3.38}$$

$$\left.\begin{aligned} \Phi_{n+1} = \|\boldsymbol{t}^\flat_{T_{n+1}}\| - \mu(\alpha_{n+1})\; t_{N\,n+1} \le 0 \\ \gamma_{n+1} \ge 0 \\ \gamma_{n+1}\; \Phi_{n+1} = 0 \end{aligned}\right\} \tag{3.39}$$

A rigorous stability and accuracy analysis of the two-stage, implicit, PMP algorithm, within the context of J2 plasticity was provided by Simo (1994). The accuracy and stability analysis show that the generalized PMP algorithm is obviously consistent, second order accurate for the PMP algorithm ($\vartheta = 0.5$), B-stable for $\vartheta \ge 0.5$ and ensures that the final stage is on the admissible domain. Remarkably, in sharp contrast with others second order accurate algorithms, i.e. mid-point rule, second order accuracy is achieved performing a *radial return mapping* in each of the Stages and thus a solution will be always guaranteed to exist for arbitrarily large time-steps. However, the long-term behaviour of this scheme is not optimal when compared with that exhibited by the, less accurate, BE algorithm. In contrast, this scheme becomes optimal for short-term behavior.

(B) *Linearization of the frictional time-stepping algorithm.* The frictional time-stepping algorithms presented above are amenable to exact linearization, leading to the corresponding terms of the *consistent* or *algorithmic* tangent operator. In order to accomodate the linearization of the BE and PMP return mapping algorithms into a single expression, we will derive the linearization of the frictional traction at time $t_{n+\vartheta}$, at the generic configuration $\mathcal{C}_{n+\vartheta}$, where $\vartheta = 1$ for the BE algorithm and $\vartheta \in (0, 1]$ for the PMP algorithm. We point out that the implementation of the PMP IRK algorithm actually requires *only* the linearization of the Stage I, while Stage II can be viewed as an update procedure to provide the initial conditions for the next time step, after convergence has been achieved.

Using the directional derivative, the linearization of the frictional time integration algorithm leads to the following expressions.

Step **1.** *Trial state.* The linearization of the trial state tak es the form

$$\begin{aligned} \Delta t_{T_{n+\vartheta}\alpha} &:= \Delta t^{trial}_{T_{n+\vartheta}\alpha} \\ \Delta\alpha_{n+\vartheta} &:= \Delta\alpha^{trial}_{n+\vartheta} = 0 \end{aligned} \tag{3.40}$$

Step **2.** *Return mapping.* The linearization of the return mapping takes the form

$$\begin{aligned} \Delta t_{T_{n+\vartheta}\alpha} &:= \mu(\alpha_{n+\vartheta})\ \Delta t_{N\,n+\vartheta}\ p^{trial}_{T_{n+\vartheta}\alpha} + \mu(\alpha_{n+\vartheta})\ t_{N\,n+\vartheta}\ \Delta p^{trial}_{T_{n+\vartheta}\alpha} \\ &\quad + \partial_\alpha\mu(\alpha_{n+\vartheta})\ \Delta\alpha_{n+\vartheta}\ t_{N\,n+\vartheta}\ p^{trial}_{T_{n+\vartheta}\alpha} \\ \Delta\alpha_{n+\vartheta} &:= \Delta\gamma_{n+\vartheta}\ [(1-w) + w\ \mu(\alpha_{n+\vartheta})\ t_{N\,n+\vartheta} - w\ \epsilon_T\ \gamma_{n+\vartheta}] \\ &\quad + \gamma_{n+\vartheta}\ w\ \Delta\|\boldsymbol{t}^{\flat\,trial}_{T_{n+\vartheta}}\| \\ &:= \Delta\gamma_{n+\vartheta}\ [(1-w) + w\ \mu(\alpha_{n+\vartheta})\ t_{N\,n+\vartheta}] \\ &\quad + \gamma_{n+\vartheta}\ w\ [\partial_\alpha\mu(\alpha_{n+\vartheta})\ t_{N\,n+\vartheta}\ \Delta\alpha_{n+\vartheta} + \mu(\alpha_{n+\vartheta})\ \Delta t_{N_{n+\vartheta}}] \end{aligned} \tag{3.41}$$

with

$$\begin{aligned} \Delta t_{N_{n+\vartheta}} &:= \epsilon_N H(g_{N_{n+\vartheta}})\ \Delta g_{N_{n+\vartheta}} \\ \Delta g_{N_{n+\vartheta}} &:= -\vartheta\ [\Delta\boldsymbol{\varphi}^{(1)h} - \Delta\boldsymbol{\varphi}^{(2)h} \circ \boldsymbol{\psi}^{(2)}_0(\bar{\boldsymbol{\xi}}_{n+\vartheta})] \cdot \boldsymbol{\nu} \\ \Delta t^{trial}_{T_{n+\vartheta}\alpha} &:= \Xi_{\alpha\beta}\ \Delta\bar{\xi}^\beta_{n+\vartheta} \end{aligned} \tag{3.42a}$$

$$\begin{aligned} \Delta p^{trial}_{T_{n+\vartheta}\alpha} &:= (\delta^\beta_\alpha - \pi^\beta_\alpha)\ \frac{\Delta t^{trial}_{T_{n+\vartheta}\beta}}{\|\boldsymbol{t}^{\flat\,trial}_{T_{n+\vartheta}}\|} + \pi^\beta_\alpha\ \boldsymbol{p}^{\flat\,trial}_{T_{n+\vartheta}} \cdot [\vartheta\ \Delta\boldsymbol{\varphi}^{(2)h}_{,\beta}(\bar{\boldsymbol{\xi}}) + \boldsymbol{e}_{\beta,\gamma}(\bar{\boldsymbol{\xi}})\ \Delta\bar{\xi}^\gamma_{n+\vartheta}] \\ \Delta\|\boldsymbol{t}^{\flat\,trial}_{T_{n+\vartheta}}\| &:= p^{trial\ \alpha}_{T_{n+\vartheta}}\ \Delta t^{trial}_{T_{n+\vartheta}\alpha} - p^{trial\ \alpha}_{T_{n+\vartheta}}\ \boldsymbol{t}^{\flat\,trial}_{T_{n+\vartheta}} \cdot [\vartheta\ \Delta\boldsymbol{\varphi}^{(2)h}_{,\alpha}(\bar{\boldsymbol{\xi}}) + \boldsymbol{e}_{\alpha,\beta}(\bar{\boldsymbol{\xi}})\ \Delta\bar{\xi}^\beta_{n+\vartheta}] \\ \Delta\bar{\xi}^\alpha_{n+\vartheta} &:= \vartheta A^{\alpha\beta}\{[\Delta\boldsymbol{\varphi}^{(1)h} - \Delta\boldsymbol{\varphi}^{(2)h}(\bar{\boldsymbol{\xi}}_{n+\vartheta})] \cdot \boldsymbol{\tau}_\beta - g_{N_{n+\vartheta}}\boldsymbol{\nu} \cdot [\Delta\boldsymbol{\varphi}^{(2)h}_{,\beta}(\bar{\boldsymbol{\xi}}_{n+\vartheta})]\} \\ \Delta\gamma_{n+\vartheta} &:= \frac{1}{\epsilon_T}[\Delta\|\boldsymbol{t}^{\flat\,trial}_{T_{n+\vartheta}}\| - \mu(\alpha_{n+\vartheta})\ \Delta t_{N_{n+\vartheta}}] - \frac{1}{\epsilon_T}\partial_\alpha\mu(\alpha_{n+\vartheta})\ t_{N_{n+\vartheta}}\ \Delta\alpha_{n+\vartheta} \end{aligned} \tag{3.42b}$$

where,

$$\begin{aligned} \Xi_{\alpha\beta} &:= \epsilon_T\ (M_{\alpha\beta} + M_{\alpha\gamma,\beta}\ g^\gamma_T) \\ g^\alpha_T &:= \bar{\xi}^\alpha_{n+\vartheta} - \bar{\xi}^\alpha_n \\ \pi^\beta_\alpha &:= p^{trial}_{T_{n+\vartheta}\alpha}\ p^{trial\ \beta}_{T_{n+\vartheta}} \end{aligned} \tag{3.43}$$

with the, in general, *non-symmetric* operator $\Xi_{\alpha\beta}$ evaluated at $t_{n+\vartheta}$. Here, $\Delta\boldsymbol{\varphi}^{(1)h}$ and $\Delta\boldsymbol{\varphi}^{(2)h}$ refers to the incremen tal displacemen ts in the whole step, i.e. from t_n to t_{n+1}, and it is implicitly assumed that all the objects involved in the expressions are evaluated at time $t_{n+\vartheta}$.

Introducing $\Delta\gamma_{n+\vartheta}$ into the expression of $\Delta\alpha_{n+\vartheta}$ and collecting terms, leads to

$$\Delta\alpha_{n+\vartheta} := \beta_1\ \Delta\|\boldsymbol{t}^{\flat\,trial}_{T_{n+\vartheta}}\| - \beta_2\ \mu(\alpha_{n+\vartheta})\ \Delta t_{N_{n+\vartheta}} \tag{3.44}$$

with

$$\begin{aligned} \beta_1 &:= \frac{\partial\alpha/\partial\gamma|_{n+\vartheta} + w\ \epsilon_T\ \gamma_{n+\vartheta}}{\epsilon_T + \partial\alpha/\partial\gamma|_{n+\vartheta}\ \partial_\alpha\mu(\alpha_{n+\vartheta})\ t_{N_{n+\vartheta}}} \\ \beta_2 &:= \frac{\partial\alpha/\partial\gamma|_{n+\vartheta}}{\epsilon_T + \partial\alpha/\partial\gamma|_{n+\vartheta}\ \partial_\alpha\mu(\alpha_{n+\vartheta})\ t_{N_{n+\vartheta}}} \end{aligned} \tag{3.45}$$

where

$$\partial\alpha/\partial\gamma|_{n+\vartheta} := (1-w) + w\ \mu(\alpha_{n+\vartheta})\ t_{N\,n+\vartheta} - w\ \epsilon_T\ \gamma_{n+\vartheta} \tag{3.46}$$

REMARK 3.2. As it is clear from (3.43) the lack of symmetry of $\Xi_{\alpha\beta}$ arises from the variation of the surface metric in the reference configuration as the closest-point projection varies. As it was pointed out by Laursen & Simo (1993,1994), a simple procedure to remove this non-symmetry is to use the metric at the center of the master element rather than at the reference placement of the current closest-point projection. □

3.4 FE-implementation. Matrix Form of the Residual and Tangent Operator

In what follows, attention will be restricted to the finite element discretization of the contact surfaces, leading to the matrix form of the frictional contact residual and tangent operators.

Let n_{sele} and n_{mele} the total number of slave and master elements, n_{snod} and n_{mnod} the total number of slave and master nodes in a triangularization of the slave and master contact surfaces, respectively, and n^e_{snod} and n^e_{mnod} the number of nodes in a generic slave and master surface elements $\Gamma^{(1)h}_e$ and $\Gamma^{(2)h}_e$, labeled as $\{\boldsymbol{X}^e_a \in \mathbb{R}^{n_{dim}} : a = 1, \dots, n^e_{snod}\}$ and $\{\boldsymbol{Y}^e_a \in \mathbb{R}^{n_{dim}} : a = 1, \dots, n^e_{mnod}\}$, respectively.

This local numbering system is related to the global numbering system via the following standard convention:

$$\begin{aligned} \boldsymbol{X}_A &= \boldsymbol{X}^e_a \quad \text{with } A = ID^{(1)}_s(e,a),\ e = 1, \dots, n_{sele}, \quad A = 1, \dots, n^e_{snod} \\ \boldsymbol{Y}_A &= \boldsymbol{Y}^e_a \quad \text{with } A = ID^{(2)}_s(e,a),\ e = 1, \dots, n_{mele}, \quad A = 1, \dots, n^e_{mnod} \end{aligned} \tag{3.47}$$

where the $n_{sele} \times n^e_{snod}$ array $ID^{(1)}_s(\cdot,\cdot)$ and the $n_{mele} \times n^e_{mnod}$ array $ID^{(2)}_s(\cdot,\cdot)$ are defined by the geometry of the triangularization $\mathcal{T}^{(i)h}$. A rather convenient formulation of the Galerkin projection is achieved by writing the local polynomial basis as $\{N^a(\boldsymbol{\zeta})\}$, where $\boldsymbol{\zeta} = (\zeta_1, \dots, \zeta_{n_{dim}-1})$ are normalized coordinates with domain the unit square $\square$ in $\mathbb{R}^{n_{dim}-1}$ and introducing the isoparametric map:

$$\begin{aligned} \boldsymbol{\zeta} \in \square \mapsto \boldsymbol{X}^h &:= \boldsymbol{\psi}^{e(1)}_0(\boldsymbol{\zeta}) = \sum_{a=1}^{n^e_{snod}} N^a(\boldsymbol{\zeta}) \boldsymbol{X}^e_a \in \Gamma^{(1)}_e \\ \boldsymbol{\zeta} \in \square \mapsto \boldsymbol{Y}^h &:= \boldsymbol{\psi}^{e(2)}_0(\boldsymbol{\zeta}) = \sum_{a=1}^{n^e_{mnod}} N^a(\boldsymbol{\zeta}) \boldsymbol{Y}^e_a \in \Gamma^{(2)}_e \end{aligned} \tag{3.48}$$

where the local polynomial basis functions $N^a : \square \to \mathbb{R}$ are referred to as the local element shape functions and satisfy the completeness condition $N^a(\boldsymbol{\zeta}_b) = \delta^a_b$, where $\boldsymbol{\zeta}_a = (\zeta_{1\ a}, \dots, \zeta_{n_{dim}-1\ a})$ are the vertices of the bi-unit square.

The Galerkin projection of the mechanical and thermal frictional contact contribution to the weak form given by (3.14) and to the bilinear form given by (3.15)-(3.19), can be written as the assembly of integrals over the n_{sele} slave surface elements of $\Gamma^{(1)h}$ as:

$$\begin{aligned} G^{mech}_c(\boldsymbol{\varphi}^h, \boldsymbol{\eta}^h_0) &:= \bigcup_{e=1}^{n_{sele}} G^{mech\ e}_c(\boldsymbol{\varphi}^h, \boldsymbol{\eta}^h_0) \\ G^{ther}_c(\Theta^h, \zeta^h_0) &:= \bigcup_{e=1}^{n_{sele}} G^{ther\ e}_c(\Theta^h, \zeta^h_0) \\ B^{mech}_{\varphi^h_t}(\boldsymbol{\eta}^h_0, \Delta\boldsymbol{\varphi}^h) &:= \bigcup_{e=1}^{n_{sele}} B^{mech\ e}_{\varphi^h_t}(\boldsymbol{\eta}^h_0, \Delta\boldsymbol{\varphi}^h) \end{aligned}$$

$$B^{ther}_{\Theta^h_t}(\zeta^h_0, \Delta\Theta^h) := \bigcup_{e=1}^{n_{sele}} B^{mech\ e}_{\Theta^h_t}(\zeta^h_0, \Delta\Theta^h) \tag{3.49}$$

where $G^{mech\ e}_c(\boldsymbol{\varphi}^h, \boldsymbol{\eta}^h_0)$ and $G^{ther\ e}_c(\Theta^h, \zeta^h_0)$, and $B^{mech\ e}_{\varphi^h_t}(\boldsymbol{\eta}^h_0, \Delta\boldsymbol{\varphi}^h)$ and $B^{mech\ e}_{\Theta^h_t}(\zeta^h_0, \Delta\Theta^h)$ represent the mechanical and thermal frictional contact contribution to the weak form and bilinear form, over a typical slave element surface $\Gamma^{(1)h}_e \subset \Gamma^{(1)h}$, given by (3.14) and (3.15)-(3.19) with L_2-inner products over the element domain.

Numerical integration of these element frictional contact contributions leads to the following expressions:

$$\begin{aligned}
G^{mech\ e}_c(\boldsymbol{\varphi}^h_e, \boldsymbol{\eta}^h_{0\,e}) &:= -\sum_{i=1}^{n_{int}} W_i\ j(\zeta_i)\ \delta\boldsymbol{\Phi}^{e,i}_c \cdot \boldsymbol{R}^{mech\ e,i}_c \\
G^{ther\ e}_c(\Theta^h_e, \zeta^h_{0\,e}) &:= -\sum_{i=1}^{n_{int}} W_i\ j(\zeta_i)\ \delta\boldsymbol{\Theta}^{e,i}_c \cdot \boldsymbol{R}^{ther\ e,i}_c \\
B^{mech\ e}_{\varphi^h_t}(\boldsymbol{\eta}^h_0, \Delta\boldsymbol{\varphi}^h) &:= \sum_{i=1}^{n_{int}} W_i\ j(\zeta_i)\ \delta\boldsymbol{\Phi}^{e,i}_c \cdot \boldsymbol{K}^{mech\ e,i}_c \cdot \Delta\boldsymbol{\Phi}^{e,i}_c \\
B^{ther\ e}_{\Theta^h_t}(\zeta^h_0, \Delta\Theta^h) &:= \sum_{i=1}^{n_{int}} W_i\ j(\zeta_i)\ \delta\boldsymbol{\Theta}^{e,i}_c \cdot \boldsymbol{K}^{ther\ e,i}_c \cdot \Delta\boldsymbol{\Theta}^{e,i}_c
\end{aligned} \tag{3.50}$$

where n_{int} is the number of integration points to be used in the quadrature rule over the domain $\Gamma^{(1)h}_e$, W_i is the weight of the quadrature point ζ_i, $j(\zeta_i) = \|\boldsymbol{X}_{,1}(\zeta_i) \times \boldsymbol{X}_{,2}(\zeta_i)\|$, where $\boldsymbol{X}_{,\alpha} = d\boldsymbol{X}/d\zeta^\alpha$, $\alpha = 1, 2$, is the jacobian of the isoparametric map at the quadrature point ζ_i, $\delta\boldsymbol{\Phi}^{e,i}_c$ and $\Delta\boldsymbol{\Phi}^{e,i}_c$ are vectors of involved nodal displacement variations corresponding to the quadrature point i of element e, $\delta\boldsymbol{\Theta}^{e,i}_c$ and $\Delta\boldsymbol{\Theta}^{e,i}_c$ are vectors of involved nodal temperature variations corresponding to the quadrature point i of element e, $\boldsymbol{R}^{mech\ e,i}_c$ and $\boldsymbol{K}^{mech\ e,i}_c$ are the mechanical frictional contact local element residual vector and tangent matrix corresponding to the quadrature point i, respectively, and $\boldsymbol{R}^{ther\ e,i}_c$ and $\boldsymbol{K}^{ther\ e,i}_c$ are the thermal frictional contact local element residual vector and tangent matrix corresponding to the quadrature point i, respectively.

REMARK 3.3. As it is evident from (3.50), the element residual and tangent finite element operators have been organized by (slave) quadrature point rather than by (slave) element. This scheme proves to be more convenient, taking into account that each (slave) quadrature point may involve degrees-of-freedom of (master) nodes of different (master) elements. Finite element operators associated to a typical (slave) quadrature point in a typical (slave) element, will involve the dof's of the (slave) nodes of its (slave) element and the dof's of the (master) nodes of the (master) element containing the contact point. On the other hand, finite element operators associated to a typical (slave) element, will involve the dof's of the (slave) nodes of its (slave) element and the dof's of the (master) nodes of the, possibly different, (master) elements containing each one of the contact points associated to each (slave) quadrature point. □

REMARK 3.4. Associated to each (slave) quadrature point we define a *contact element* involving degrees-of-freedom of the slave and master surface elements. When nodal quadrature points are used, the contact element involves the degrees-of-freedom of the slave node and the degrees-of-freedom of the master element surface containing the closest-point projection. When a different quadrature rule is used, the contact element involves all the degrees-of-freedom of the slave and master surface elements. □

(A) *Application: Residual and tangent operator for a n-node 3D surface element discretization.* In this section we will present the finite element implementation of the frictional contact model, assuming an arbitrary n-node finite element 3D spatial discretization of contact (master) surfaces. Furthermore, we will assume that nodal quadrature is used to define (3.50).

In what follows, we will restrict our attention to a typical slave quadrature point, i.e. a slave node using nodal quadrature, with current placement denoted as $\boldsymbol{x}$ and to the n-node master element surface containing its projection $\bar{\boldsymbol{y}} \in \gamma^{(2)h}$, denoted as $\gamma_e^{(2)h}$. It is assumed that the projection point $\bar{\boldsymbol{y}}$ lies in the interior domain of the surface element $\gamma_e^{(2)h}$.

We will denote as *contact element* the set of nodes consisting of the slave node (playing the role of quadrature point) and the n-master nodes defining the surface element $\gamma_e^{(2)h}$. Taking the nodal displacements as nodal degrees of freedom we will get the *mechanical contact element* while taking the nodal temperatures as nodal degrees of freedom we will get the *thermal contact element*.

(A.1) *Mechanical contact element.* Associated to each mechanical contact element we define the vectors of nodal displacement variations $\delta\boldsymbol{\Phi}_c$ and $\Delta\boldsymbol{\Phi}_c$ containing the displacement variation of the slave (quadrature) node, denoted as $\delta\boldsymbol{d}_s$ and $\Delta\boldsymbol{d}_s$ respectively, and those of the n-master nodes in $\gamma_e^{(2)h}$, denoted as $\delta\boldsymbol{d}_a$ and $\Delta\boldsymbol{d}_a$, $a = 1, \ldots, n$, respectively, as

$$\delta\boldsymbol{\Phi}_c := \left\{ \begin{array}{c} \delta\boldsymbol{d}_s \\ \delta\boldsymbol{d}_1 \\ \cdot \\ \cdot \\ \delta\boldsymbol{d}_n \end{array} \right\}, \qquad \Delta\boldsymbol{\Phi}_c := \left\{ \begin{array}{c} \Delta\boldsymbol{d}_s \\ \Delta\boldsymbol{d}_1 \\ \cdot \\ \cdot \\ \Delta\boldsymbol{d}_n \end{array} \right\} \tag{3.51}$$

Furthermore we introduce the following operators

$$\boldsymbol{N} = \left\{ \begin{array}{c} \boldsymbol{\nu} \\ -N_1(\bar{\boldsymbol{\xi}})\ \boldsymbol{\nu} \\ \cdot \\ \cdot \\ -N_n(\bar{\boldsymbol{\xi}})\ \boldsymbol{\nu} \end{array} \right\}, \quad \boldsymbol{T}_\alpha = \left\{ \begin{array}{c} \boldsymbol{\tau}_\alpha \\ -N_1(\bar{\boldsymbol{\xi}})\ \boldsymbol{\tau}_\alpha \\ \cdot \\ \cdot \\ -N_n(\bar{\boldsymbol{\xi}})\ \boldsymbol{\tau}_\alpha \end{array} \right\}, \quad \boldsymbol{N}_\alpha = \left\{ \begin{array}{c} 0 \\ -N_{1,\alpha}(\bar{\boldsymbol{\xi}})\ \boldsymbol{\nu} \\ \cdot \\ \cdot \\ -N_{n,\alpha}(\bar{\boldsymbol{\xi}})\ \boldsymbol{\nu} \end{array} \right\}, \tag{3.52}$$

where $\alpha = 1, 2$, and N_a, $a = 1, \ldots, n$ are the standard isoparametric shape functions of the arbitrary n-node element. Using the operators introduced above, we also define:

$$\begin{aligned} \boldsymbol{D}^\alpha &:= A^{\alpha\beta}(\boldsymbol{T}_\beta + g_N \boldsymbol{N}_\beta) \\ \bar{\boldsymbol{N}}_\alpha &:= \boldsymbol{N}_\alpha - \kappa_{\alpha\beta}\boldsymbol{D}^\beta \end{aligned} \tag{3.53}$$

where the indices α and β ranges from 1 to 2 and the summatory on repeated indices is assumed. Here, $A^{\alpha\beta}$ are the components of the inverse of matrix $\boldsymbol{A}$ defined in (2.99).

With the preceding notation in hand, and using the key discrete relations,

$$\begin{aligned} \delta g_N^h &:= -\boldsymbol{N} \cdot \delta\boldsymbol{\Phi}_c \\ \delta\bar{\xi}^{\alpha h} &:= \boldsymbol{D}^\alpha \cdot \delta\boldsymbol{\Phi}_c \end{aligned} \tag{3.54}$$

the mechanical frictional contact residual $\boldsymbol{R}_c^{mech}$ takes the expression,

$$\boxed{\boldsymbol{R}_c^{mech} := t_N\ \boldsymbol{N} - t_{T\alpha}\boldsymbol{D}^\alpha} \tag{3.55}$$

where $\alpha = 1, 2$.

The mechanical frictional contact tangent operator can be split into the *normal* and *tangent* contributions.

$$\boldsymbol{K}_c^{mech} := \boldsymbol{K}_{c_N}^{mech} + \boldsymbol{K}_{c_T}^{mech} \tag{3.56}$$

Additionally , from the mechanical *material* and *geometric* terms in the bilinear form (3.15), the mechanical normal con tact and frictional tangent operators, can be split as

$$\begin{aligned} \boldsymbol{K}_{c_N}^{mech} &:= \boldsymbol{K}_{c_N}^{mech,mat} + \boldsymbol{K}_{c_N}^{mech,geo} \\ \boldsymbol{K}_{c_T}^{mech} &:= \boldsymbol{K}_{c_T}^{mech,mat} + \boldsymbol{K}_{c_T}^{mech,geo} \end{aligned} \tag{3.57}$$

where $\boldsymbol{K}_{c_N}^{mech,mat}$ and $\boldsymbol{K}_{c_N}^{mech,geo}$ are the material and geometric contributions to the mechanical normal con tact tangent operator, respectively,and $\boldsymbol{K}_{c_T}^{mech,mat}$ and $\boldsymbol{K}_{c_T}^{mech,geo}$ are the material and geometric contributions to the mec hanical frictional tangent operator, respectively.

Using the operators defined abo ve, the mec hanical normal con tact tangent operators can be written as

$$\boxed{\begin{aligned} \boldsymbol{K}_{c_N}^{mech,mat} &:= \epsilon_N H(g_N)\ \boldsymbol{N} \otimes \boldsymbol{N} \\ \boldsymbol{K}_{c_N}^{mech,geo} &:= t_N\ [g_N\ m^{\alpha\beta} \bar{\boldsymbol{N}}_\alpha \otimes \bar{\boldsymbol{N}}_\beta - (\boldsymbol{D}^\alpha \otimes \boldsymbol{N}_\alpha + \boldsymbol{N}_\alpha \otimes \boldsymbol{D}^\alpha) + \kappa_{\alpha\beta} \boldsymbol{D}^\alpha \otimes \boldsymbol{D}^\beta] \end{aligned}} \tag{3.58}$$

To define the mec hanical frictional tangent operators, we introduce first the following operators:

$$\begin{aligned} \boldsymbol{T}_{\alpha\beta} &:= [0^T,\ -N_{1,\beta}(\bar{\boldsymbol{\xi}})\ \boldsymbol{\tau}_\alpha^T,\ \ldots,\ -N_{n,\beta}(\bar{\boldsymbol{\xi}})\ \boldsymbol{\tau}_\alpha^T]^T \\ \boldsymbol{N}_{\alpha\beta} &:= [0^T,\ -N_{1,\alpha\beta}(\bar{\boldsymbol{\xi}})\boldsymbol{\nu}^T,\ \ldots,\ -N_{n,\alpha\beta}(\bar{\boldsymbol{\xi}})\boldsymbol{\nu}^T]^T \\ \boldsymbol{P}_\alpha &:= [0^T,\ -N_{1,\alpha}(\bar{\boldsymbol{\xi}})\ \boldsymbol{p}_T^{\flat T},\ \ldots,\ -N_{n,\alpha}(\bar{\boldsymbol{\xi}})\ \boldsymbol{p}_T^{\flat T}]^T \end{aligned} \tag{3.59}$$

where $\alpha, \beta = 1, 2$, and the shape functions are evaluated at $\bar{\boldsymbol{\xi}}$. Based on the definitions (3.52), (3.53) and (3.59), we introduce the additional operators

$$\begin{aligned} \bar{\boldsymbol{T}}_{\alpha\beta} &:= \boldsymbol{T}_{\alpha\beta} - (\boldsymbol{e}_{\beta,\gamma}(\bar{\boldsymbol{\xi}}) \cdot \boldsymbol{\tau}_\alpha) \boldsymbol{D}^\gamma \\ \bar{\boldsymbol{P}}_\alpha &:= \boldsymbol{P}_\alpha - (\boldsymbol{e}_{\alpha,\gamma}(\bar{\boldsymbol{\xi}}) \cdot \boldsymbol{p}_T^\flat) \boldsymbol{D}^\gamma \\ \hat{\boldsymbol{T}}_{\alpha\beta} &:= \boldsymbol{T}_{\alpha\beta} + g_N \boldsymbol{N}_{\alpha\beta} \\ \hat{\boldsymbol{D}}^\alpha &:= \boldsymbol{D}^\alpha - m^{\alpha\beta} \boldsymbol{T}_\beta \end{aligned} \tag{3.60}$$

where $\alpha, \beta = 1, 2$

With the preceding definitions in hand and the key expressions

$$\begin{aligned} (\delta\boldsymbol{\varphi}^{(1)h} - \delta\boldsymbol{\varphi}^{(2)h}) \cdot \boldsymbol{\tau}_\alpha &:= \boldsymbol{T}_\alpha \cdot \delta\boldsymbol{\Phi}_c \\ \delta\boldsymbol{\varphi}_{,\alpha}^{(2)h} \cdot \boldsymbol{\nu} &:= -\boldsymbol{N}_\alpha \cdot \delta\boldsymbol{\Phi}_c \\ \delta\boldsymbol{\varphi}_{,\alpha}^{(2)h} \cdot \boldsymbol{\tau}_\beta &:= -\boldsymbol{T}_{\beta\alpha} \cdot \delta\boldsymbol{\Phi}_c \\ \delta\boldsymbol{\varphi}_{,\alpha\beta}^{(2)h} \cdot \boldsymbol{\nu} &:= -\boldsymbol{N}_{\alpha\beta} \cdot \delta\boldsymbol{\Phi}_c \end{aligned} \tag{3.61}$$

the geometric part of the mechanical frictional tangent operator can be written as

$$\boxed{\begin{aligned}
\boldsymbol{K}_{c_T}^{mech,geo} &:= t_{T_\alpha} A^{\alpha\beta} \boldsymbol{K}_{c_T\beta}^{mech,geo} \\
\boldsymbol{K}_{c_T\alpha}^{mech,geo} &:= \hat{\boldsymbol{T}}_{\alpha\beta} \otimes \boldsymbol{D}^\beta + \boldsymbol{D}^\beta \otimes \hat{\boldsymbol{T}}_{\alpha\beta} \\
&\quad + \hat{\boldsymbol{D}}^\beta \otimes \bar{\boldsymbol{T}}_{\beta\alpha} + \bar{\boldsymbol{T}}_{\beta\alpha} \otimes \hat{\boldsymbol{D}}^\beta \\
&\quad - (\boldsymbol{N} \otimes \bar{\boldsymbol{N}}_\alpha + \bar{\boldsymbol{N}}_\alpha \otimes \boldsymbol{N}) \\
&\quad - (\boldsymbol{e}_{\beta,\gamma}(\bar{\boldsymbol{\xi}}) \cdot \boldsymbol{\tau}_\alpha + g_N \; \boldsymbol{e}_{\alpha,\beta\gamma}(\bar{\boldsymbol{\xi}}) \cdot \boldsymbol{\nu}) \; \boldsymbol{D}^\beta \otimes \boldsymbol{D}^\gamma
\end{aligned}} \tag{3.62}$$

The material part of the mechanical frictional tangent operator will depend of the slip/stick frictional state. Using the above definitions, the mechanical *stick* material frictional tangent operator, denoted as $\boldsymbol{K}_{c_T}^{mech,mat,stick}$ and the mechanical *slip* material frictional tangent operator, denoted as $\boldsymbol{K}_{c_T}^{mech,mat,slip}$, can be written as

$$\boxed{\begin{aligned}
\boldsymbol{K}_{c_T}^{mech,mat,stick} &:= \Xi_{\alpha\beta} \; \boldsymbol{D}^\alpha \otimes \boldsymbol{D}^\beta \\
\boldsymbol{K}_{c_T}^{mech,mat,slip} &:= -(1-\bar{\beta}_2) \; \mu(\alpha) \; \epsilon_N \; H(g_N) \; p_{T_\alpha} \; \boldsymbol{D}^\alpha \otimes \boldsymbol{N} \\
&\quad + [\frac{\mu(\alpha) \; t_N}{\| \boldsymbol{t}_T^{trial} \|} (\delta_\alpha^\gamma - \pi_\alpha^\gamma) + \bar{\beta}_1 \; \pi_\alpha^\gamma] \; \Xi_{\gamma\beta} \; \boldsymbol{D}^\alpha \otimes \boldsymbol{D}^\beta \\
&\quad - [\mu(\alpha) \; t_N - \frac{\bar{\beta}_1}{\| \boldsymbol{t}_T^{trial} \|}] \; \pi_\alpha^\beta \; \boldsymbol{D}^\alpha \otimes \bar{\boldsymbol{P}}_\beta
\end{aligned}} \tag{3.63}$$

where $\bar{\beta}_1 := \beta_1 \; \partial_\alpha \mu(\alpha) \; t_N$ and $\bar{\beta}_2 := \beta_2 \; \partial_\alpha \mu(\alpha) \; t_N$ and β_1 and β_2 are given in (3.45).

REMARK 3.5. *Bi-linear surface elements.* Note that for the particular case of 4-node bi-linear surface finite elements, $\boldsymbol{N}_{\alpha\beta} = 0$ for $\alpha = \beta$, $\boldsymbol{e}_{\alpha,\beta} = 0$ for $\alpha = \beta$, $\boldsymbol{e}_{\alpha,\beta\gamma} = 0$ for any α, β, γ, $\boldsymbol{E}_{\alpha,\beta} = 0$ for $\alpha = \beta$ and the components of the *non-symmetric* operator $\Xi_{\alpha\beta}$ $(3.43)_1$ take the form:

$$\begin{aligned}
\Xi_{11} &:= \epsilon_T \; (M_{11} + \lambda_1 g_T^2) \\
\Xi_{12} &:= \epsilon_T \; (M_{12} + 2\lambda_1 g_T^1 + \lambda_2 g_T^2) \\
\Xi_{21} &:= \epsilon_T \; (M_{21} + \lambda_1 g_T^1 + 2\lambda_2 g_T^2) \\
\Xi_{22} &:= \epsilon_T \; (M_{22} + \lambda_2 g_T^1)
\end{aligned} \tag{3.64}$$

where the short hand notation $\lambda_\alpha := \boldsymbol{E}_{1,2}(\bar{\boldsymbol{\xi}}) \cdot \boldsymbol{\tau}_\alpha^{ref}$ and $g_T^\alpha := \bar{\xi}_{n+\vartheta}^\alpha - \bar{\xi}_n^\alpha$ has been introduced. In the above expressions, greek indices α, β, γ varies from 1 to 2. □

(A.2) *Thermal contact element.* Associated to each thermal contact element we define the vectors of nodal temperature variations $\delta\boldsymbol{\Theta}_c$ and $\Delta\boldsymbol{\Theta}_c$ containing the temperature variation of the slave (quadrature) node, denoted as $\delta\Theta_s$ and $\Delta\Theta_s$ respectively, and those of the n-master nodes in $\gamma_e^{(2)h}$, denoted as $\delta\Theta_a$ and $\Delta\Theta_a$, $a = 1, \ldots, n$, respectively, as

$$\delta\boldsymbol{\Theta}_c := \left\{ \begin{array}{c} \delta\Theta_s \\ \delta\Theta_1 \\ \cdot \\ \cdot \\ \delta\Theta_n \end{array} \right\}, \qquad \Delta\boldsymbol{\Theta}_c := \left\{ \begin{array}{c} \Delta\Theta_s \\ \Delta\Theta_1 \\ \cdot \\ \cdot \\ \Delta\Theta_n \end{array} \right\} \tag{3.65}$$

Furthermore we introduce the following operators

$$\boldsymbol{T}_{\Theta} = \left\{ \begin{array}{c} 1 \\ -N_1(\bar{\boldsymbol{\xi}}) \\ \cdot \\ \cdot \\ -N_n(\bar{\boldsymbol{\xi}}) \end{array} \right\}, \quad \boldsymbol{T}_{G} = \left\{ \begin{array}{c} h_{\epsilon} \\ (1-h_{\epsilon})\ N_1(\bar{\boldsymbol{\xi}}) \\ \cdot \\ \cdot \\ (1-h_{\epsilon})\ N_n(\bar{\boldsymbol{\xi}}) \end{array} \right\}, \tag{3.66}$$

where h_{ϵ} is the relative effusivity of the slave surface and N_a, $a = 1, \ldots, n$ are the standard isoparametric shape functions of the arbitrary n-node master element.

With the preceding notation in hand, and using the key discrete relations,

$$\begin{aligned} \delta g_{\theta}^{h} &:= \boldsymbol{T}_{\Theta} \cdot \delta \boldsymbol{\Theta}_c \\ \delta \theta_{G}^{h} &:= \boldsymbol{T}_{G} \cdot \delta \boldsymbol{\Theta}_c \end{aligned} \tag{3.67}$$

the thermal frictional con tact residual $\boldsymbol{R}_c^{ther}$ takes the expression,

$$\boxed{\boldsymbol{R}_c^{ther} := -Q_{hc}\ \boldsymbol{T}_{\Theta} + \mathcal{D}_{fric}\ \boldsymbol{T}_{G}} \tag{3.68}$$

The thermal frictional contact tangent operator can be split into the *conduction* $\boldsymbol{K}_{c_N}^{ther}$ and *frictional dissipation* $\boldsymbol{K}_{c_T}^{ther}$ contributions.

$$\boldsymbol{K}_c^{ther} := \boldsymbol{K}_{c_N}^{ther} + \boldsymbol{K}_{c_T}^{ther} \tag{3.69}$$

Additionally, from the thermal *material* and *geometric* terms in the bilinear form (3.15), the thermal normal contact and frictional tangent operators, can be split as

$$\begin{aligned} \boldsymbol{K}_{c_N}^{ther} &:= \boldsymbol{K}_{c_N}^{ther,mat} + \boldsymbol{K}_{c_N}^{ther,geo} \\ \boldsymbol{K}_{c_T}^{ther} &:= \boldsymbol{K}_{c_T}^{ther,mat} + \boldsymbol{K}_{c_T}^{ther,geo} \end{aligned} \tag{3.70}$$

where $\boldsymbol{K}_{c_N}^{ther,mat}$ and $\boldsymbol{K}_{c_N}^{ther,geo}$ are the material and geometric contributions to the thermal normal con tact tangent operator, respectively, and $\boldsymbol{K}_{c_T}^{ther,mat}$ and $\boldsymbol{K}_{c_T}^{ther,geo}$ are the material and geometric con tributions to the thermal frictional tangen t operator, respectively.

Using the thermal operators defined above, the thermal normal contact tangent operators can be written as

$$\boxed{\begin{aligned} \boldsymbol{K}_{c_N}^{ther,mat} &:= \hat{h}(t_{N\,n+1}, \theta_{G\,n+1}) H(g_{N\,n+1})\ \boldsymbol{T}_{\Theta} \otimes \boldsymbol{T}_{\Theta} \\ &\quad + \partial_{\theta_G} \hat{h}(t_{N\,n+1}, \theta_{G\,n+1})\ \boldsymbol{T}_{\Theta} \otimes \boldsymbol{T}_{G} \\ \boldsymbol{K}_{c_N}^{ther,geo} &:= 0 \end{aligned}} \tag{3.71}$$

where the last expression arise from the fact that $\Delta(\delta g_{\theta}) = 0$ for a fixed configuration.

The thermal frictional tangent operators take the form

$$\boxed{\begin{aligned} \boldsymbol{K}_{c_T}^{ther,mat} &:= -\partial_{\theta_G} \mathcal{D}_{fric}\ \boldsymbol{T}_{G} \otimes \boldsymbol{T}_{G} \\ \boldsymbol{K}_{c_T}^{ther,geo} &:= 0 \end{aligned}} \tag{3.72}$$

where the last expression arise from the fact that a constant effusivity parameter has been implicitly assumed and then $\Delta(\delta \theta_G) = 0$ for a fixed configuration.

(B) *Application: Residual and tangen t operator for a n-node 2D surface elemen t discretization.* Here we will presen t the finite elemen t implemen tation of the frictional contact

model, assuming an arbitrary n-node finite element 2D spatial discretization of contact (master) surfaces. Furthermore, we will assume that nodal quadrature is used to define (3.50).

In what follows, we will restrict our attention to a typical slave quadrature point, i.e. a slave node using nodal quadrature, with current placement denoted as $\boldsymbol{x}$ and to the n-node master element surface containing its projection $\bar{\boldsymbol{y}} \in \gamma^{(2)h}$, denoted as $\gamma_e^{(2)h}$. It is assumed that the projection point $\bar{\boldsymbol{y}}$ lies in the interior domain of the surface element $\gamma_e^{(2)h}$.

We will denote as *contact element* the set of nodes consisting of the slave node (playing the role of quadrature point) and the n-master nodes defining the surface element $\gamma_e^{(2)h}$. Taking the nodal displacements as nodal degrees of freedom we will get the *mechanical contact element* while taking the nodal temperatures as nodal degrees of freedom we will get the *thermal contact element*

(B.1) *Mechanical contact element.* Associated to each contact element we define the vectors of nodal variations $\delta\boldsymbol{\Phi}_c$ and $\Delta\boldsymbol{\Phi}_c$ containing the variation of the slave (quadrature) node, denoted as $\delta\boldsymbol{d}_s$ and $\Delta\boldsymbol{d}_s$ respectively, and those of the n-master nodes in $\gamma_e^{(2)h}$, denoted as $\delta\boldsymbol{d}_a$ and $\Delta\boldsymbol{d}_a$, $a = 1, \ldots, n$, respectively, as

$$\delta\boldsymbol{\Phi}_c := \left\{ \begin{array}{c} \delta\boldsymbol{d}_s \\ \delta\boldsymbol{d}_1 \\ \cdot \\ \cdot \\ \delta\boldsymbol{d}_n \end{array} \right\}, \qquad \Delta\boldsymbol{\Phi}_c := \left\{ \begin{array}{c} \Delta\boldsymbol{d}_s \\ \Delta\boldsymbol{d}_1 \\ \cdot \\ \cdot \\ \Delta\boldsymbol{d}_n \end{array} \right\} \tag{3.73}$$

Furthermore we introduce the following operators

$$\boldsymbol{N} = \left\{ \begin{array}{c} \boldsymbol{\nu} \\ -N_1(\bar{\boldsymbol{\xi}})\ \boldsymbol{\nu} \\ \cdot \\ \cdot \\ -N_n(\bar{\boldsymbol{\xi}})\ \boldsymbol{\nu} \end{array} \right\}, \quad \boldsymbol{T}_1 = \left\{ \begin{array}{c} \boldsymbol{\tau}_1 \\ -N_1(\bar{\boldsymbol{\xi}})\ \boldsymbol{\tau}_1 \\ \cdot \\ \cdot \\ -N_n(\bar{\boldsymbol{\xi}})\ \boldsymbol{\tau}_1 \end{array} \right\}, \quad \boldsymbol{N}_1 = \left\{ \begin{array}{c} 0 \\ -N_{1,1}(\bar{\boldsymbol{\xi}})\ \boldsymbol{\nu} \\ \cdot \\ \cdot \\ -N_{n,1}(\bar{\boldsymbol{\xi}})\ \boldsymbol{\nu} \end{array} \right\}, \tag{3.74}$$

where N_a, $a = 1, \ldots, n$, are the standard isoparametric shape functions of the arbitrary n-node element. Using the operators introduced above, we also define:

$$\begin{aligned} \boldsymbol{D}^1 &:= A^{11}(\boldsymbol{T}_1 + g_N \boldsymbol{N}_1) \\ \bar{\boldsymbol{N}}_1 &:= \boldsymbol{N}_1 - \kappa_{11}\boldsymbol{D}^1 \end{aligned} \tag{3.75}$$

were, A^{11} is the inverse of $A_{11} = m_{11} + g_N\ \kappa_{11}$.

With the preceding notation in hand, and using the key discrete relations,

$$\begin{aligned} \delta g_N^h &:= -\boldsymbol{N} \cdot \delta\boldsymbol{\Phi}_c \\ \delta\bar{\xi}^{1h} &:= \boldsymbol{D}^1 \cdot \delta\boldsymbol{\Phi}_c \end{aligned} \tag{3.76}$$

the frictional contact residual $\boldsymbol{R}_c$ takes the expression,

$$\boxed{\boldsymbol{R}_c := t_N\ \boldsymbol{N} - t_{T1}\boldsymbol{D}^1} \tag{3.77}$$

The frictional contact tangent operator can be split into the *normal* and *tangent* contributions.

$$\boldsymbol{K}_c := \boldsymbol{K}_{c_N} + \boldsymbol{K}_{c_T} \tag{3.78}$$

Additionally, from the *material* and *geometric* terms in the bilinear form (3.15), the normal contact and frictional tangent operators, can be split as

$$\begin{aligned} \boldsymbol{K}_{c_N} &:= \boldsymbol{K}_{c_N}^{mat} + \boldsymbol{K}_{c_N}^{geo} \\ \boldsymbol{K}_{c_T} &:= \boldsymbol{K}_{c_T}^{mat} + \boldsymbol{K}_{c_T}^{geo} \end{aligned} \tag{3.79}$$

where $\boldsymbol{K}_{c_N}^{mat}$ and $\boldsymbol{K}_{c_N}^{geo}$ are the material and geometric contributions to the normal contact tangent operator, respectively, and $\boldsymbol{K}_{c_T}^{mat}$ and $\boldsymbol{K}_{c_T}^{geo}$ are the material and geometric contributions to the frictional tangent operator, respectively.

Using the operators defined above, the normal contact tangent operators can be written as

$$\boxed{\begin{aligned} \boldsymbol{K}_{c_N}^{mat} &:= \epsilon_N H(g_N)\ \boldsymbol{N} \otimes \boldsymbol{N} \\ \boldsymbol{K}_{c_N}^{geo} &:= t_N\ [g_N\ m^{11} \bar{\boldsymbol{N}}_1 \otimes \bar{\boldsymbol{N}}_1 - (\boldsymbol{D}^1 \otimes \boldsymbol{N}_1 + \boldsymbol{N}_1 \otimes \boldsymbol{D}^1) + \kappa_{11} \boldsymbol{D}^1 \otimes \boldsymbol{D}^1] \end{aligned}} \tag{3.80}$$

To define the frictional tangent operators, we introduce first the following operators:

$$\begin{aligned} \boldsymbol{T}_{11} &:= [0^T,\ -N_{1,1}(\bar{\boldsymbol{\xi}})\ \boldsymbol{\tau}_1^T,\ \ldots,\ -N_{n,1}(\bar{\boldsymbol{\xi}})\ \boldsymbol{\tau}_1^T]^T \\ \boldsymbol{N}_{11} &:= [0^T,\ -N_{1,11}(\bar{\boldsymbol{\xi}})\boldsymbol{\nu}^T,\ \ldots,\ -N_{n,11}(\bar{\boldsymbol{\xi}})\boldsymbol{\nu}^T]^T \\ \boldsymbol{P}_1 &:= [0^T,\ -N_{1,1}(\bar{\boldsymbol{\xi}})\ \boldsymbol{p}_T^{\flat T},\ \ldots,\ -N_{n,1}(\bar{\boldsymbol{\xi}})\ \boldsymbol{p}_T^{\flat T}]^T \end{aligned} \tag{3.81}$$

where the shape functions are evaluated at $\bar{\boldsymbol{\xi}}$. Based on the definitions (3.74),(3.75) and (3.81), we introduce the additional operators

$$\begin{aligned} \bar{\boldsymbol{T}}_{11} &:= \boldsymbol{T}_{11} - (\boldsymbol{e}_{1,1}(\bar{\boldsymbol{\xi}}) \cdot \boldsymbol{\tau}_1)\boldsymbol{D}^1 \\ \bar{\boldsymbol{P}}_1 &:= \boldsymbol{P}_1 - (\boldsymbol{e}_{1,1}(\bar{\boldsymbol{\xi}}) \cdot \boldsymbol{p}_T^{\flat})\boldsymbol{D}^1 \\ \hat{\boldsymbol{T}}_{11} &:= \boldsymbol{T}_{11} + g_N \boldsymbol{N}_{11} \\ \hat{\boldsymbol{D}}^1 &:= \boldsymbol{D}^1 - m^{11}\boldsymbol{T}_1 \end{aligned} \tag{3.82}$$

With the preceding notation in hand, and using the key discrete relations,

$$\begin{aligned} (\delta\boldsymbol{\varphi}^{(1)h} - \delta\boldsymbol{\varphi}^{(2)h}) \cdot \boldsymbol{\tau}_1 &:= \boldsymbol{T}_1 \cdot \delta\boldsymbol{\Phi}_c \\ \delta\boldsymbol{\varphi}_{,1}^{(2)h} \cdot \boldsymbol{\nu} &:= -\boldsymbol{N}_1 \cdot \delta\boldsymbol{\Phi}_c \\ \delta\boldsymbol{\varphi}_{,1}^{(2)h} \cdot \boldsymbol{\tau}_1 &:= -\boldsymbol{T}_{11} \cdot \delta\boldsymbol{\Phi}_c \\ \delta\boldsymbol{\varphi}_{,11}^{(2)h} \cdot \boldsymbol{\nu} &:= -\boldsymbol{N}_{11} \cdot \delta\boldsymbol{\Phi}_c \end{aligned} \tag{3.83}$$

the geometric part of the frictional tangent operator can be written as

$$\boxed{\begin{aligned} \boldsymbol{K}_{c_T}^{geo} &:= t_{T_1} A^{11} \boldsymbol{K}_{c_{T_1}}^{geo} \\ \boldsymbol{K}_{c_{T_1}}^{geo} &:= \hat{\boldsymbol{T}}_{11} \otimes \boldsymbol{D}^1 + \boldsymbol{D}^1 \otimes \hat{\boldsymbol{T}}_{11} \\ &\quad + \hat{\boldsymbol{D}}^1 \otimes \bar{\boldsymbol{T}}_{11} + \bar{\boldsymbol{T}}_{11} \otimes \hat{\boldsymbol{D}}^1 \\ &\quad - (\boldsymbol{N} \otimes \bar{\boldsymbol{N}}_1 + \bar{\boldsymbol{N}}_1 \otimes \boldsymbol{N}) \\ &\quad - (\boldsymbol{e}_{1,1}(\bar{\boldsymbol{\xi}}) \cdot \boldsymbol{\tau}_1 + g_N\ \boldsymbol{e}_{1,11}(\bar{\boldsymbol{\xi}}) \cdot \boldsymbol{\nu})\ \boldsymbol{D}^1 \otimes \boldsymbol{D}^1 \end{aligned}} \tag{3.84}$$

The material part of the frictional tangent operator will depend of the slip/stick frictional state. Using the above definitions, the *stick* material frictional tangent operator, denoted as $\boldsymbol{K}_{c_T}^{mat,stick}$ and the *slip* material frictional tangent operator, denoted as $\boldsymbol{K}_{c_T}^{mat,slip}$, can be written as

$$\boxed{\begin{aligned}\boldsymbol{K}_{c_T}^{mat,stick} &:= \Xi_{11}\ \boldsymbol{D}^1 \otimes \boldsymbol{D}^1 \\ \boldsymbol{K}_{c_T}^{mat,slip} &:= -(1-\bar{\beta}_2)\ \mu(\alpha)\ \epsilon_N\ H(g_N)\ p_{T_1}\ \boldsymbol{D}^1 \otimes \boldsymbol{N} \\ &\quad + \bar{\beta}_1\ \Xi_{11}\ \boldsymbol{D}^1 \otimes \boldsymbol{D}^1 \\ &\quad - [\mu(\alpha)\ t_N - \frac{\bar{\beta}_1}{\|\boldsymbol{t}_T^{b\,trial}\|}]\ \ \boldsymbol{D}^1 \otimes \bar{\boldsymbol{P}}_1\end{aligned}} \tag{3.85}$$

where $\bar{\beta}_1 := \beta_1\ \partial_\alpha \mu(\alpha)\ t_N$ and $\bar{\beta}_2 := \beta_2\ \partial_\alpha \mu(\alpha)\ t_N$ and β_1 and β_2 are given in (3.45).

REMARK 3.6. *Linear surface elements.* Note that for the particular case of 2-node linear surface finite elements, $\boldsymbol{N}_{11} = 0$, $\boldsymbol{e}_{1,1} = 0$, $\kappa_{11} = 0$, $\boldsymbol{e}_{1,11} = 0$, $\boldsymbol{E}_{1,1} = 0$, $A^{11} = m^{11}$ and $\Xi_{11} := \epsilon_T\ M_{11}$. □

(B.2) *Thermal contact element.* The thermal contact finite element matrices and vectors for a 2D surface element discretization are the same than the ones given above for the general 3D surface element discretization.

4. NUMERICAL SIMULATIONS

The formulation presented in the preceding sections is illustrated below in a number of numerical simulations. The goals are to provide a practical accuracy assessment of the thermal frictional contact model and to demonstrate the robustness of the overall frictional contact formulation in different numerical simulations and particularly in metal forming operations. The calculations are performed with an enhanced version of the finite element program FEAP developed by R.L. Taylor and J.C. Simo and documented in Zienkiewicz & Taylor (1991).

(A) *Frictional Heating of a Block on a Rigid Surface.* This example is taken from Wriggers & Miehe (1992) and is concerned mainly with the mechanism of heating due to frictional dissipation. We consider an elastic block sliding over a rigid block. Both bodies are considered to be heat conductors. The upper body, a square block of 1.25 mm, moves within $3.75 \cdot 10^{-3}$ s from the left to the right end of the lower block. This lower block is a rectangle of 5.00 mm length by 1.25 mm height. During this process a pressure of 10 N/mm^2 is applied on the top of the upper block. Both bodies are considered to be of aluminium. The material parameters for aluminium are given in Table IV.1. Frictional behavior at the interface is considered through a constant frictional coefficient of 0.2 within a Coulomb frictional model.

The geometry of the problem was modeled with 25 continuum elements being utilized for the discretization of the upper elastic block and 100 continuum elements being utilized for the discretization of the lower rigid block. Frictional contact constraints were regularized by means of penalty method and the normal and tangential penalty parameters were taken as $\varepsilon_N = 1 \cdot 10^5$ N/mm^2 and $\varepsilon_T = 1 \cdot 10^5$ N/mm^2, respectively. The displacement of the upper block has been imposed by prescribing the driving tangential displacements at the top of the upper block. The sliding process has been achieved in 100 time steps. The sides of the blocks

Bulk Modulus	$\kappa = 58,333\ N/mm^2$
Shear Modulus	$G = 26,926\ N/mm^2$
Density	$\rho_0 = 2.7 \cdot 10^{-9}\ N\ s^2/mm^4$
Thermal Expansion Coefficient	$\alpha = 23.86 \cdot 10^{-6}\ K^{-1}$
Thermal Conductivity	$k = 150\ N/s\ K$
Thermal Capacity	$c = 0.9 \cdot 10^9\ mm^2/s^2\ K$
Thermal Resistance Coefficient	$h_{co} = 150\ N/s\ K$
Vickers Hardness	$H_e = 932\ N/mm^2$
Exponent	$\varepsilon = 0.95$
Relative Thermal Effusivity	$h_\epsilon = 0.5$

Table IV.1. Aluminium material properties

which are not in contact have been assumed thermally isolated. Heat conduction flux and frictional dissipation heat source at the contact interface have been considered. Plane strain conditions have been assumed in the analysis. A fractional step method, arising from an (isothermal) operator split of the momentum and reduced dissipation balance equations, was used to solve the coupled thermomechanical nonlinear system of equations. The Newton-Raphson method, combined with a line search optimization procedure, was used to solve the nonlinear system of equations arising from the spatial and temporal discretization of the weak form of the momentum and reduced dissipation balance equations. Convergence of the incremental iterative solution procedure was monitored by requiring a tolerance of 10^{-20} in the energy norm.

Table IV.2 shows the Euclidean norm of the residual at three typical mechanical + thermal time steps. For each step, the boldface line separates the mechanical and thermal entries of the Euclidean norm of the residual obtained in the solution of the mechanical and thermal problem, respectively.

Step 20	*Step* 50	*Step* 80
1.67464E+03	1.67464E+03	1.67463E+03
1.48534E+02	1.48549E+02	1.48556E+02
3.27963E+01	3.27688E+01	3.27540E+01
1.25703E+02	1.25322E+02	1.25152E+02
5.26016E+00	5.18675E+00	5.15008E+00
4.78359E-03	4.60015E-03	4.50579E-03
1.90039E-09	1.79104E-09	1.74612E-09
3.77591E+02	3.53182E+02	3.59583E+02
4.11398E-02	3.20033E-02	3.93119E-02
9.07564E-10	6.40018E-10	9.97886E-10

Table IV.2. Frictional Heating of an Elastic Block on a Rigid Surface. Euclidean norm of the residual at three typical mechanical + thermal time steps

Figures 4.1 and 4.2 show the (relative) temperature distribution and vertical component of the heat flux, respectively, for each one of the blocks, at three different stages of the sliding process: (a) Step=20, Time=$7.500 \cdot 10^{-4}$; (b) Step=50, Time=$1.875 \cdot 10^{-3}$; (c) Step=100, Time=$3.000 \cdot 10^{-3}$.

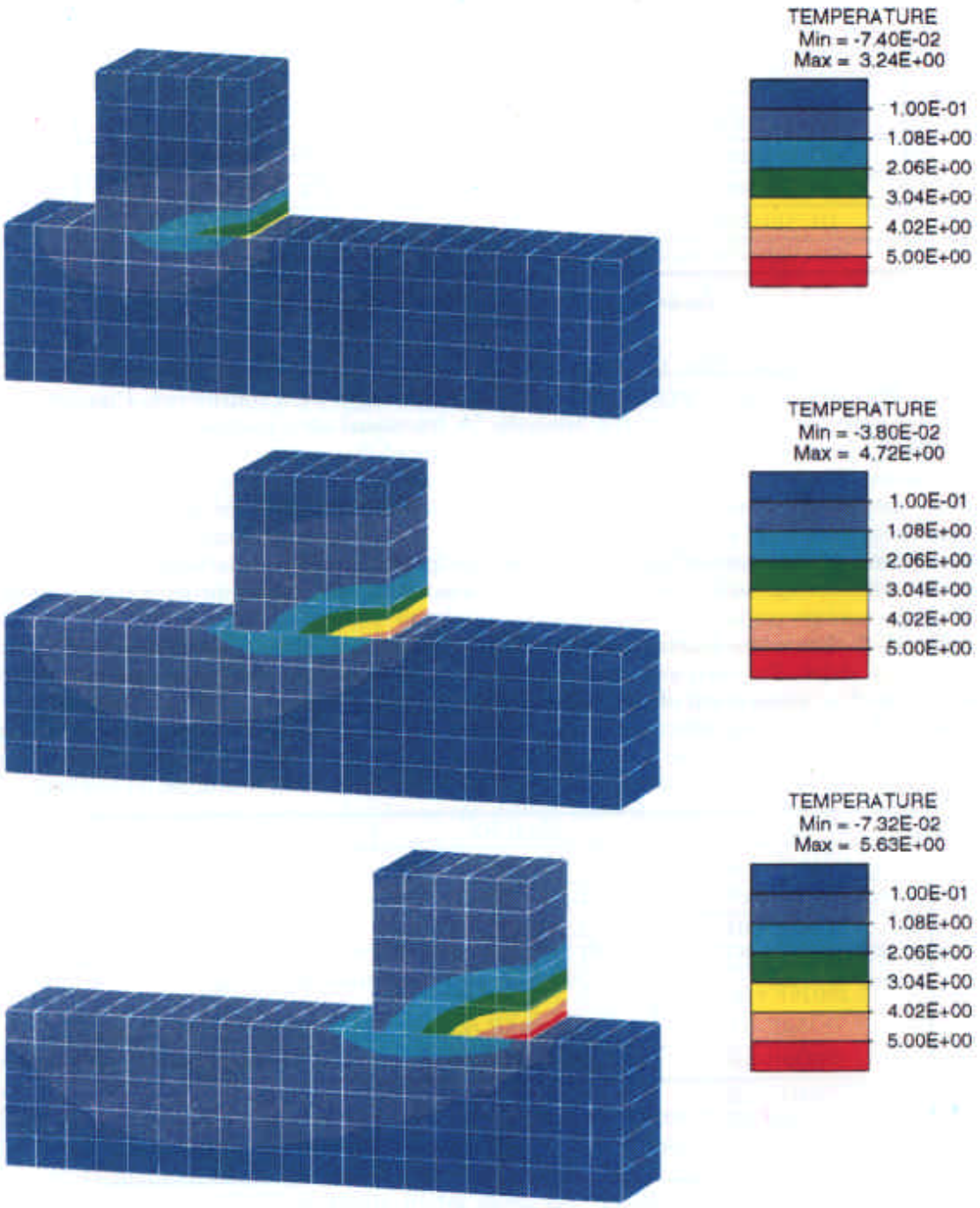

Figure 4.1. Frictional Heating of an Elastic Bloc k on a Rigid Surface. Relative temperature distribution at three different stages of the sliding process: (a) Step=20, Time=$7.500 \cdot 10^{-4}$; (b) Step=50, Time=$1.875 \cdot 10^{-3}$; (c) Step=100, Time=$3.000 \cdot 10^{-3}$

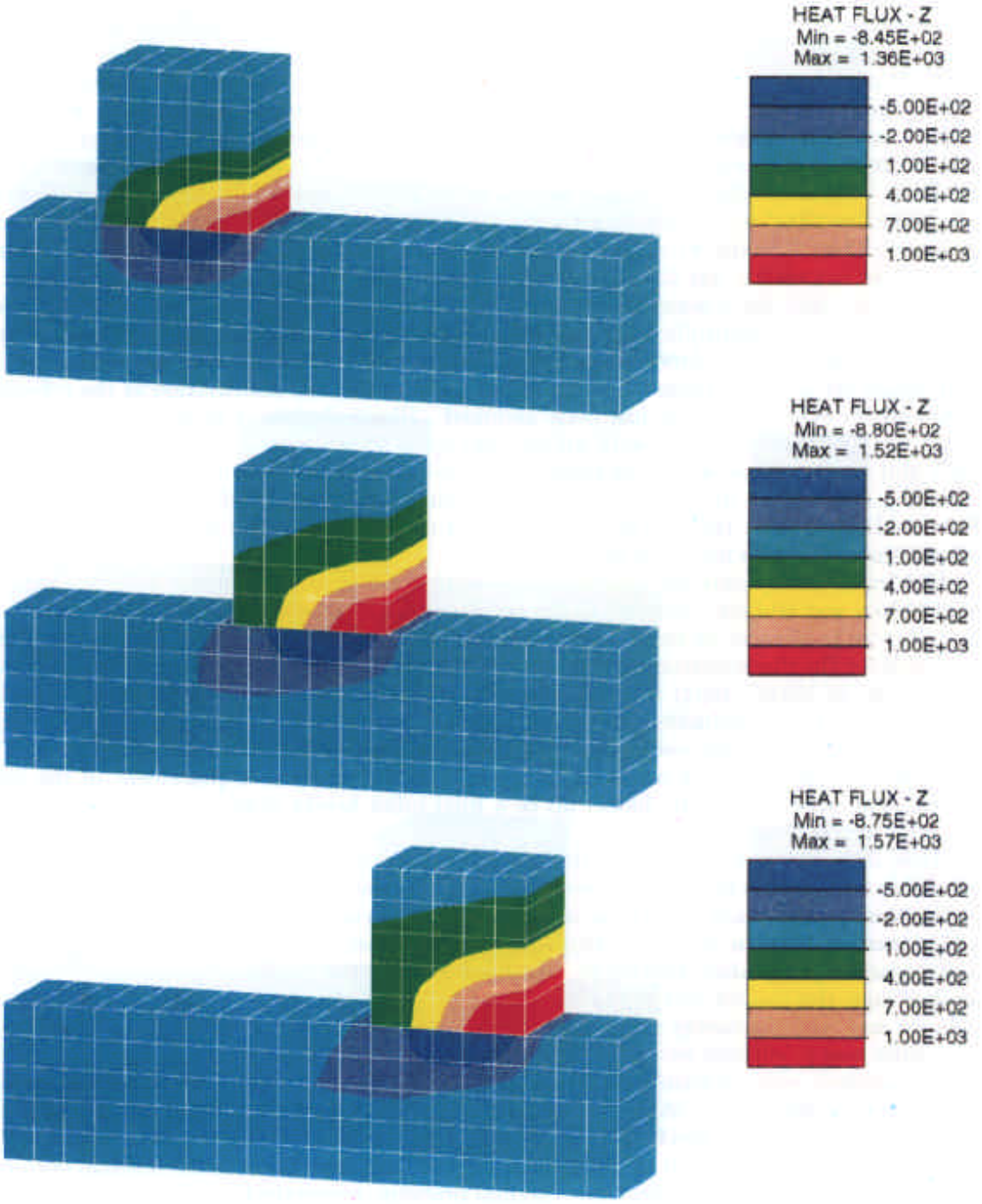

Figure 4.2. Frictional Heating of an Elastic Block on a Rigid Surface. Vertical heat flux distribution at three different stages of the sliding process: (a) Step=20, Time=$7.500 \cdot 10^{-4}$; (b) Step=50, Time=$1.875 \cdot 10^{-3}$; (c) Step=100, Time=$3.000 \cdot 10^{-3}$

Figures 4.3 and 4.4 show the frictional dissipation and contact pressure at the contact interface, at the same three different stages of the sliding process.

(B) *Upsetting of a Billet.* This example is taken from Wriggers & Miehe (1992) and is concerned with the numerical simulation of the thermoplastic upsetting process of an aluminium block. The block is pressed between two rigid plates which are able to conduct heat. Within this process heating of the block occurs due to plastic internal dissipation within the block and frictional dissipation on the contact surface. We consider a thermoplastic model of J_2-flow at finite strains, with a logarithmic stored free energy function and isotropic saturation hardening combined with thermal softening, summarized in Table IV.3. This model falls within the format of the general class of models for multiplicative plasticity described in Section 2, with the plastic incompressibility constraint $\det[\boldsymbol{F}^p] = 1$ enforced. Then $J := \det[\boldsymbol{F}] = \det[\boldsymbol{F}^e]$ and we denote as $\bar{\boldsymbol{b}}^e := J^{-2/3}\ \boldsymbol{b}^e$ the volume preserving part of the elastic left Cauchy-Green tensor $\boldsymbol{b}^e$. See Simo (1992,1994) and Armero & Simo (1992b,1993) for a detailed description of a particular class of exponential return mapping algorithms for multiplicative plasticity, which preserve the classical scheme of return mapping algorithms developed for infinitesimal plasticity. The material properties for the aluminium are given in Table IV.1. An initial uniform thermal distribution at the reference temperature $\Theta_0 = 293.15$ K has been assumed. Plastic behavior is characterized by an isotropic linear hardening law with initial yield stress at reference temperature $y_0(\Theta_0) = 70$ MPa and hardening parameter at reference temperature $h(\Theta_0) = 210$ MPa. Linear thermal softening is given by the thermal softening parameters $w_0 = 3 \cdot 10^{-4}$ and $w_h = 3 \cdot 10^{-4}$. Frictional behavior at the interface is considered through a constant frictional coefficient of 0.2 within a Coulomb frictional model.

Due to symmetry only one quarter of the system was discretized using 50 finite elements in the block and 60 finite elements in the rigid plate. The Q1/E12 assumed enhanced strain tri-linear finite element at finite deformations developed by Simo, Armero & Taylor (1993) was used for the discretization of the billet. The finite element mesh size used for the block in Wriggers & Miehe (1992) was not small enough to capture the temperature distribution generated by heat conduction and frictional dissipation at the contact surface, for high values of the billet height reduction. The billet is deformed within a time of 0.0035 s. The upsetting process has been achieved by prescribing the vertical displacement of the rigid plates. The upsetting of the block, up to a final billet height reduction of 60%, has been achieved in 100 time steps.

Time integration of the coupled thermoplastic problem was performed using a staggered algorithm based on an isothermal operator split of the governing equations. Time integration of the transient thermal equations, as well as the internal variables, has been done using a Backward-Euler time-stepping algorithm. The Newton-Raphson method, combined with a line search optimization procedure, was used to solve the nonlinear systems of equations arising from the spatial and temporal discretization of the weak form of the momentum balance and reduced energy equations. Convergence of the incremental iterative solution procedure was monitored by requiring a tolerance of 10^{-20} in the energy norm.

The analysis was performed in a Silicon Graphics Power Challenge L Workstation and it was accomplished in $7:58$ min CPU time. Table IV.4 shows the Euclidean norm of the residual at three typical mechanical + thermal time steps. For each step, the boldface line separates the mechanical and thermal entries of the Euclidean norm of the residual obtained in the solution of the mechanical and thermal problem, respectively.

Figures 4.5 and 4.6 show the (relative) temperature and equivalent plastic strain distribution, respectively, at different stages of the upsetting process, corresponding to billet height reductions of 30%, 45% and 60%.

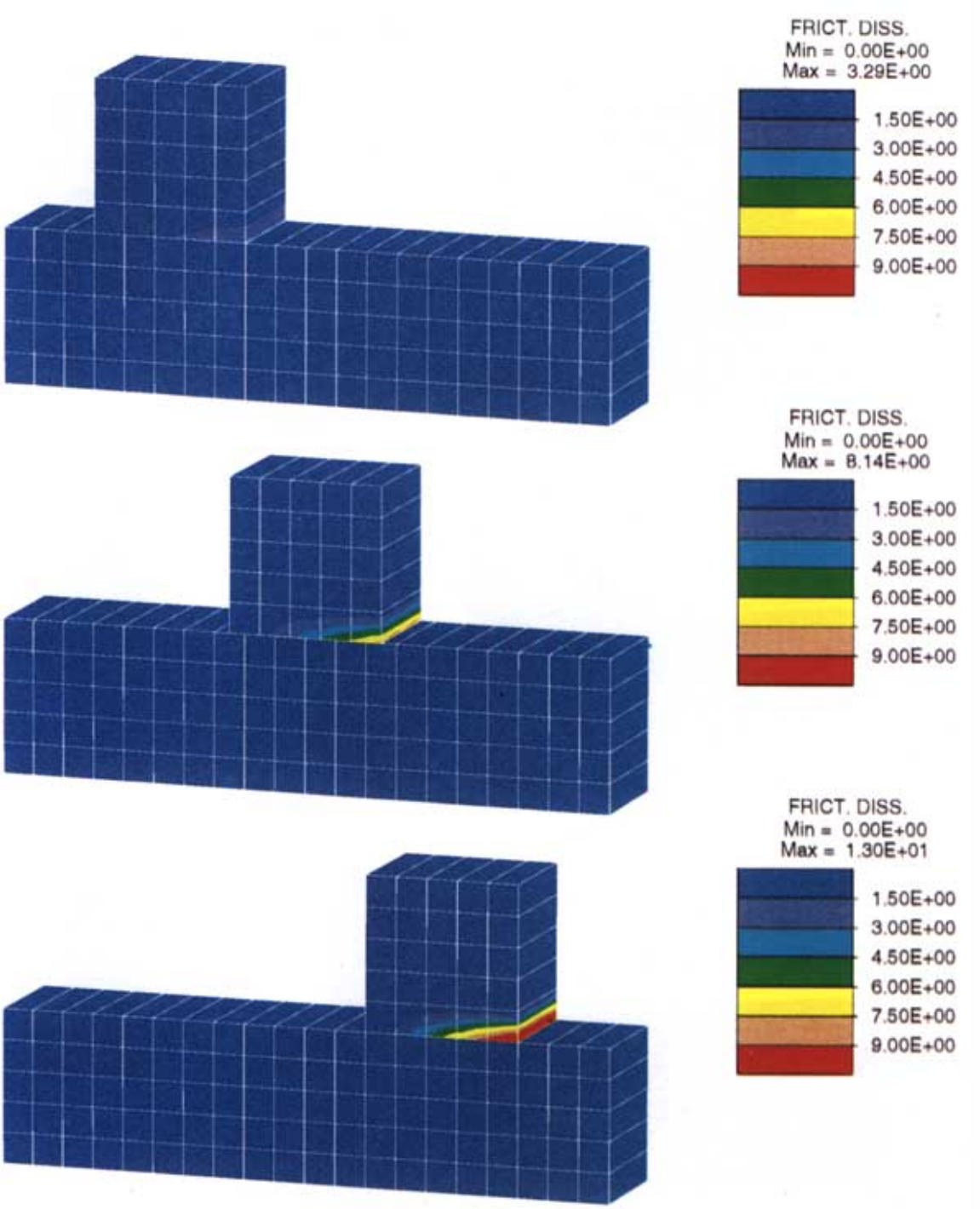

Figure 4.3. Frictional Heating of an Elastic Bloc k on a Rigid Surface. Frictional dissipation distribution at the contact interface at three different stages of the sliding process: (a) Step=20, Time=$7.500 \cdot 10^{-4}$; (b) Step=50, Time=$1.875 \cdot 10^{-3}$; (c) Step=100, Time=$3.000 \cdot 10^{-3}$

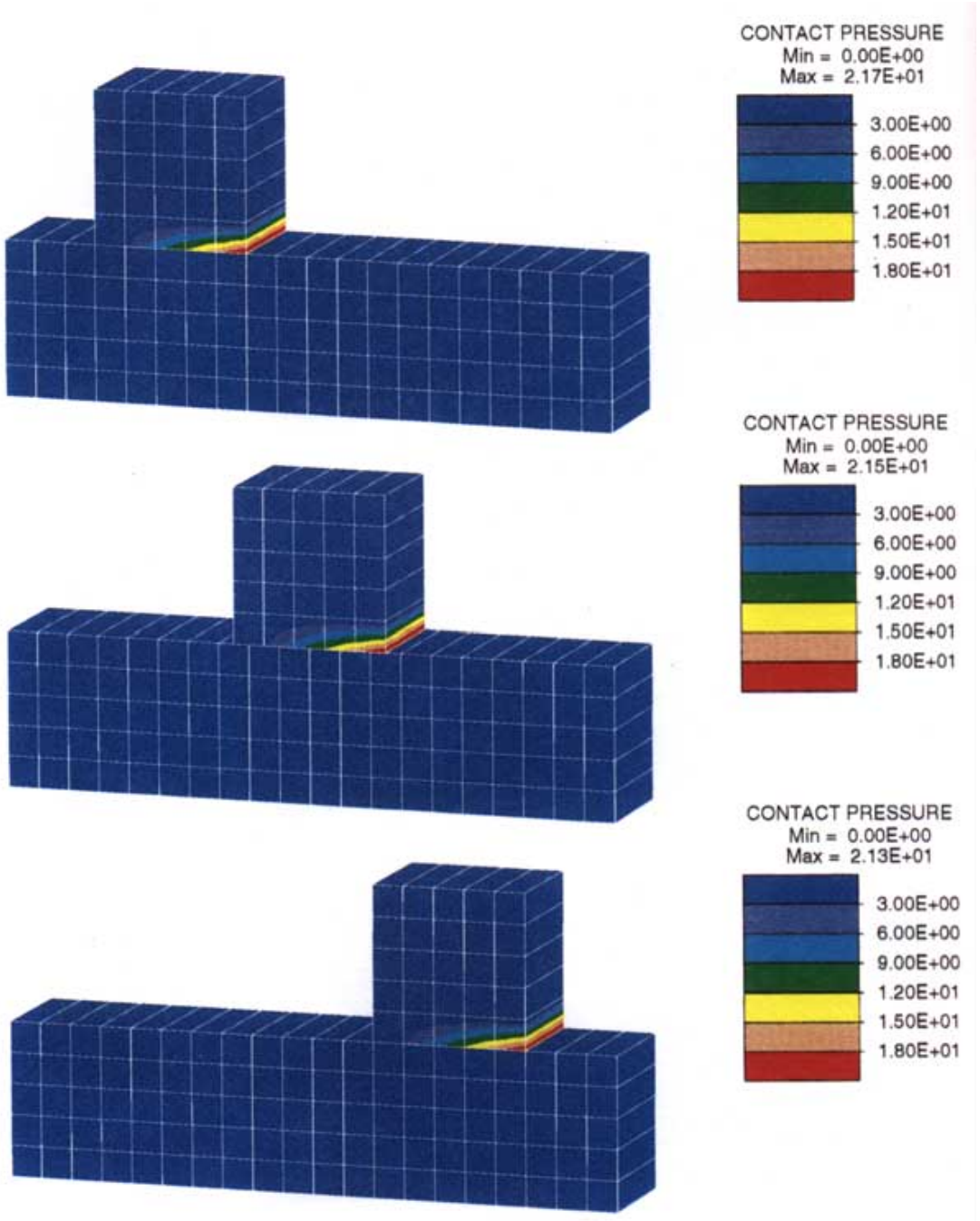

Figure 4.4. Frictional Heating of an Elastic Bloc k on a Rigid Surface. Con tact pressure distribution at the contact interface at three different stages of the sliding process: (a) Step=20, Time=$7.500 \cdot 10^{-4}$; (b) Step=50, Time=$1.875 \cdot 10^{-3}$; (c) Step=100, Time=$3.000 \cdot 10^{-3}$

1. *Free energy function:*

$$\hat{\psi}(\boldsymbol{b}^e, \xi, \Theta) = W(\bar{\boldsymbol{b}}^e) + U(J) + M(J, \Theta) + T(\Theta) + K(\xi, \Theta),$$

i. Logarithmic h yperelastic response ($\mu > 0$ and $\kappa > 0$ constants),

$$W(\bar{\boldsymbol{b}}^e) = \mu \sum_{A=1,3} [\log(\bar{\lambda}^e_A)]^2 \qquad \text{and} \qquad U(J) = \frac{1}{2}\kappa \log^2 J,$$

where $\bar{\lambda}^e_A = J^{-1/3}\ \lambda^e_A$ and λ^e_A are the elastic principal stretches.

ii. Thermoelastic coupling,

$$M(J, \Theta) = -3\kappa\alpha(\Theta - \Theta_0) \log J.$$

iii. Thermal con tribution,

$$T(\Theta) = c_0[(\Theta - \Theta_0) - \Theta \log(\Theta/\Theta_0)].$$

iv. Hardening poten tial,

$$K(\xi, \Theta) = \frac{1}{2}h(\Theta)\xi^2 - [y_0(\Theta) - y_\infty(\Theta)]\ H(\xi),$$

where

$$H(\xi) := \begin{cases} \xi - (1 - \exp^{-\delta\xi})/\delta, & \text{if } \delta \neq 0; \\ 0, & \text{if } \delta = 0. \end{cases}$$

2. *Plastic response:*

i. V on Mises yield criterion with flow stress $\sigma_Y(\Theta) := y_0(\Theta)$,

$$\hat{\phi}(\boldsymbol{\tau}, \beta, \Theta) = \sqrt{\frac{3}{2}}\|\mathrm{dev}[\boldsymbol{\tau}]\| + \beta - \sigma_Y(\Theta) \leq 0,$$

ii. Hardening v ariable β conjugate to ξ,

$$\beta := -\partial_\xi \hat{\psi} = -[h(\Theta)\xi - (y_0(\Theta) - y_\infty(\Theta))(1 - \exp^{-\delta\xi})].$$

iii. Linear thermal softening,

$$\left.\begin{aligned} y_0(\Theta) &= y_0(\Theta_0)[1 - w_0(\Theta - \Theta_0)] \\ h(\Theta) &= h(\Theta_0)[1 - w_h(\Theta - \Theta_0)] \\ y_\infty(\Theta) &= y_\infty(\Theta_0)[1 - w_h(\Theta - \Theta_0)] \end{aligned}\right\}$$

Table IV.3. Thermoplastic model: J_2-flow theory

Figures 4.7 and 4.8 sho w the frictional dissipation and con tact pressure distribution, respectively, at the contact surface, at the same differen t stages of the upsetting process.

Step 50	*Step* 75	*Step* 100
8.15773E+02	8.13804E+02	8.05270E+02
5.91627E+01	6.20615E+01	6.78419E+01
1.26919E+01	3.25550E+01	6.89033E+01
1.21883E+00	7.96927E+00	3.43222E+01
1.11981E-02	1.41444E-01	5.82032E+00
9.33841E-07	6.39979E-05	6.48231E-02
9.66732E-11	9.39676E-11	1.90928E-05
		1.20049E-10
1.45432E+04	2.75136E+04	7.88499E+04
1.03186E+01	4.29962E+01	3.91760E+02
1.09560E-05	1.88359E-04	2.21231E-02
8.65355E-10	8.86778E-10	9.28287E-10

Table IV.4. Upsetting of a Billet. Euclidean norm of the residual for three typical mechanical + thermal time steps

5. CONCLUDING REMARKS

A numerical model for the analysis of coupled thermomechanical multi-body frictional contact problems at finite deformations has been presented. The multi-body frictional contact formulation has been fully developed on a continuum setting within a fully non-linear kinematics. A contact pressure and temperature dependent thermal contact model has been considered.

The solution of the coupled problem was performed within the context of fractional step methods by a product formula algorithm arising from an operator split of the local evolution governing equations. This method leads to a partitioning of the coupled problem into a mechanical phase and a thermal phase to be solved sequentially by a staggered algorithm.

Within the context of the displacement-driven formulation of frictional contact problems, exploiting the computational framework developed for plasticity, two frictional return mapping algorithms have been considered: the BE and the implicit PMP rules. An exact linearization of the algorithms allows to derive the consistent frictional contact tangent operator.

Numerical simulations shown the suitability of the proposed model to deal with the analysis of fully coupled thermomechanical problems.

ACKNOWLEDGEMENT

Support for this work was provided by the European Commission through the BRITE-EURAM Project no. BE-5248-92, under contract no. BRE2-CT92-0180 and by the "Dirección General de Investigación Científica y Técnica, DGICYT" of the "Ministerio de Educación y Ciencia, MEC" of Spain, under grant no. 93-013. These support are gratefully acknowledged.

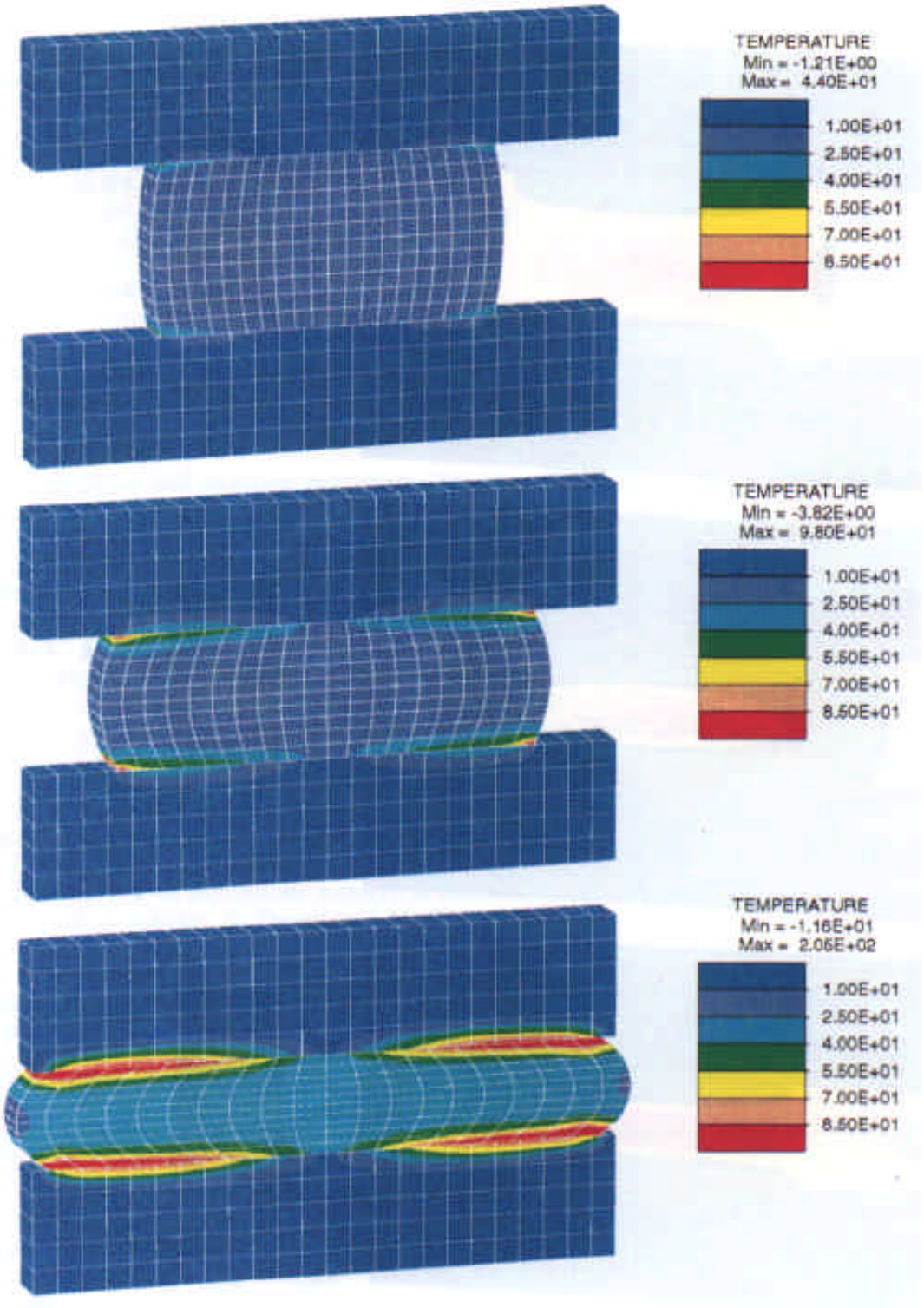

Figure 4.5. Upsetting of a Billet. Temperature distribution at three different time steps, corresponding to billet height reductions of 30%, 45% and 60%

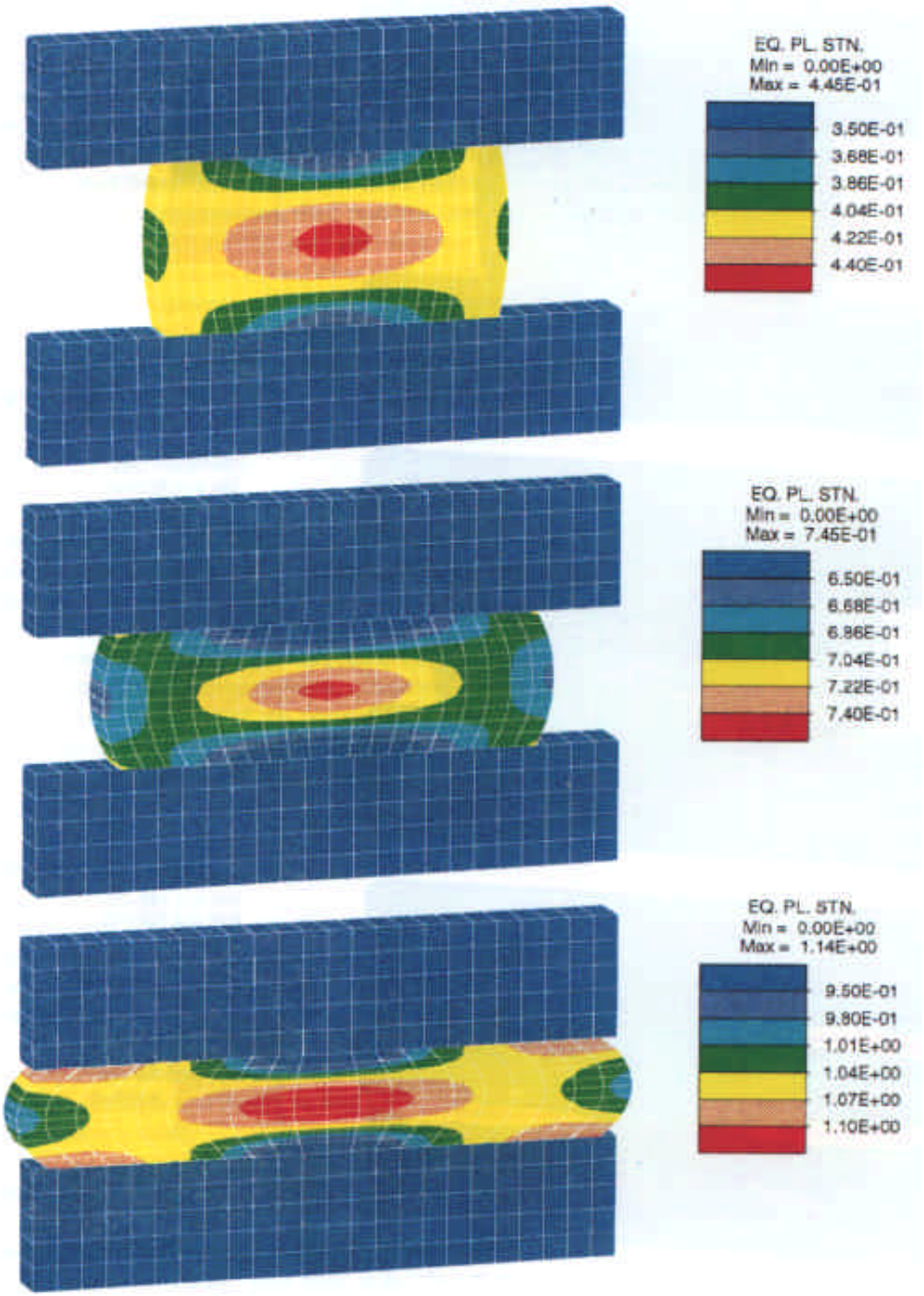

Figure 4.6. Upsetting of a Billet. Equivalent plastic strain distribution at three different time steps, corresponding to billet height reductions of 30%, 45% and 60%

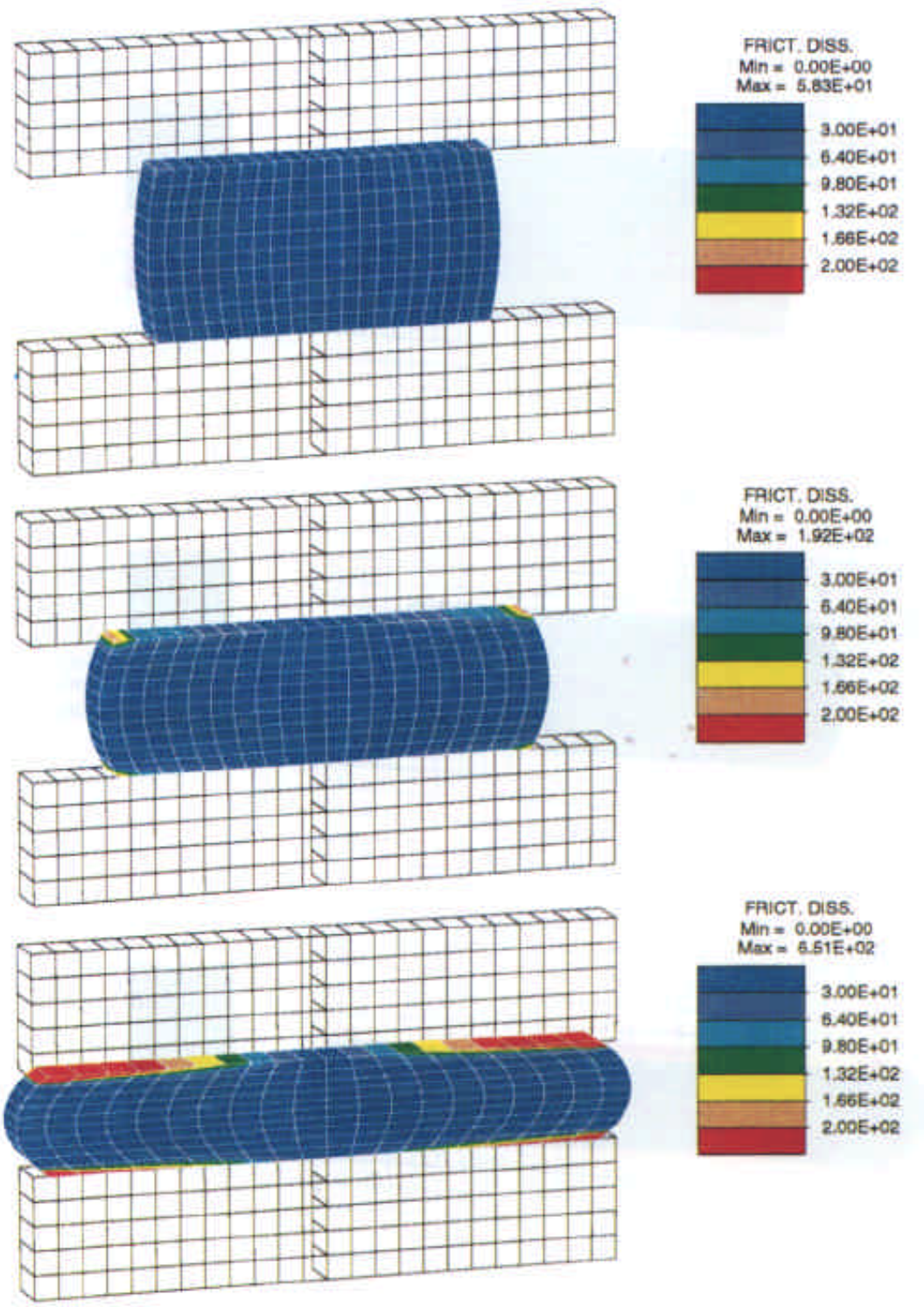

Figure 4.7. Upsetting of a Billet. Frictional dissipation distribution at the contact surface for three different time steps, corresponding to billet height reductions of 30%, 45% and 60%

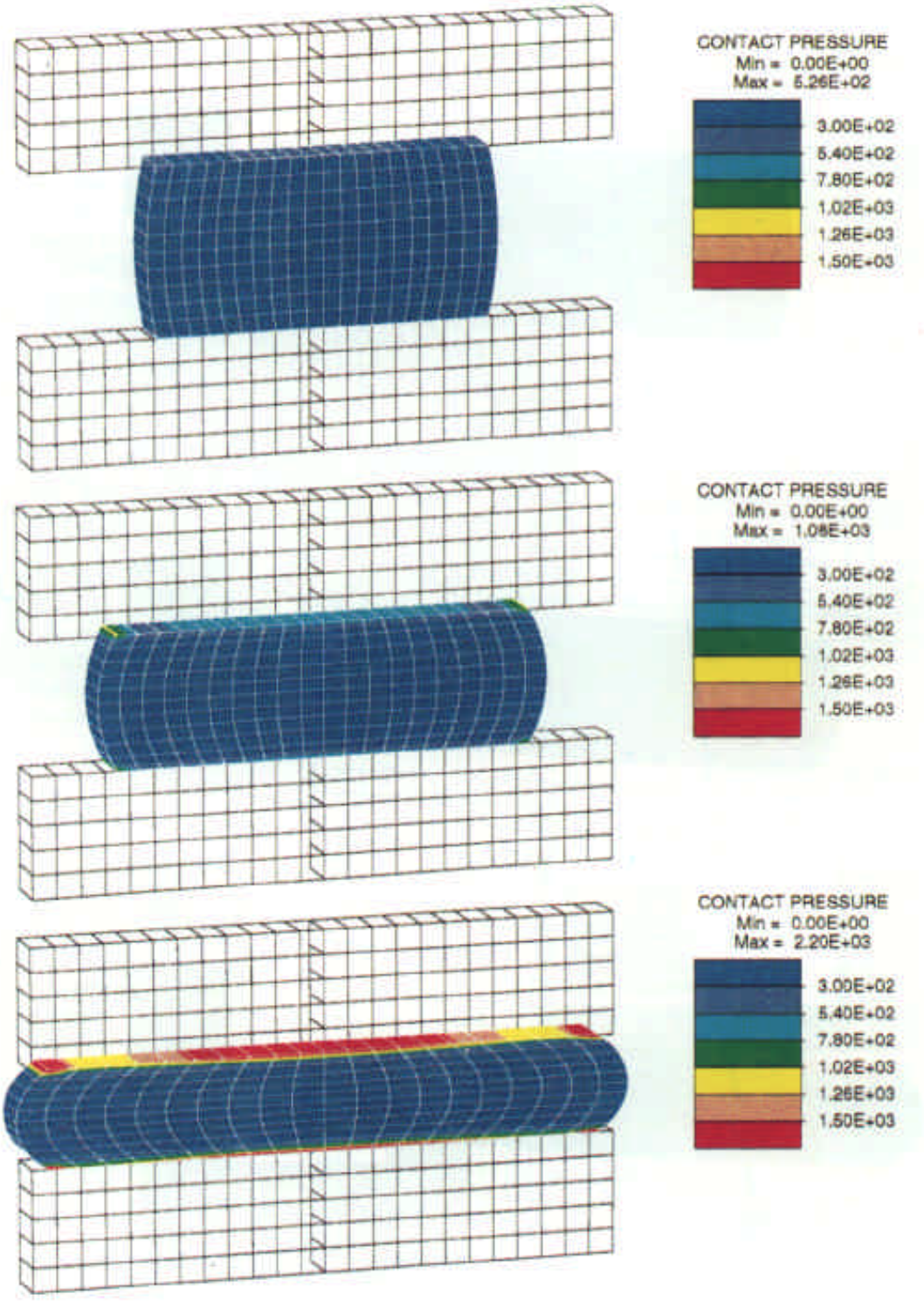

Figure 4.8. Upsetting of a Billet. Contact pressure distribution at the contact surface for three different time steps, corresponding to billet height reductions of 30%, 45% and 60%

REFERENCES

Agelet de Saracibar, C. (1995a), "A New Frictional Time Integration Algorithm for Multi-Body Large Slip Frictional Contact Problems", *Computer Methods in Applied Mechanics and Engineering*, **142**, 303–334.

Agelet de Saracibar, C. (1995b), "Numerical Analysis of Frictional Contact Problems", *Lecture notes of Short Course on Computational Techniques for Plasticity*, International Center for Numerical Methods in Engineering, Barcelona, Spain.

Agelet de Saracibar, C. & M. Chiumenti (1995), "Numerical Analysis of Frictional Wear Contact Problems. Computational Model and Applications", to be published in *Computer Methods in Applied Mechanics and Engineering*.

Armero, F. & J.C. Simo (1992a), "A new Unconditionally Stable Fractional Step Method for Nonlinear Coupled Thermomechanical Problems", *International Journal for Numerical Methods in Engineering*, **35**, 737-766.

Armero F. & J.C. Simo (1992b), "Product Formula Algorithms for Nonlinear Coupled Thermoplasticity: Formulation and Nonlinear Stability Analysis", *Division of Applied Mechanics, Department of Mechanical Engineering, Stanford University, Stanford, California*, SUD AM Report no. 92-4, March 1992.

Armero F. & J.C. Simo (1993), "A Priori Stability Estimates and Unconditionally Stable Product Algorithms for Nonlinear Coupled Thermoplasticity", *International Journal of Plasticity*, **9**, 749-782.

Bathe, K.-J. & A. Chaudhary (1985), "A Solution Method for Planar and Axisymmetric Contact Problems", *International Journal for Numerical Methods in Engineering*, **21**, 65-88.

Belytschko, T. & M.O. Neal (1991), "Contact-Impact by the Pinball Algorithm with Penalty and Lagrangian Methods", *International Journal for Numerical Methods in Engineering*, **31**(3), 547-572.

Benson, D.J. & J.O. Hallquist (1990), "A Single Surface Contact Algorithm for the Post-Buckling Analysis of Shell Structures", *Computer Methods in Applied Mechanics and Engineering*, **78**, 141-163.

Campos, L.T., J.T. Oden & N. Kikuchi (1982), "A Numerical Analysis of a Class of Contact Problems with Friction in Elastostatics", *Computer Methods in Applied Mechanics and Engineering*, **34**, 821-845.

Carpenter, N.J., R.L. Taylor & M.G. Katona (1991), "Lagrange Constraints for Transient Finite Element Surface Contact", *International Journal for Numerical Methods in Engineering*, **32**, 103-128.

Cheng, J.-H. & N. Kikuchi (1985), "An Analysis of Metal Forming Processes Using Large Deformation Elastic-Plastic Formulations", *Computer Methods in Applied Mechanics and Engineering*, **49**, 71-108.

Ciarlet, P.G. (1988), *Mathematical Elasticity. Volume 1: Three-Dimensional Elasticity*, North-Holland, Amsterdam.

Curnier, A. (1984), "A theory of friction", *International Journal of Solids and Structures*, **20**, 637-647.

Curnier, A. & P. Alart (1988), "A Generalized Newton Method for Contact Problems with Friction", *Journal de Mecanique Theorique et Appliquee*, supplement no. 1 to **7**, 67-82.

Duvaut, G. & J.L. Lions (1972), *Les Inequations en Mecanique et en Physique*, Dunod, Paris.

Gallego, F.J. & J.J. Anza (1989), "A Mixed Finite Element Model for the Elastic Contact Problem", *International Journal for Numerical Methods in Engineering*, **28**, 1249-1264.

Giannakopoulos, A.E. (1989), "The Return Mapping Method for the Integration of Friction Constitutive Relations", *Computers and Structures*, **32**, 157-167.

Hallquist, J.O., G.L. Goudreau & D.J. Benson (1985), "Sliding Interfaces with Contact-Impact in Large-Scale Lagrangian Computations", *Computer Methods in Applied Mechanics and Engineering*, **51**, 107-137.

Hughes, T.J.R. (1987), *The Finite Element Method: Linear Static and Dynamic Finite Element Analysis*, Prentice-Hall, Englewood Cliffs, NJ.

Ju, J.-W. & R.L. Taylor (1988), "A Perturbed Lagrangian Formulation for the Finite Element Solution of Nonlinear Frictional Contact Problems", *Journal de Mecanique Theorique et Appliquee*, supplement no. 1 to volume **7**, 1-14.

Ju, J.-W., R.L. Taylor & L.Y. Cheng (1987), "A Consistent Finite Element Formulation of Nonlinear Frictional Contact Problems", *Proceedings of the International Conference NUMETA'87*, J. Middleton & G.N. Pande, eds., Nijhoff, Dordrecht.

Kikuchi, N. & J.T. Oden (1988), *Contact Problems in Elasticity: A Study of Variational Inequalities and Finite Element Methods*, SIAM, Philadelphia.

Klarbring, A. & G. Björkman (1992), "Solution of Large Displacement Contact Problems with Friction Using Newton's Method for Generalized Equations", *International Journal for Numerical Methods in Engineering* **34**, 249-269.

Laursen, T.A. (1992), "Formulation and Treatment of Frictional Contact Problems Using Finite Elements", *Ph.D. Dissertation*, Stanford University, Division of Applied Mechanics, Report no. 92-6.

Laursen, T.A. & S. Govindjee (1994), "A Note on the Treatment of Frictionless Contact Between Non-smooth Surfaces in Fully Non-linear Problems", *Communications in Applied Numerical Methods*, **10**, 869-878

Laursen, T.A. & J.C. Simo (1991), "On the Formulation and Numerical Treatment of Finite Deformation Frictional Contact Problems", in *Nonlinear Computational Mechanics–State of the Art*, P. Wriggers & W. Wagner, eds., Springer-Verlag, Berlin, pp. 716-736.

Laursen, T.A. & J.C. Simo (1992), "Formulation and Regularization of Frictional Contact Problems for Lagrangian Finite Element Computations", in *Proc. of The Third International Conference on Computational Plasticity: Fundamentals and Applications, COMPLAS III*, D.R.J. Owen, E. Oñate & E. Hinton, eds., Pineridge Press, Swansea, pp. 395-407.

Laursen, T.A. & J.C. Simo (1993a), "A Continuum-Based Finite Element Formulation for the Implicit Solution of Multi-Body, Large Deformation Frictional Contact Problems", *International Journal for Numerical Methods in Engineering* **36**(20), 3451-3485.

Laursen, T.A. & J.C. Simo (1993b), "Algorithmic Symmetrization of Coulomb Frictional Problems Using Augmented Lagrangians", *Computer Methods in Applied Mechanics and Engineering*, **108**, 133-146.

Lee, E.H. (1969), "Elastic-plastic Deformation at Finite Strains", *Journal of Applied Mechanics*, **36**, 1-6.

Lee, E.H. & D.T. Liu (1967), "Finite Strain Elastic-Plastic Theory Particularly for Plane Wave Analysis", *Journal of Applied Physics*, **38**.

Luenberger, D.G. (1984), *Linear and Nonlinear Programming*, Addison-Wesley, Reading, Massachusetts.

Mandel, J. (1974), "Thermodynamics and Plasticity", in *Foundations of Continuum Thermodynamics*, J.J. Delgado et al. eds., McMillan, London, 283-304.

Marsden, J.E. & T.J.R. Hughes (1983), *Mathematical Foundations of Elasticity*, Prentice-Hall, Inc., Englewood Cliffs, New Jersey.

Moran, B., M. Ortiz & C.F. Shih (1990), "Formulation of Implicit Finite Element Methods for Multiplicative Deformation Plasticity", *International Journal for Numerical Methods in Engineering*, **29**, 483-514.

Oden, J.T. & J.A.C. Martins (1985), "Models and Computational Methods for Dynamic Friction Phenomena", *Computer Methods in Applied Mechanics and Engineering*, **52**, 527-634.

Oden, J.T. & E.B. Pires (1984), "Algorithms and Numerical Results for Finite Element Approximations of Contact Problems with Non-Classical Friction Laws", *Computer and Structures*, **19**, 137-147.

Owen, D.R.J., D. Perić, A.J.L. Crook, E.A. de Souza Neto, J. Yu & M. Dutko (1995), "Advanced Computational Strategies for 3D Large Scale Metal Forming Simulations", *Proceedings of the Fifth International Conference on Numerical Methods in Industrial Forming Processes*, to appear

Papadopoulos, P. & R.L. Taylor (1990), "A Mixed Formulation for the Finite Element Solution of Contact Problems", *UCB/SEMM Report*, 90/18, University of California at Berkeley.

Parisch, H. (1989), "A Consistent Tangent Stiffness Matrix for Three-Dimensional Non-Linear Contact Analysis", *International Journal for Numerical Methods in Engineering*, **28**, 1803-1812.

Shai, I. & M. Santo (1982), "Heat transfer with contact resistance", *International Journal of Heat and Mass Transfer*, **24**, 465-470.

Simo, J.C. (1988), "A Framework for Finite Strain Elastoplasticity Based on the Multiplicative Decomposition and Hyperelastic Relations. Part II: Computational Aspects", *Computer Methods in Applied Mechanics and Engineering*, **68**, 1-31.

Simo, J.C. (1992), "Algorithms for Static and Dynamic Multiplicative Plasticity that Preserve the Classical Return Mapping Schemes of the Infinitesimal Theory", *Computer Methods in Applied Mechanics and Engineering*, **99**, 61-112.

Simo, J.C. (1994), "Numerical Analysis Aspects of Plasticity", in *Handbook of Numerical Analysis, Volume IV*, P.G. Ciarlet and J.J. Lions, eds., Nort-Holland.

Simo, J.C. & F. Armero (1991), "Recent Advances in the Formulation and Numerical Analysis of Thermoplasticity at Finite Strains", in *Finite Inelastic Deformations - Theory and Applications* E. Stein and D. Besdo, eds., IUTAM/IACM Symposium, Hannover, FRG, August, 19-23, 1991 Springer-Verlag, Berlin, 1991.

Simo J.C. & F. Armero (1992), "Geometrically Nonlinear Enhanced Strain Mixed Methods and the Method of Incompatible Modes", *International Journal for Numerical Methods in Engineering*, **33**, 1413-1449.

Simo, J.C., F. Armero & R.L. Taylor (1993), "Improved Versions of Assumed Enhanced Strain Tri-Linear Elements for 3D Finite Deformation Problems", *Computer Methods in Applied Mechanics and Engineering*, .

Simo, J.C. & T.J.R. Hughes (1994), "Elastoplasticity and Viscoplasticity: Computational Aspects", to be published by Springer-Verlag, Berlin.

Simo, J.C. & T.A. Laursen (1992), "An Augmented Lagrangian Treatment of Contact Problems Involving Friction", *Computers and Structures*, **42**, 97-116.

Simo, J.C. & C. Miehe (1992), "Associative Coupled Thermoplasticity at Finite Strains: Formulation, Numerical Analysis and Implementation", *Computer Methods in Applied Mechanics and Engineering*, **98**, 41-104.

Simo, J.C., P. Wriggers, K. Schweizerhof & R.L. Taylor (1986), "Finite Deformation Postbuckling Analysis Involving Inelasticity and Contact Constraints", *International Journal for Numerical Methods in Engineering*, **23**, 779-800.

Simo, J.C., P. Wriggers & R.L. Taylor (1985), "A Perturbed Lagrangian Formulation for the Finite Element Solution of Contact Problems", *Computer Methods in Applied Mechanics and Engineering*, **50**, 163-180.

Song, S. & M.M. Yovanovich (1987), "Explicit relative contact pressure expression: dependence upon surface roughness parameters aand Vickers microhardness coefficients", *AIAA*, Paper 87-0152.

de Souza Neto, K. Hashimoto, D. Perić & D.R.J. Owen (1995), "A Phenomenological Model for Frictional Contact of Coated Steel Sheets Accounting for Wear Effects: Theory, Experiments and Numerical Simulation", *International Journal for Numerical Methods in Engineering*, to appear.

Wriggers, P. (1987), "On Consistent Tangent Matrices for Frictional Contact Problems", in *Proceedings of the International Conference NUMETA'87*, J. Middleton & G.N. Pande, eds., Nijhoff, Dordrecht.

Wriggers, P. (1995), "Finite Element Algorithms for Contact Problems", *Archives of Computational Methods in Engineering* **2**, 4, 1-50.

Wriggers, P. & M. Imhof (1993), "On the Treatment of Nonlinear Unilateral Contact Problems", *Ing. Archiv*, **63**, 116-129.

Wriggers, P. & C. Miehe (1992), "Recent Advances in the Simulation of Thermomechanical Contact Processes", in *Proc. of The Third International Conference on Computational Plasticity: Fundamentals and Applications, COMPLAS III*, D.R.J. Owen, E. Oñate & E. Hinton, eds., Pineridge Press, Swansea, pp. 325-347.

Wriggers, P. & C. Miehe (1994), "Contact Constraints within Coupled Thermomechanical Analysis. A Finite Element Model", *Computer Methods in Applied Mechanics and Engineering*, **113**, 301-319.

Wriggers, P& O. Scherf (1995), "An adaptive finite element method for elastoplastic contact problems", in *Proc. of The Fourth International Conference on Computational Plasticity: Fundamentals and Applications, COMPLAS IV*, D.R.J. Owen, E. Oñate & E. Hinton, eds., Pineridge Press, Swansea.

Wriggers, P, O. Scherf & C. Carstensen (1995), "Adaptive Techniques for the Contact of Elastic Bodies", in *Recent Developments in Finite Element Analysis*, T.J.R. Hughes, E. Oñate & O.C. Zienkiewicz, eds. CIMNE, Barcelona.

Wriggers, P. & J.C. Simo (1985), "A Note on Tangent Stiffness for Fully Nonlinear Contact Problems", *Communications in Applied Numerical Methods*, **1**, 199-203.

Wriggers, P., J.C. Simo & R.L. Taylor (1985), "Penalty and Augmented Lagrangian Formulations for Contact Problems", *Proceedings of the International Conference NUMETA'85*, J. Middleton & G.N. Pande, eds., A.A. Balkema, Rotterdam.

Wriggers, P, T. Vu Van & E. Stein (1990), "Finite Element Formulation of Large Deformation Impact-Contact Problems with Friction", *Computers and Structures*, **37**, 319-331.

Wriggers, P & G. Zavarise (1993), "On the Application of Augmented Lagrangian Techniques for Nonlinear Constitutive Laws in Contact Interfaces", *Communications in Numerical Methods in Engineering*, **9**, 815-824.

Wriggers, P& G. Zavarise (1993), "Thermomechanical Contact. A Rigorous but Simple Numerical Approach", *Computers and Structures*, **46**, 47-53.

Yovanovich, M.M. (1981), "Thermal Contact Correlations", *AIAA*, Paper 81-1164.

Zavarise, G., P. Wriggers & B. A. Schrefler (1995), "On Augmented Lagrangian Algorithms for Thermomechanical Contact Problems With Friction", *International Journal for Numerical Methods in Engineering*, **38**(17), 2929-2949.

Zavarise, G., P. Wriggers, E. Stein & B. A. Schrefler (1992), "Real Contact Mechanisms and Finite Element Formulation–A Coupled Thermomechanical Approach", *International Journal for Numerical Methods in Engineering*, **35**(4), 767-785.

Zienkiewicz, O.C. & R.L. Taylor (1991), *The Finite Element Method, 4th ed., Volume 2: Solid and Fluid Mechanics, Dynamics and Non-linearity*, McGraw-Hill, London.

Please address your comments or questions on this paper to:
International Center for Numerical Methods in Engineering
Edificio C-1, Campus Norte UPC
Gran Capitán s/n
08034 Barcelona, Spain
Phone: 34-93-4016035; Fax: 34-93-4016517